The domino problem of the hyperbolic plane is undecidable

Maurice Margenstern

Laboratoire d'Informatique Théorique et Appliquée, EA 3097,
Université de Metz, I.U.T. de Metz,
Département d'Informatique,
Île du Saulcy,
57045 Metz Cedex, France,
e-mail : margens@univ-metz.fr

Abstract

In this paper, we prove that the general tiling problem of the hyperbolic plane is undecidable by proving a slightly stronger version using only a regular polygon as the basic shape of the tiles. The problem was raised by a paper of Raphael Robinson in 1971, in his famous simplified proof that the general tiling problem is undecidable for the Euclidean plane, initially proved by Robert Berger in 1966.

1 Introduction

The question, whether it is possible to tile the plane with copies of a fixed set of tiles was raised by Wang, [30] in the late 50's of the previous century. Wang solved the *origin-constrained* problem which consists in fixing an initial tile in the above finite set of tiles. Indeed, fixing one tile is enough to entail the undecidability of the problem. The general case, later called the **general tiling problem** in this paper, without condition, in particular with no fixed initial tile, was proved undecidable by Berger in 1966, [1]. Both Wang's and Berger's proofs deal with the problem in the Euclidean plane. In 1971, Robinson found an alternative, simpler proof of the undecidability of the general problem in the Euclidean plane, see [27]. In this 1971 paper, he raises the question of the general problem for the hyperbolic plane. Seven years later, in 1978, he proved that in the hyperbolic plane, the origin-constrained problem is undecidable, see [28]. Up to now, the general tiling problem remained open.

In 2006, a step forward was made with a technical report, see [17], which will be soon published, see [25]. This step consists in a generalization of the origin-constrained problem. Later, In 2007, I deposited on *arXiv* several improvements of a first version of the proof that the domino problem of the hyperbolic plane is

undecidable, see[16, 21] and also on my web-page [18] . In [22], I give a synthetic presentation of the techniques contained on these different technical papers. In this paper, I provide the complementary material to fully understand [22]. In particular, full proofs with auxiliary lemmas, tables and more illustrations are given in order to make the proof as complete as possible.

In this introduction, we remind the general strategy to attack the tiling problem, as it was already established in the famous proofs dealing with the Euclidean case. We also remind the basic properties we need about hyperbolic geometry and of the tiling $\{7, 3\}$, in the frame of which our solution of the problem takes place. The reader familiar with hyperbolic geometry can skip this part of the paper. We also refer the reader to [24] and to [13] for a more detailed introduction and for other bibliographical references. Also, in order the paper could be self-contained, we sketchily reminds the notion of a space-time diagram of a Turing machine.

In the second section, we establish the properties of the particular tiling which we consider within the tiling $\{7, 3\}$, the **mantilla**. There, we recall the properties already established in [17, 15] and we append the new properties established in [18, 16].

In the third section, we present a needed interlude, a parenthesis on brackets, which is a basic ingredient of the proof. In the fourth section, we lift up this line construction to a planar Euclidean one. In the fifth section, we show how to implement the Euclidean construction in the hyperbolic plane, using the specific properties indicated in the second section. In the sixth section, we complete the proof of the main result:

THEOREM **1** *The domino problem of the hyperbolic plane is undecidable.*

From theorem 1, we immediately conclude that the general tiling problem is undecidable in the hyperbolic plane.

Still in the sixth section, we again complete the proof by a detailed description and a counting of the tiles.

In the seventh section, we give several corollaries of the construction and we conclude in two directions. The first one wonders whether it is possible to simplify the construction. The second direction tries to see what might be learned from the construction leading to theorem 1.

Before turning to sub-section 1.1, let us remark that an alternative proof of the general tiling problem is claimed by Jarkko Kari, see [8, 9]. His proof is completely different of this one. It is completely combinatoric and it makes use of a non-effective argument. It is not the place, here, to discuss this latter point.

1.1 The general strategy

In the proofs of the general tiling problem in the Euclidean plane by Berger and by Robinson, there is an assumption which is implicit and which was, most probably, considered as obvious at that time.

Consider a finite set S of **prototiles**. We call **solution** of the tiling of the plane by S a partition $\mathcal{P}$ such that the closure of any element of $\mathcal{P}$ is a copy of

an element of S. We notice that this definition contains the traditonal condition on matching signs in the case when the elements of S possess signs.

Note that the general tiling problem can be formalized as follows:

$$\forall S \ \ (\exists\, \mathcal{P} \ sol(\mathcal{P}, S) \vee \neg(\exists\, \mathcal{P} \ sol(\mathcal{P}, S))),$$

where $\vee$ is interpreted in a constructive way: there is an algorithm which, applied to S provides us with 'yes' if there is a solution and 'no' if there is none.

The origin-constrained problem can be formalized in a similar way by:

$$\forall (S, a) \ \ (\exists\, \mathcal{P} \ sol(\mathcal{P}, S, a) \vee \neg(\exists\, \mathcal{P} \ sol(\mathcal{P}, S, a))),$$

where $a \in S$, with the same algorithmic interpretation of $\vee$.

Now, note that if we have a solution of the general tiling problem for the considered instance, we also have a solution of the origin-constrained problem, with the facility that we may choose the first tile. However, to prove that the general tiling problem, in the considere instance, has no solution, we have to prove that, whatever the initial tile, the corresponding origin-constrained problem also has no solution.

However, Berger's and Robinson's proofs consider that we start the construction with a special tile, called the **origin**. There is no contradiction with what we have just said, because they force the tiling to have a dense subset of origins. In the construction, the origins start the simulation of the space-time diagram of the computation of a Turing machine M. All origins compute the same machine M which can be assumed to start from an empty tape. The origins define infinitely many domains of computation of infinitely many sizes. If the machine does not halt, starting from an origin, it is possible to tile the plane. If the machine halts, whatever the initial tile, we nearby find an origin and, from this one, we shall eventually fall into a domain which contains the halting of the machine: at this point, it is easy to prevent the tiling to go on.

The present construction aims at the same goal.

1.2 The tiling $\{7, 3\}$

In this sub-section, we very sketchily remember the minimal data about hyperbolic geometry and about the tiling which constitutes the general frame of our construction.

The hyperbolic plane

Hyperbolic geometry appeared in the first half of the 19^{th} century, as the conclusion of the very long quest to prove the famous axiom of parallels of Euclid's *Elements* from the other axioms. As presently known, the axiom on parallels is independent from the others. The discovery of hyperbolic geometry also raised the notion of independency in an axiomatic theory. In the second half of the 19^{th} century, several models were devised in which the axioms of hyperbolic geometry are satisfied. Among these models, Poincaré's models became very popular. One model makes use of the half-plane in the Euclidean plane, the other makes use of a disc, also in the Euclidean plane. Each time we shall

need to refer to a model, especially for illustrations, we shall use Poincaré's disc model.

Let us fix an open disc U of the Euclidean plane. Its points constitute the points of the hyperbolic plane $\mathbb{H}^2$. The border of U, ∂U, is called the set of **points at infinity**. Lines are the trace in U of its diameters or the trace in U of circles which are orthogonal to ∂U. The model has a very remarkable property, which it shares with the half-plane model: hyperbolic angles between lines are the euclidean angles between the corresponding circles. The model is easily generalized to higher dimension, see [24] for definitions and properties of such generalizations as well as references for further reading.

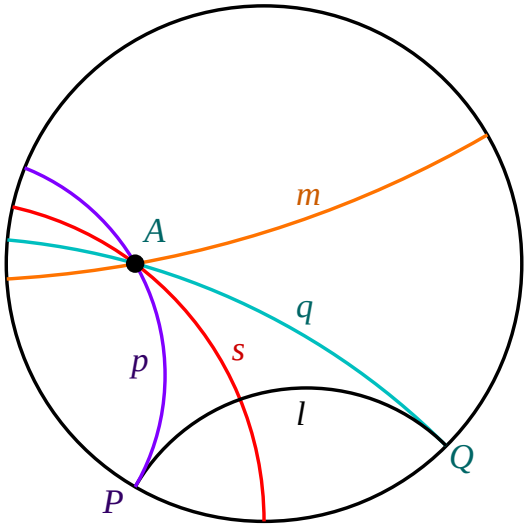

FIG. **1** An illustration of the Poincaré model.

On Figure 1, the lines p and q pass through the point A and they are parallel to the line ℓ. We notice that each of them has a common point at infinity with ℓ: P in the case of p and Q in the case of q. The line s which also passes through A cuts the line ℓ: it is a **secant** to this line. However, the line m, which also passes through A does not meet ℓ, neither in U, nor at infinity, *i.e.* on ∂U. Such a line is called **non-secant** with ℓ. Non-secant lines have a nice characterisitic property: two lines are non-secant if and only if they have a common perpendicular which is unique.

A tiling of the hyperbolic plane: the ternary heptagrid

Tessellations are a particular case of tilings. They are generated from a regular polygon by reflection in its sides and, recursively, of the images in their sides. In the Euclidean case, there are, up to isomorphism and up to similarities, three tesselations, respectively based on the square, the equilateral triangle and on the regular hexagon.

In the hyperbolic plane, there are infinitely many tessellations. They are based on the regular polygons with p sides and with $\frac{2\pi}{q}$ as vertex angle and they are denoted by $\{p, q\}$. This is a consequence of a famous theorem by Poincaré which characterizes the triangles starting from which a tiling can be generated by the recursive reflection process which we already mentioned. Any triangle tiles the hyperbolic plane if its vertex angles are of the form $\frac{\pi}{p}$, $\frac{\pi}{q}$ and $\frac{\pi}{r}$ with the condition that $\frac{1}{p} + \frac{1}{q} + \frac{1}{r} < 1$.

Among these tilings, we choose the tiling $\{7, 3\}$ which we called the thernary heptagrid in [2]. It is below illustrated by Figure 2.

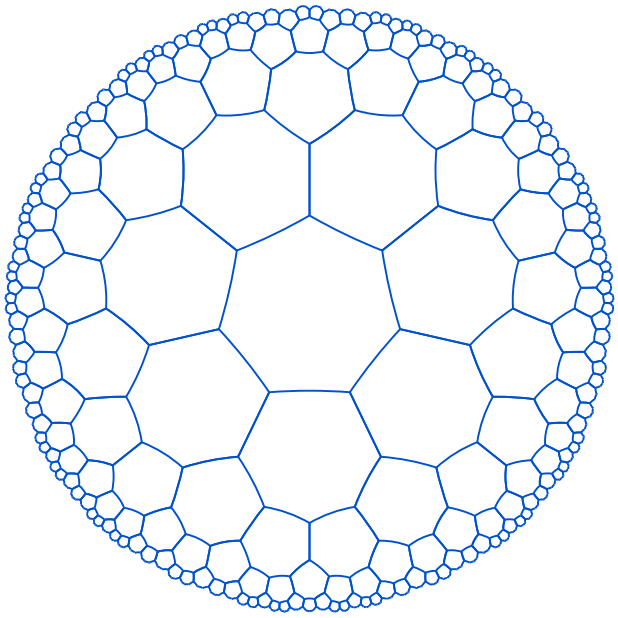

FIG. **2** The tiling $\{7, 3\}$ of the hyperbolic plane in the Poincaré's disc model.

In [2, 24], many properties of the ternary heptagrid are described. An important tool to establish them is the splitting method, prefigured in [12] and for which we refer to [24]. Here, we just suggest the use of this method which allows to exhibit a tree, spanning the tiling: the **Fibonacci tree**. Below, the left-hand side of Figure 3 illustrates the splitting of $\mathbb{H}^2$ into a central tile T and seven sectors dispatched around T. Each sector is spanned by a Fibonacci tree. The right-hand side of Figure 3 illustrates how the sector can be split into sub-regions. Now, we notice that two of these regions are copies of the same sector and that the third region S can be split into a tile and then a copy of a sector and a copy of S. Such a process gives rise to a tree which is in bijection with the tiles of the sector. The tree structure will be used in the sequence and other illustrations will allow the reader to better understand the process.

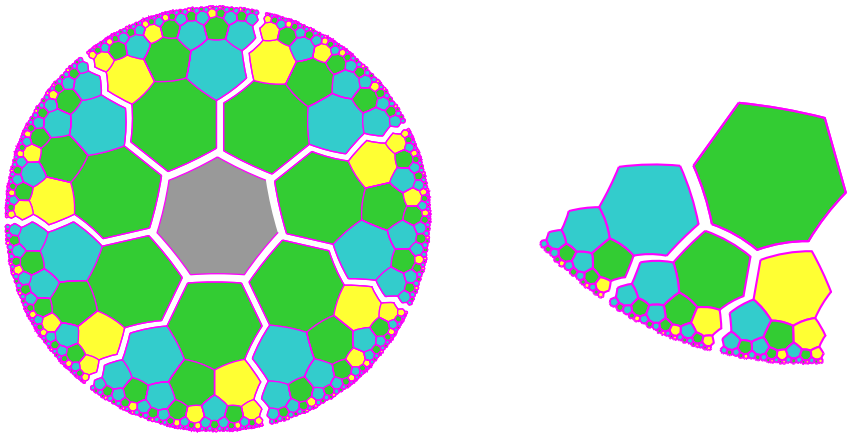

FIG. **3** Left-hand side: the standard Fibonacci trees which span the tiling $\{7, 3\}$ of the hyperbolic plane. Right-hand side: the mid-point lines.

Another important tool to study the tiling $\{7, 3\}$ is given by the **mid-point** lines, which are illustrated by Figure 4, below. The lines have this name because they join the mid-points of contiguous edges of tiles. We can see on the figure how such lines allow to delimit a sector, a property which is proved in [2, 24].

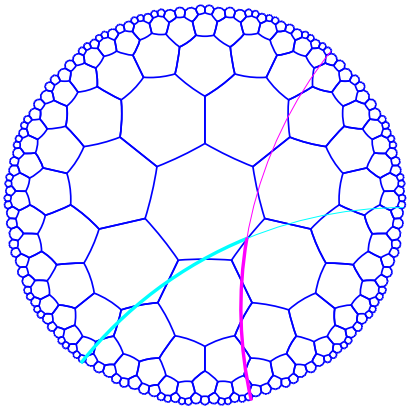

FIG. **4** The mid-point lines.

The space-time diagram of a Turing machine

As our proof of Theorem 1 makes use of the simulation of a Turing machine, we skecthily remind a few features of the Turing machines, see [29, 7]. We shall specifically remind the use of space-time diagrams.

A Turing machine is a device which consists of an infinite **tape** and of a **head**. The tape is constituted of adjacent **squares**, each one containing a

symbol belonging to a finite alphabet A. The head looks at a square, the **scanned square** and it is in a given **state**. Depending on its state and on the symbole read in the scanned square, the machine performs an action specified by an **instruction**: replace the read letter by a new letter, possibly the same one, turn to a new state, possibly the same one, and go to the next scanned square which is either the right-hand side neighbour of the scanned square, or its left-hand side neighbour or again, the same scanned square. There are finitely many instructions whose set constitutes the **program** of the machine. One symbol of A plays a special rôle. It is called the **blank** and a square containing the blank is called **empty**.

The configuration of a Turing machine is defined by two squares: the leftmost and the rightmost ones, called the **borders** of the configuration. For the initial configuration, these borders define the smallest finite interval of the tape which contains both the square scanned by the head of the machine and all the non-empty squares. It is assumed that at the initial time, there are finitely non-empty squares in the tape. When the borders of the current configuration are defined, the borders of the next configuration are either the same or one of them is move by one square further: this is the case when the head scans a border and when its action moves outside the current configuration.

Now, a **space-time diagram** of the execution of a Turing machine M consists in placing successive configurations of the computation of M on the plane. The initial configuration C_0 is put along the X-axis with the origin at a fixed position of the tape: it corresponds to the absissa 0. The configuration i which is obtained after i steps of computation is placed on the parallel to the X-axis which has the absissa i.

As can immediately be seen, the important feature is not that we have strictly parallel lines, and that squares are alined along lines which are perpendicular to the tapes. What is important is that we have a **grid**, which may be a more or less distorted image of the just described representation.

2 The mantilla

In this section, we remind the construction of the tiling which will be the frame in which our proof of the main theorem takes place. We start with the motivation of this special tiling which we call the **mantilla**.

2.1 The flowers

Remind that a **ball** is the set of tiles which are within a fixed distance from a fixed tile which we call its **centre**, where the **distance** of a tile to this centre is the number of tiles constituting the shortest path between the tile and the centre, the centre not being taken into account. The distance which defines the ball is called its **radius**. In what follows, we denote a ball of radius n by B_n. But as we shall be very often concerned by balls of radius 1 only, we give them a special name, we call them **flowers**.

In [24], we proved that flowers tile the hyperbolic plane.

But here, we shall use another object in which we partially **merge** flowers. This will give rise to another way of tiling the ternary heptagrid which will be at the basis of our construction.

The idea of merging the flowers comes from the following consideration. Robinson's proof of the undecidability of tiling the Euclidean plane is based upon a simple tiling consisting of two tiles represented by Figure 5, below.

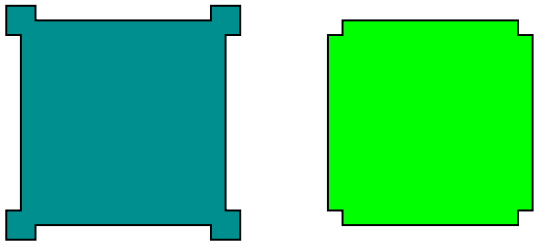

FIG. **5** Robinson's basic tiles for the undecidability of the tiling problem in the Euclidean case.

In the Euclidean case, this fixes the tiling immediately and we refer the reader to Robinson's paper [27] to see the very nice consequences deduced from these simple tiles.

If we try to apply the same idea to the ternary heptagrid, we get the tiles of Figure 6.

It is not very difficult to see that this cannot work. Indeed, tile a requires seven copies of b around it and once we put three tiles a around a tile b, we arrive to an impossibility to go on.

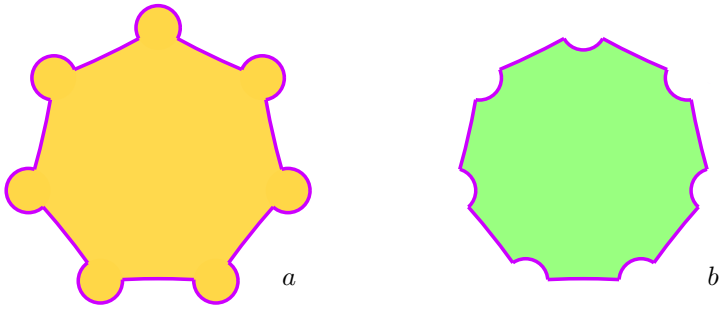

FIG. **6** A 'literal' translation of Robinson's basic tiles to the situation of the ternary heptagrid.

However, it is not very difficult to change a bit the tile b to make things to work much better, perfectly well as will be seen later. Consider the new couple of tiles given by Figure 7.

This time we can see that we always must put seven copies of tile c around a tile a and that we need three copies of a around a tile c. Also, we can see that three tiles c abut around their untouched vertex.

What we shall call later the mantilla and the set of tiles which we shall later derive to represent it can be seen as a rigourous proof that there are tilings of the hyperbolic plane based only on tiles a and c of Figure 7. However, by contrast with the Euclidean case, we have here infinitely many such tilings, even continuously many of them.

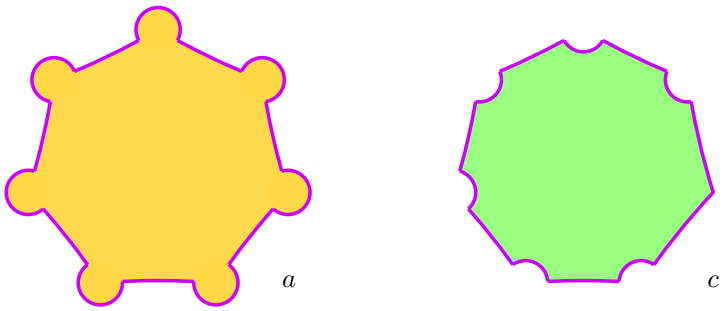

FIG. **7** An adaptation of Robinson's basic tiles to the ternary heptagrid.

The seven copies of c around a tile a give immediately the idea of a flower. Also, we shall modify the representation in order to obtain strict *à la Wang* tiles. Moreover, the tiles will abut simply, only requiring that abutting edges have the same colour.

Using the notion of flower, we introduce two kind of tiles: blank ones which, later on will be called **centres**, and the others will be called the **petals**. The tiles are represented by Figure 8. As can be more or less guessed, centres correspond to tile a of Figure 7 and petals correspond to tile c of the same figure. Petals can be seen as a *pedagogic* version of tile c: green and red marks indicate the edges where a petal abut with another petal, the other sides being shared with a centre.

The basic figure of the mantilla is the flower. Later, we will re-define the tiling in such a way that a condition will be put on the tiles: a centre may be surrounded by petals only; it cannot abut with another centre. A consequence of this constraint is that any petal belongs to three flowers and so, we can view petals and centres as meshes and holes of a vast crochet, whence the name *mantilla*.

It will turn out that there can be infinitely many mantillas if any. Indeed, we shall find an **algorithmic way** to combine petals and centres in order to get a tiling. We shall do this a bit later.

Assuming that solutions exist, let us investigate to what they look like. Considering a centre, it is not difficult to see that it is surrounded by centres, not immediately but at a small distance. Indeed, the first row of surrounding tiles are petals but on the second row, centres necessarily appear. Note in Figure 11

that the red vertex of three petals must be glued together. This will define the **red vertices** of the configurations we shall study. Also, two green dots are connected by the sides of two neighbouring petals. Accordingly, we say that the corresponding side is **green**. Now, we note that red vertices are always at the end of a side where the other belongs to the border of a centre. We shall say that the considered red vertex is **at distance 1** from this centre. Note that any red vertex is always at distance 1 of exactly three distinct centres.

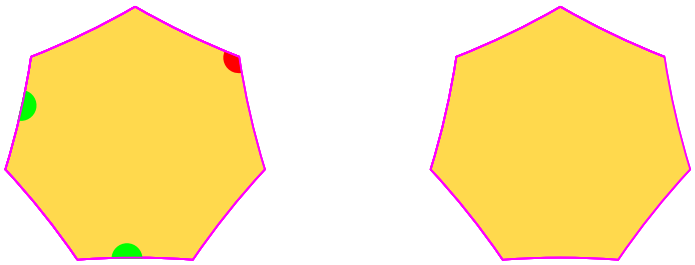

FIG. **8** The basic two kinds of tiles, translation of tiles a and c into dominoes.

LEMMA **1** *A petal can abut at a blank edge only with a centre. Two petals can abut either by their red-vertex and an edge of this vertex or by an edge with a green mark.*

Proof of Lemma 1. If we consider a petal, it cannot abut with itself or with another one by the blank edges. To see this point, we fix one petal and an edge and we make the other rotate three times in order to present all its blank edges to the chosen blank edge of the fixed petal. As we can see in Figure 9, in two cases, this would require a tile where two adjacent edges bear a green mark, which is impossible. In the remaining case, it would require a tile with an edge marked by a green side and an adjacent edge with, at the non-common vertex, a red vertex. This is also impossible.

The possibilities between two petals are indicated by Figure 10.

From Figure 10 which indicates the way of how petals can be connected we can see that the number of centres of the second row ranges in the interval $\{7..10\}$. Call **centre ring** the set of centres in the second row of tiles around a given centre. The centre defining the centre ring is again called the **centre** of the centre ring or simply centre if no confusion may arise. Then, it can be noted that the number of elements in the centre ring is directly connected with the number of red vertices which are at distance 1 from the centre of the centre ring. The correspondence is given by the following formula:

$$\#centres = \#red\_vertices + 7$$

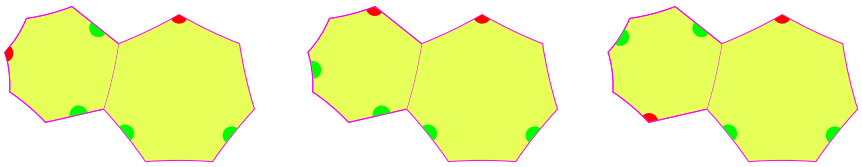

FIG. **9** The three ways of abutting petals along blank edges: in all cases, it is impossible.

This comes from the fact that a green side connects directly two centres, and that a red vertex is at distance 1 of three centres and for each of these three centres, both remaining centres belong to its centre ring. Accordingly, a red vertex generates 2 centres of the centre ring while a green side exactly generates one of them. Now,

$$\#red\_vertices + \#green\_sides = 7$$

and so,

$$\#centres = 2\#red\_vertices + \#green\_sides = \#red\_vertices + 7.$$

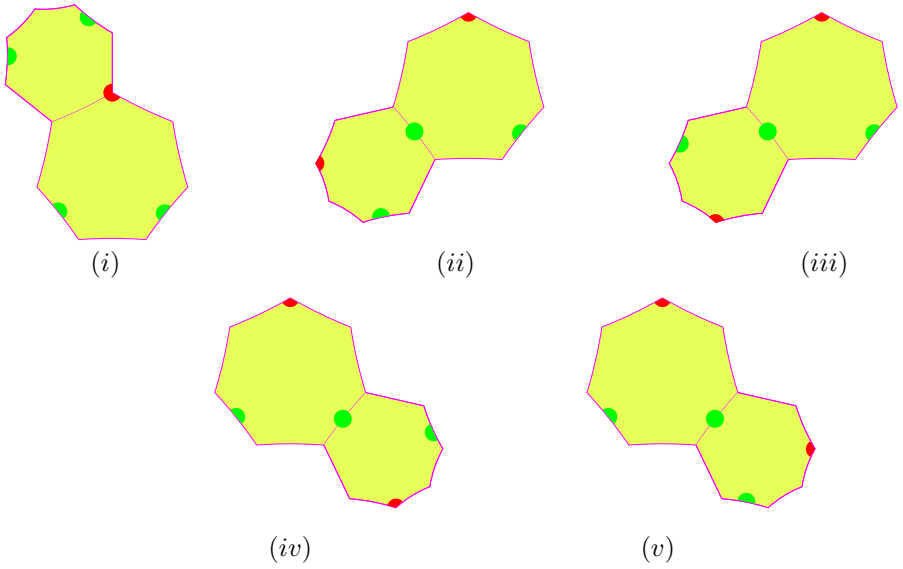

FIG. **10** The five ways to correctly abut two petals. Note that (iv) is obtained from (iii) by reflection in the vertical axis of the big heptagon. However, by rotating the small heptagon around the bigger one, (iii) is easily transformed into (v) which is also the reflection of (ii) in the same vertical axis. Then we obtain (iv) from (v) by rotating the smaller heptagon around its centre.

Next, it is not very difficult to see that there cannot be tilings where all centres have a centre ring of 7 elements or all centres have a centre ring of 10 elements. Indeed, if a centre is surrounded by seven green sides, then any element of its centre ring has at least two red vertices at distance 1 and so, the corresponding centre has a centre ring with at least 9 elements. The same remark applies also to a centre whose centre ring contains 8 elements. And so, there cannot be tilings of this kind where centres are all centres of a centre ring with 8 elements.

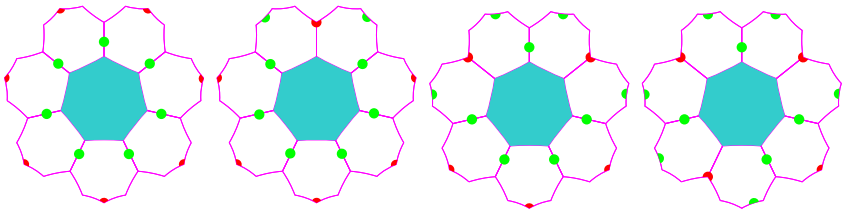

FIG. **11** Flowers with, respectively, 7, 8, 9 and 10 centres in their centre ring.

It remains to see that all centres cannot have a centre ring with 10 elements. Indeed, consider a centre with a centre ring of 10 elements. As a red vertex at distance 1 of a centre defines two green sides in contact with the centre, the 3 red vertices of such a flower are separated either by a single green side touching the centre of the flower, or by two such green sides. Now, consider two red vertices of a centre surrounded by 10 centres which are separated by a single green vertex. This green vertex connects the centre of the considered centre ring with another centre C. Now, from what we said, C has 3 consecutive green sides around itself and so, it cannot be the centre of a centre ring of 10 elements.

I don't know whether all centres can be surrounded by a centre ring of 9 elements. My conjecture is that this is the case, but I could not construct such a tiling algorithmically.

2.2 The mantilla

On the other side, we have the following:

LEMMA **2** *There is a tiling of* $\{7, 3\}$ *with the petals and centres such that all flowers of the tiling have a centre ring of* 9 *elements or of* 8 *elements. Moreover, it is possible to algorithmically construct such a tiling.*

In this proof, we distinguish between flowers with 9 elements in a centre ring as there are two different possible patterns, see Figure 12. Indeed, the two red vertices of the flower may be separated by one green edge or by two, considering the shortest number between them in the centre ring. We call **F-flowers** the flowers for which the two red-vertices are separated by only one green edge. We call **G-flowers** the others: their red vertices are separated by two green edges. We shall call **8-flowers** the flowers with 8 elements in their centre ring.
Proof of Lemma 2. The proof consists in showing that the new tiling can also be generated by the splitting method. This is performed by induction.

Below, Figures 13, 14 and 15 indicate how we split F-, G- and **8**-flowers. In the case of an F-flower, we call **parental petals** the petals of the flower which are between the two red vertices, considering the minimal possible number.

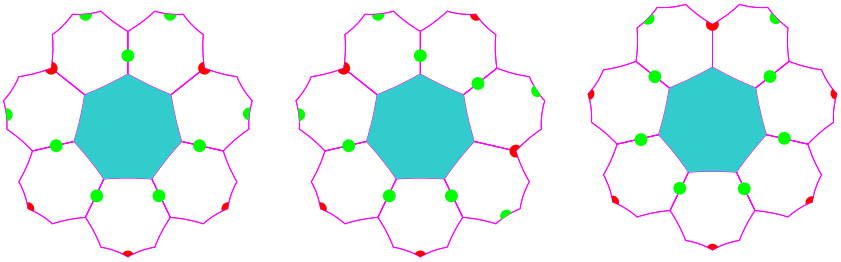

FIG. **12** The flowers of the mantilla : they consist of flowers with 8 or 9 elements in their centre ring. Note the representation of **F-** and **G-flowers** for the flowers with 9 centres.

In the case of a G-flower, the parental petals are also taken among the three petals which realize the shorter path between the main two red-vertices of the flower. The central petal of this triple is a parental petal, call it p. The red vertex of p defines two centres which are in contact with the triple. By induction on the splitting, we shall show that one of these two centres defines an **8**-flower. The other non-parental petal of the G-flower is the petal which belongs to this **8**-flower.

In the case of an **8**-flower, the parental petals are the two petals which are in contact with the single red vertex.

Important convention: from now on, if not otherwise indicated, we shall not mention green sides, only red vertices in order to make the figures more easily readable.

In the case of F- and G-flowers, the splitting is defined as follows: let β_ℓ be the line which supports an edge of the non-parental petal sharing the left-hand red vertex and which is not in contact with the centre. We define β_r to be the reflection of β_ℓ in the bisector of the segment which joins the two red-vertices of the flower. We call F- or G-**sector** the region delimited by β_ℓ, β_r and the lower border of the non-parental petals of the considered flower, see figures 13 and 14.

Note that we have two kinds of G-flowers: left-hand side and right-hand side flowers, depending on the side of the **8**-flower which is in contact with a parental flower. However, a G-sector is symmetric.

In the case of an **8**-flower, let u and v be the parental petals and let p and q be the non-parental neighbouring petal of, respectively, u and v. Denote by A the red vertex of p and by B the one of q. Note that B and q are the respective reflections of A and p in the line σ which passes through the red-vertex of the **8**-flower and through the mid-point O of its centre.

Define the line which starts from O and which passes through A. Then denote by β_ℓ the ray on this line which is issued from A and which does not cut the centre of the flower. Symmetrically, define β_r to be the reflection of β_ℓ in σ.

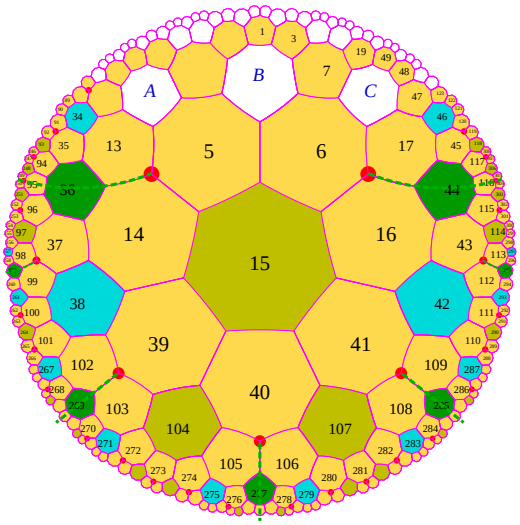

FIG. **13** Splitting the sector associated to an F-flower of the mantilla. The line β_ℓ crosses the tile 36 and the line β_r crosses the tile 44.

The **8-sector** is defined by β_ℓ and β_r and by the part of the lower border of the non-parental petals of the flower which falls inside inside the angular sector defined by β_ℓ and β_r.

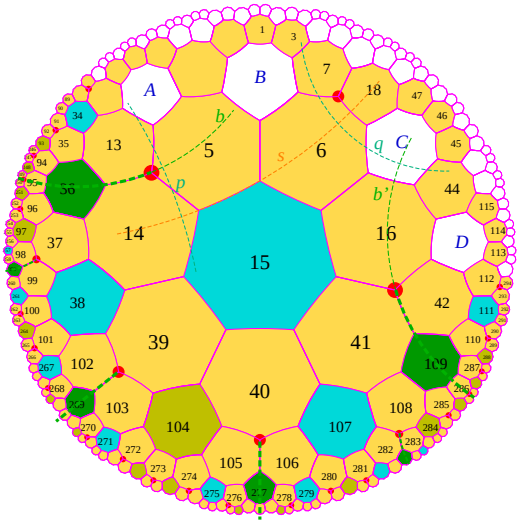

FIG. **14** Splitting the sector associated to a G-flower of the mantilla. Here, the line β_r crosses the tile 109.

We note that the parental petals also belong to another flower. They both belong to the same other flower in the case of an F-flower. They belong to different flowers in the cases of a G- or an **8**-flower.

Note that the distinction between parental and nonparental petals introduces the notions of **top** and **bottom** in a flower of the tiling. In sub-section 2.5, we shall come back to this point by the introduction of the notion of **levels** and of **isoclines** of the mantilla. In the above figures 13, 14 and 15, we say that the central tile is the **centre** of the sector.

It is not difficult to see how the splitting indicated in each case of figures 13, 14 and 15 can go on *downwards*, from the non-parental petals of the flower. The non-parental petals of the central flower of the pictures in figures 13, 14 and 15 induce the flowers which are the head of the sectors into which the above sectors can be split.

In the case of an **8-flower**, the splitting defines four sectors exactly. We consider that the G-flowers which appear outside the sector and around its head are defined by another flower: this property also belongs to the induction hypothesis. Also by induction, we will check the following property. Consider the three centres which are around a red vertex. Then, exactly one of them is the centre of an **8**-flower. The others are either both centres of F-flowers or one centre is from a G-flower, the other from an F-flower.

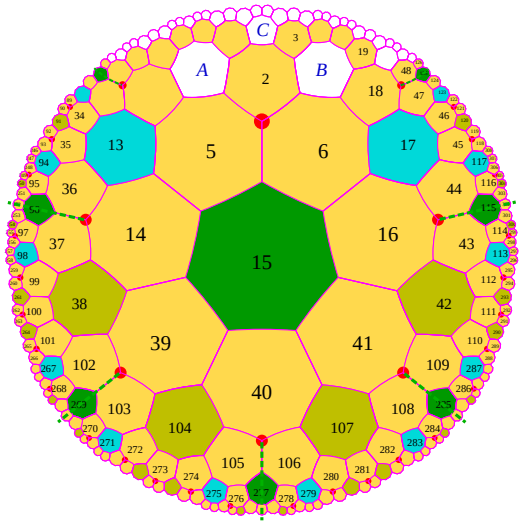

FIG. **15** Splitting the sector associated to an 8-flower of the mantilla.

In the case of F- and G-flowers, beyond the side of the G-sector which is not shared by an F-sector, we have the half of an **8**-sector: a right-hand half on the left-hand side and a left-hand half on the right-hand side.

Accordingly, as half- and right-hand sides are isometric, the splitting can be given by the following rules:

$$\begin{array}{lcl} F & \longrightarrow & 2F,\, 2G,\, 2\times\frac{1}{2}\mathbf{8} \\ G & \longrightarrow & F,\, 2G,\, 2\times\frac{1}{2}\mathbf{8} \\ \mathbf{8} & \longrightarrow & 4F \end{array}$$

For counting the elements of the spanning tree on the same level, we may replace 2 halves of an **8**-sector by a whole sector, and so, we get the following matrix:

$$\begin{array}{ccc} 2 & 2 & 1 \\ 1 & 2 & 1 \\ 4 & 0 & 0 \end{array}$$

accordingly, the characteristic polynomial P of the splitting is:

$$P(X) = X^2 - 4X - 2.$$

We note that it is a Pisot polynomial whose greatest real root is $2 + \sqrt{6}$.

At this point, we note that we have a tiling of any sector, neglecting the fact that the borders of a sector may involve half-tiles: we know that such halves will be completed by another sector which must necessarily be present.

Now, to tile the plane, we use the argument of [14]: consider a sector whose head is a flower **F**. The parental petals of **F** are non-parental petals of another flower **H**, **higher** than **F** in the tiling. It is clear that the sector Σ defined by **H** contains the sector defined by **F** as a sub-sector in the above tiling of Σ. Call **H** a **completing** sector of **F**.

It remains to prove that, whatever the choices are for the completing sector of the head of a given sector, we obtain a sequence of sectors whose union is the hyperbolic plane.

To prove this point, define the **augmented** sector of a given sector S to be the union of the sector and its heading flower, its parental petals being ruled out. Let B_n be the greatest ball around a once for all fixed origin O, contained in an augmented sector. Then, by completing the sector, we define a new sector of the splitting which, when augmented, contains S and B_{n+1} around O.

First, consider the case of an F-flower **F**. Figure 13 indicates three centres which share a petal with **F**. Call them A, B and C, from the left to the right in Figure 13.

Taking into account the already realised splittings, as the red-vertex shared by tiles 13, 5 and 14 is at distance 1 of the centre A and the **8**-centre situated at tile 36, A cannot be the centre of an **8**-flower. It may be the centre of a 9-flower, either F or G. The same conclusion holds for C. Now, the following chains of consequences hold as the reader can easily check it:

$$\begin{array}{lll} A = F & \Rightarrow B = 8 & \Rightarrow C = G \\ & & \Rightarrow C = F \\ & \Rightarrow B = F & \Rightarrow C = G \\ \\ A = G & \Rightarrow B = 8 & \Rightarrow C = F \\ & \Rightarrow B = F & \Rightarrow C = F \\ & \Rightarrow B = G & \Rightarrow C = G \end{array}$$

We could also start with B and the above chains also indicate the possible choices: we note that B may be any kind of centre. But once it is fixed, it also fixes the choices for A and B when B is the centre of a G-flower, and we have two solutions in both cases when B is the centre of either an **8**-flower or an F-flower.

In all these situation, as tiles 5 and 6 in Figure 13 belong to the sector headed by B, the ball obtained from B_n by appending a new level of tiles is also in the sector. And this new ball is exactly B_{n+1}. And so, our claim is proved in this case.

Next, consider the case of a G-flower which is illustrated by Figure 14.

In this case, we have to discuss the situation of four centres denoted by respectively A, B, C and D in the figure.

It is not difficult to note that A and D are occupied by the centre of an F-flower. Indeed, A cannot be the centre of an **8**-flower, because there is already such a centre at distance 1 from the red vertex shared by tiles 13, 5 and 14 in Figure 14. Also, A cannot be the centre of a G-flower as there cannot be two adjacent G-sectors in the splitting of any sector. And so, A must be the centre of an F-flower. By symmetry of the figure, this is also the case for D.

Now, the possible cases for B and C are indicated by the following diagram:

$$\begin{aligned} B = 8 \quad &\Rightarrow C = F \\ &\quad\ \ C = G \\ B = F \quad &\Rightarrow C = 8 \\ B = G \quad &\Rightarrow C = 8 \end{aligned}$$

It is not difficult to check that, in all these cases, tiles 36, 13, 5, 6, 16, 42 and 109 do belong to the new appended augmented sector, either in B or in C and so, accordingly, the new augmented sector contains B_{n+1}.

At last, we remain with the case of an **8**-sector which is illustrated by Figure 15.

Here, we have the union of the four F-sectors defined by its splitting. The augmented sectors contains tiles 14, 15 and 16, as it can easily be checked.

As the red vertex shared by 5 and 6 is at distance 1 from the centre of the considered **8**-flower, A and B cannot be the centre of an **8**-flower as they are at distance 1 from this red vertex.

This leaves four cases a priori. But A and B cannot be both centres of a G-flowers, as two G-sectors cannot be adjacent. And so we remain with three cases: A and B are both centres of an F-flower, or A is the centre of a G-flower and B, that of an F-flower, or, conversely, B is the centre of a G-flower and A, that of an F-flower.

In all cases, tiles 5 and 6 also belong to the union of the new augmented sectors and so, whatever the tile appended in C, it is the centre of a flower and the considered tiles together with 36, 13, 17 and 44 are in the sector defined

by C.

And so, the following property is proved:

LEMMA **3** *Completing a sector S by any of the possible centres which will give rise to a new sector Σ in which S enters its splitting, in at most two steps of such a completion, if S contains the ball B_n around a fixed in advance tile T, Σ contains the ball B_{n+1} around T.*

With this property, the proof of Lemma 2 is completed.

2.3 The set of tiles

Now, we show that the tiling which we have described in general terms in the previous section can effectively be generated from a small finite set of tiles: we simply need 21 of them.

We have to implement the construction of F-, G- and **8**-flowers and the rules of generations of the carpet structure of the mantilla, see [24, 14] for the notion of carpet.

To this aim, remember that in the flowers we have two categories of tiles: the petals and the centres. Also remember that we started with two kind of tiles: tiles with a red vertex and two green sides and tiles with no marks. In sub-section 2.1, we postponed the solution to force the centres to be surrounded by petals. It is now time to indicate how to proceed.

A solution consists in labelling the edges of such a tile by numbers from 1 up to 7. It is very easy to check that with such a labelling, the domino tiles associated to the tile a of sub-section 2.1, see figure 8, cannot alone tile the plane as the labels cannot match. This property is not specific to tiling $\{7, 3\}$, indeed it is shared by any regular tiling $\{p, 2q+1\}$[1]. Due to the matching condition on edges, the tiles which support the petals should be dotted with similar labels. But the labels are needed only on the edges of petals which are shared by a centre. A priori, this would give 7^3 different tiles for the initial set of tiles which, after Berger, we call the **prototiles**. As we shall soon see, we need only 21 prototiles to construct the mantilla: 17 petals and 4 centres.

To see this, let us fix where we put number 1 in a tile which is a centre. For F-flowers, it seems natural to put 1 and 7 at symmetric places with respect to the vertical axis of reflection of the flower. It is also easy to fix 1 and 7 for an **8**-flower: the red vertex is exactly on the vertical axis of reflection of the flower. We have a different situation with G-flowers. We already noted that there are left- and right-hand side flowers. Here, we shall stress on this difference by giving to G-flowers a different numbering: instead of clockwise increasing around the edges of the tile, the numbers will increase while **counter-clockwise** going around the edges of the tile. Also, in order to distinguish between petals, we introduce two sets of numbers: we shall consider **marked** and **unmarked** numbers. Unmarked numbers in $\{1..7\}$ are those which we

[1] The property does not hold for $\{p, q\}$ when q is even.

ordinarily use. Marked numbers are in $\{\overline{1}..\overline{7}\}$. The difference appears below, on table 1 and figure 16.

TABLE **1** Table of the distribution of colours on the sides of the central tiles. The labels are given for sides numbered from 1 up to 7 clockwise running around the tile. For centres of G-flowers, we indicate the reverse ordering on the labels. The labels 1 and 7 are not indicated: they are the same for F- and **8**-flowers, and they are exchanged for G-flowers.

	2	3	4	5	6
F	2	$\overline{3}$	$\overline{4}$	$\overline{5}$	6
G_ℓ	$\overline{6}$	$\overline{5}$	4	3	2
G_r	6	5	4	$\overline{3}$	$\overline{2}$
8	$\overline{2}$	3	$\overline{4}$	5	$\overline{6}$

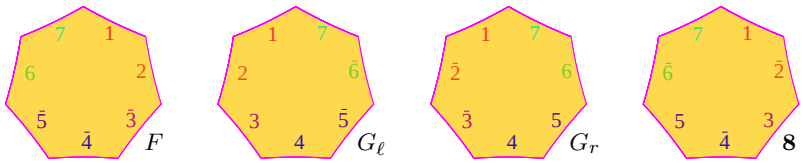

FIG. **16** The prototiles for the centres: F-, **8**-, G_ℓ- and G_r-centres.

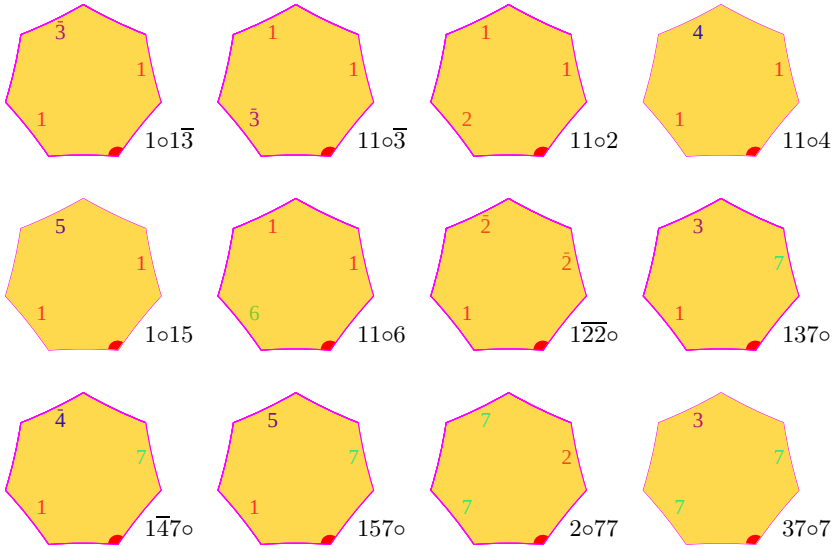

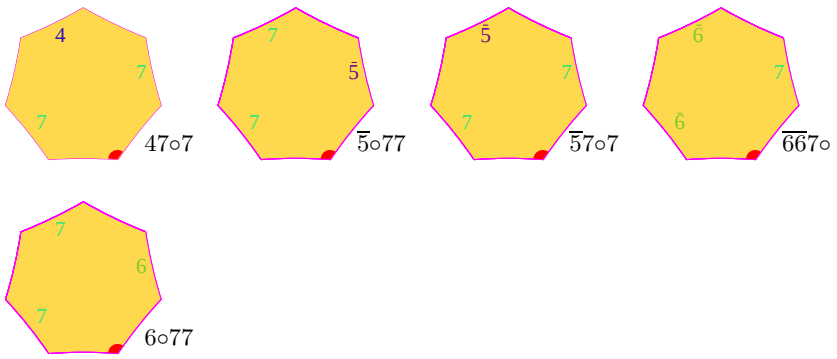

FIG. **17** The prototiles for the non-parental petals.

We remark that the new numbers do not change the fact that central tiles alone, even by mixing the labels, cannot tile the plane by themselves.

From this, we deduce 17 prototiles from the petals, looking at the different configurations of petals attached to edges numbered from 2 up to 6 of all possible centres. In this respect, we define such tiles as the **non-parental** tiles which will be the meaning of this expression until the end of the paper.

Above, Figure 17 displays the complete set of 21 tiles of the mantilla.

The non-parental petals can be grouped according to the flowers in which they occur. This is given in table 2, below. In this table, the position of the red-vertex in the petal is indicated by the occurrence of symbol ∘. The labels are indicated by putting in first position the lowest label according to the alphabetic order and then by by following the occurrence of the other labels and of the red vertex while running around the tile clockwise.

TABLE **2** Table of the non-parental petals according to their parent flower.

	2	$\overline{2}$	3	$\overline{3}$	4	$\overline{4}$	5	$\overline{5}$	6	$\overline{6}$
F	2∘77			1∘1$\overline{3}$		1$\overline{4}$7∘		$\overline{5}$7∘7	11∘6	
G_ℓ	11∘2		37∘7		1∘14			$\overline{5}$∘77		$\overline{66}$7∘
G_r		1$\overline{22}$∘		11∘$\overline{3}$	47∘7		1∘15		6∘77	
8		1$\overline{22}$∘	137∘			1$\overline{4}$7∘	157∘			$\overline{66}$7∘

Table 2 results from a careful checking. It is not difficult to check, in each case, that the configuration of each petal is unique, even when the same tile may appear in different contexts.

In this line, we note that the following petals appear only in a fixed centre:

2∘77, 1∘1$\overline{3}$, $\overline{5}$7∘7 and 11∘6 for F-flowers;

11∘2, 37∘7, 1∘14 and $\overline{5}$∘77 for G_ℓ flowers;
11∘$\overline{3}$, 47∘7, 1∘15 and ∘77 for G_r-flowers;
137∘ and 157∘ for **8**-flowers.

For the other petals:

1$\overline{4}$7∘ is common to F- and **8**-flowers;
$\overline{66}$7∘ is common to G_ℓ- and to **8**-flowers;
1$\overline{22}$∘ is common to G_r and **8**-flowers.

Now, we have to establish a converse of the table. Starting from a tile, we necessarily obtain what can be deduced from the table and nothing else.

To this aim, we first prove :

LEMMA **4** *The set of tiles defined by table* 2 *together with the four tiles for the centers entail the mantilla. Namely, starting from a tile, we precisely have the contacts which can be deduced from the table.*

In order to prove the lemma, we first note that a corollary of Lemma 1 is the following result:

COROLLARY **1** *A petal can abut at a numbered edge only with a centre, at the edge which bears the same number. If the number on the edge of the petal is marked, the same number on the edge of the centre must also be marked.*

The proof of lemma 4 is long and tedious. It is written in full extent in [17]. It consists in a careful examination of all the possible case and in showing, in particular, that no other possibility than those dictated by the tables are possible. However, the examination of [17] is a bit simplified by the two following elementary remarks: considering the petals which have been to be put around a centre, they abut with different numbers and, also, adjacent petals abut with consecutive numbers, considering here that 1 and 7 are consecutive. The checking is rather easy for an F-flower, but it is more intricate for a G-flower and also for an **8**-flower.

Now, tables 1 and 2 allow to construct the tiling **downwards**. Note that figure 18, below, illustrates the just indicated tables and it is a convenient way to represent them.

In order to construct it also **upwards**, we need another information, which we also present in the form of tables. These new tables can be seen as a reversal reading of tables 1 and 2. We again repeat that the goal of the lemma is not to establish the tables, which is rather easy, but to prove that with the set of prototiles defined by figures 16 and 17, we cannot obtain a combination which is not indicated by the tables. The tables indicate what is possible and only that.

In order to determine the reverse tables, see tables 3, 4 and 5, below, it is not difficult to see that the first thing we have to do is to determine what the parental tiles are.

Our first remark is that we should check that parental tiles do not bring in new types of tile. Indeed, a parental tile in a given flower is also a non-parental tile in another one. Accordingly, we should have already all possible types of tiles.

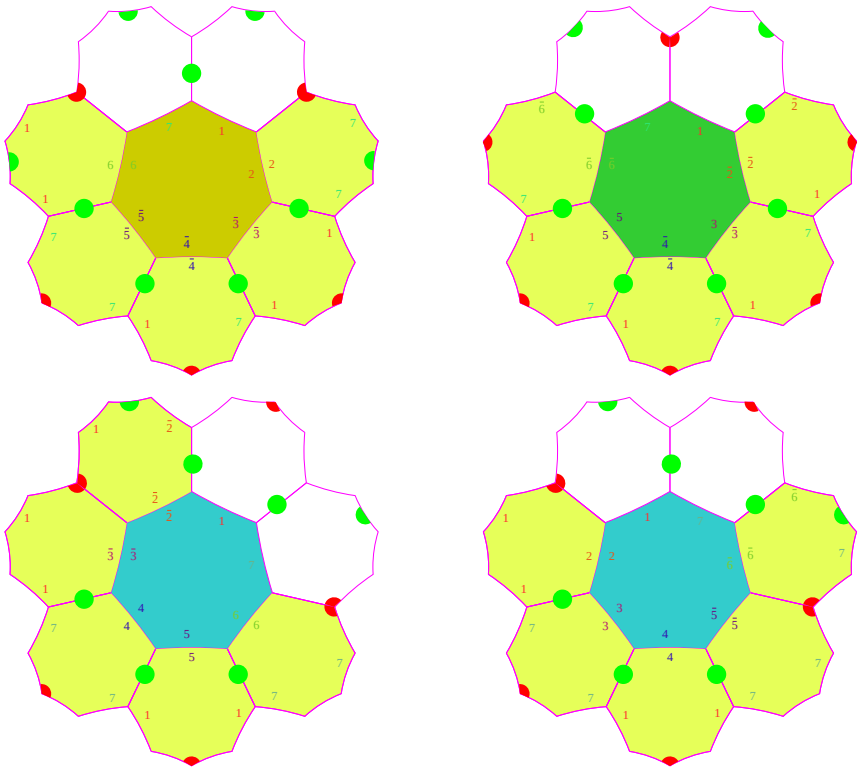

FIG. **18** All the non-parental tiles induced by the centres: above, left-hand side, an F-centre; right-hand side, an **8**-flower. Below, left-hand side, a G_r-centre; right-hand side, a G_ℓ-centre.

In cite [17], a careful checking shows that this is the case and that the property is obtained from the tiles themselves.

The tables are established for each type of flower.
First, table 3 indicates all the possible pairs of parental tiles of an F-flower.

TABLE **3** The possible values of the parental tiles of an F-flower.

	F_ℓ	F_r	G_ℓ	G_r	$\mathbf{8}_1$	$\mathbf{8}_2$	$\mathbf{8}_3$	$\mathbf{8}_4$
1	$1\overline{4}7\circ$	$1\circ1\overline{3}$	$1\circ14$	$1\circ15$	$1\overline{22}\circ$	$137\circ$	$1\overline{4}7\circ$	$157\circ$
7	$\overline{5}7\circ7$	$1\overline{4}7\circ$	$37\circ7$	$47\circ7$	$137\circ$	$1\overline{4}7\circ$	$157\circ$	$\overline{66}7\circ$

We note that the table gives additional information about the position of the flower induced by the indicated parental petals. In what we computed, we see that there is a single case for G_ℓ- and G_r-flowers. This corresponds to the fact that in a G-flower, there is a single F-son. For an F-flower, we have two cases: this is due to the fact that an F-son has two F-sons. One is on the left-hand side, it is determined by petals $\overline{5}7\circ 7$ and $1\overline{4}7\circ$ as we can see in figure 18. This is why table 3 indicates F_ℓ. The other F-son of an F-flower is determined by petals $1\overline{4}7\circ$ at edge 7 and $1\circ 1\overline{5}$ at edge 1 as we can see in figure 18. From this we understand the indication F_r of the table. Now, it is easy to understand the indications $\mathbf{8}_i$, $i \in \{1..4\}$ of the table. An **8**-flower has four F-sons and, numbering them from 1 up to 4, going clockwise around the centre as we can see from Figure 18 we obtain: the first F-son is determined by petals $1\overline{22}\circ$ at edge 1 and $137\circ$ at edge 7, the second by $137\circ$ at edge 1 and $1\overline{4}7\circ$ at edge 7, the third by $1\overline{4}7\circ$ at edge 1 and $157\circ$ at edge 7 and the last one by $157\circ$ at edge 1 and $\overline{66}7\circ$ at edge 7. These are exactly the indications of table 3.

We argue in a similar way for G-flowers, taking into account their laterality: we have G_ℓ- and G_r-flowers.

The corresponding information is given in table 4, for both cases of G_ℓ and G_r-flowers.

TABLE **4** The possible values of the parental tiles of a G-flower. On the left-hand side, the case of a G_ℓ-flower. On the right-hand side, the case of a G_r-flower.

	F	G_ℓ	G_r		F	G_ℓ	G_r
1	$1\circ 1\overline{3}$	$1\circ 14$	$1\circ 15$	1	$11\circ 6$	$11\circ 2$	$11\circ\overline{3}$
7	$2\circ 77$	$\overline{5}\circ 77$	$6\circ 77$	7	$\overline{5}7\circ 7$	$37\circ 7$	$47\circ 7$

Note a property which we have already noticed with the definition of a sector and that we find again from considerations on the tiles only: the parent of a G-flower is either an F-flower or a G-flower. It is never an **8**-flower.

Now, let us turn to the case of an **8**-flower.

To better understant table 5, we refer the reader to figure 15, where the tiles marked A, B and C play an important rôle. In the second an third sub-tables, we have three rows. The first row corresponds to what we could call the two parents of the **8**-flower, A and B in figure 15. The second row corresponds to what is called the **third tile** in [17]: it is the tile 2 of figure 15, which is a petal. The third row corresponds to the third centre, the tile C of figure 15.

Note that table 5 shows that the two centres defined by the petals at edge 7 and at edge 1 cannot be both G-centres, a situation which was already ruled out by the definition of the splitting and which can be derived from the definition of the tiles only.

Accordingly, the proof of Lemma 4 is completed. ■

TABLE **5** Above: the possible values of the parental tiles of an **8**-flower. Below, in two tables, the third petal and the third centre.

	F-*F*	*F*-G_ℓ	*F*-G_r	G_ℓ-*F*	G_r-*F*
1	11∘6	11∘2	11∘$\overline{3}$	11∘6	11∘6
7	2∘77	2∘77	2∘77	$\overline{5}$∘77	6∘77

	F-*F*			*F*-G_r	G_ℓ-*F*
3rd	1$\overline{4}$7∘	1$\overline{4}$7∘	137∘	157∘	1$\overline{22}$∘	$\overline{66}$7∘
	F	**8**	**8**	**8**	**8**	**8**

	F-G_ℓ			G_r-*F*		
3rd	1$\overline{3}$1∘	141∘	151∘	7$\overline{5}$7∘	737∘	747∘
	F	G_ℓ	G_r	*F*	G_ℓ	G_r

2.4 The trees of the mantilla

First, we define what we shall from now on call a tree.

DEFINITION **1** *Say that a set of tiles of the tiling* $\{7,3\}$ *is within a* **tree** *if the centres of the tiles belong to the angular sector defined by two mid-point lines* β_1 *and* β_2 *issued from the mid-point* A *of an edge* η *of the tiling whose angle is* α*, the angle which defines the angular sectors of the tiling* $\{7,3\}$*. We also assume that the line supporting* η *is the bisector of the angle made by* β_1 *and* β_2 *at* A*. The set of tiles is called the* **area** *delimited by the tree or, simply, the* **area of the tree**.

Next, we define where the trees are placed. To this aim, we use a very simple criterion:

DEFINITION **2** *In the mantilla, we call* **tree of the mantilla**, *the area of a tree whose root is the centre of an* F*-flower which is the* F*-son of a* G*-flower. The rrot of a tree of the mantilla is called a* **seed**.

We shall prove two basic properties of the trees of the mantilla: they are completely contained in the sector defined by the F-flower whose centre is their root. We also prove that two such trees have either distinct areas or the area of one contains the other area.

LEMMA **5** *In the mantilla, a tree of the mantilla is completely contained in the sector defined by its root.*

Proof. Consider Figure 19. Using the numbering of the tiles, note that a tree is rooted in tile 104 and that the mid-point lines which define it start on the mid-point of the edge shared by the tiles 39 and 40. Denote by β_ℓ and β_r the respective left- and right-hand side mid-point lines which we just considered. The tile 104 is the centre of an F-flower whose sector is delimited by the lines which support the common edge of the tiles 102 and 103 on the left-hand side and the common edge of the tiles 105 and 106 on the right-hand side. Denote these lines by δ_ℓ and δ_r respectively.

Now, it is not difficult to see that the line γ_ℓ which is shared by the tiles 39 and 15 in Figure 19 is perpendicular to both β_ℓ and δ_ℓ. And so, as these lines are non-secant, two of the half-planes which they define are disjoint. They are precisely the half planes containing the tree, delimited by β_ℓ, and the half-plain delimited by δ_ℓ which does not contain the sector.

A similar result holds for γ_r, the line which supports the common edge between the tile 40 and the tile 15: $\gamma_r \perp \beta_r$ and $\gamma_r \perp \delta_r$. With a similar remark about the half-planes defined by β_ℓ, β_r, δ_ℓ and δ_r, we conclude that the tree is strictly contained in the sector. ■

Indeed, we can say more: between the leftmost branch of the tree and the left-hand side border of the sector, new trees appear. This can be seen in figure 19. The configuration of the tile 104 is exactly that of the tile 2. Note that the tile 17 plays for the tile 2 the rôle which is played by the tile 277 for the tile 104. There is a shift transforming the configuration of the tile 2 into that of the tile 104. The same shift applied to the tile 104 provides us with a new tree between the rightmost branch of the tree rooted at the tile 104 and the right-hand side border of the region defined by the F-flower whose centre is the tile 104.

Now, let us start from the parental petals of an F-flower which is the F-son of a G-flower. There are two possible couples of such petals: 37∘7 and 1∘14 in the case of a G_ℓ-flower, 47∘7 and 1∘15 in the case of a G_r-flower.

Consider the right-hand side border.

We successively meet the following tiles, starting from the first one, say $1\circ 1\alpha$ with $\alpha \in \{4, 5\}$:

TABLE **6** The ultimately periodic path followed by the mid-point line of the rightmost branch of a tree of the mantilla. The table indicates the patterns of the tiles crossed by the mid-point lines. For each tile, it also indicates the sides of the tile which are crossed. The ⋄ sign indicates a green side.

rank	1	2	3	4	5	6	7	8	9	10	11
tile	7	2	6	5	15	14	39	38	102	101	267
pattern	$1\circ 1\alpha$	F	$2\circ 77$	$1\circ 1\overline{3}$	G_ℓ	$11\circ 2$	$37\circ 7$	G_r	$6\circ 77$	$1\circ 15$	G_ℓ
sides	⋄–1	1–2	2–⋄	⋄–1	1–2	2–⋄	⋄–7	7–6	6–⋄	⋄–1	1–2

We note that the sequence of tiles crossed by the mid-point lines is ultimately periodic. The period involves six tiles and the aperiodic part at the beginning of the sequence involves four tiles. Note that the table also indicates the sides which are crossed by the mid-point line for each tile involved by the border. In the table, a green side is represented by $\diamond$.

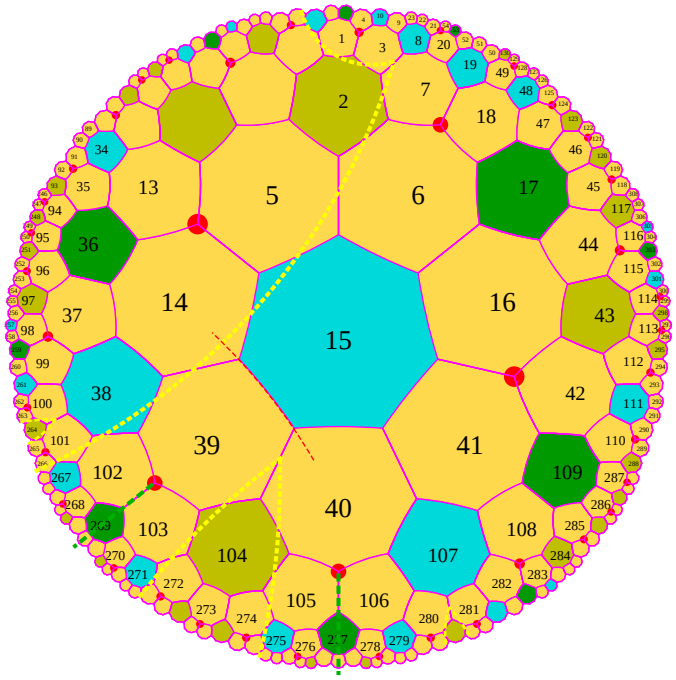

FIG. **19** The tree generated by an F-flower which is the son of a G-flower.

A similar table can be established for the left-hand side border where the first tile is $\beta 7 \circ 7$ with $\beta \in \{3, 4\}$:

TABLE **7** The ultimately periodic path followed by the mid-point line of the leftmost branch of a computing tree. Same conventions as in table 6.

rank	1	2	3	4	5	6	7	8	9	10	11
pattern	$\beta 7 \circ 7$	F	$11 \circ 6$	$\overline{5}7 \circ 7$	G_r	$6 \circ 77$	$1 \circ 15$	G_ℓ	$11 \circ 2$	$37 \circ 7$	G_r
sides	$\diamond$–7	7–6	6–$\diamond$	$\diamond$–7	7–6	6–$\diamond$	$\diamond$–1	1–2	2–$\diamond$	$\diamond$–7	7–6

Taking into account that the construction of the tiling is deterministic when we go from a centre to its non-parental petals, the sequences defined by tables 6 and 7 for the ranks, the patterns and the sides are the same for all trees.

Accordingly, we proved the following result:

LEMMA **6** *The sequence of the tiles crossed by the border of the tree is ultimately periodic. The length of the period is the same for the right-hand- and for the left-hand side borders.*

Let us look again at the tiles involved in the border.

The initial tiles $1\circ 1\alpha$ and $\beta 7\circ 7$ may occur in the period. This is the case for $\alpha = 5$ and $\beta = 3$ only. Consider a tile $1\circ 15$. When it is the first tile of a tree, the border is the right-hand side one and it crosses sides $\diamond - 1$. We note that the concerned sides are on the left-hand side of edge 5 when the red-vertex is below this edge. When it appears in the periodic part of the border, the same tile is also crossed at sides $\diamond - 1$. As we can see on Figure 19, the crossed side are on the other side of edge 5, with the red-vertex again in a below position, see the tile 101 in Figure 19. This means that another border may use this tile as indicated. A similar remark holds for the tile $37\circ 7$. It is crossed along sides $\diamond - 7$. But the crossed sides are on the right-hand side of edge 3 when the red-vertex of the tile is below this edge. When the tile $37\circ 7$ again appears in the period of a border, it is also crossed at edges $\diamond - 7$, but on the right-hand side of the tile when the red-vertex is below edge 3, as can be noted in Figure 19 with the tile 39. This means that this tile may also be crossed by another border at the same time. In Figure 19, this is the case for the tile 39.

Another tile can be crossed by two borders at the same time. It is, of course, the F-tile which is at the root of the tree. The involved edges are $1-2$ on one side and $7-6$ on the other.

Let us look at the other tiles. Using tables 6 and 7 and Figure 19, we have the following properties:

- tiles crossed by a right-hand side border only: $1\circ 14$, at edges $\diamond - 1$ only; $2\circ 77$, at edges $2 - \diamond$ only; $1\circ 1\overline{3}$, at edges $\diamond - 1$ only;
- tiles crossed by a left-hand side border only: $47\circ 7$, at edges $\diamond - 7$ only; $11\circ 6$, at edges $6 - \diamond$ only; $\overline{5}7\circ 7$, at edges $\diamond - 7$ only;
- tiles crossed by one border only, when the left-hand side border, when the right-hand side one: G_ℓ, at edges $1-2$ only; $11\circ 2$, at edges $2 - \diamond$ only; G_r, at edges $7-6$ only, $6\circ 77$ at edges $6 - \diamond$ only;
- tiles possibly crossed by two borders: F, always at both edges $1-2$ and $7-6$; $1\circ 15$ at edges $\diamond - 1$, when both, when one of them; $37\circ 7$ at edges $\diamond - 7$, when both, when one of them.

Next, we have the following property of the mid-point lines which we consider:

LEMMA **7** *Consider two mid-point lines ℓ_1 and ℓ_2 of tiling $\{7, 3\}$. Recall that we consider lines joining the mid-points of two consecutive edges of tiles of the tiling. Then if ℓ_1 and ℓ_2 do intersect, they meet at the mid-point of an edge of a tile.*

Proof. Indeed, assume that ℓ_1 and ℓ_2 meet at a point A. On a mid-point line of the tiling, any point is between two mid-points of two consecutive edges of a tile,

as can easily be seen in Figure 19. Let A_1 and B_1 be the such points for ℓ_1 with respect to A and A_2 and B_2 for ℓ_2 with respect to A too. By construction of a mid-point line of the tiling, if A is inside a tile τ, A_1 and B_1 must be vertices of τ. It is clear that A_2 and B_2 must be the same vertices as this happens also on the same tile. And so, this is impossible if $\ell_1 \neq \ell_2$. Accordingly, A belongs to the border of a tile and, by construction of a mid-point line, it is the mid-point of an edge of a tile. ■

Now, if we look at what we observed on the tiles involved in borders, the single possible meeting of two borders is the mid-point of the common edge shared by the tiles 37∘7 and 1 ∘4, or the tiles 47∘7 and 1∘15.

Consequently:

LEMMA **8** *The border of a tree of the mantilla does not meet the border of another tree of the mantilla.*

Proof. There is no tile which would allow to realize the meeting as the only ones which can contain the intersection of two mid-point lines are the parental petals of the root of the tree. ■

What we proved on the border of a tree and of a sector also proves Lemma 8. Figure 19 indicates that along a border, new trees appear, both outside and inside the area of the tree. They are generated by the G_ℓ's and G_r's tiles which periodically occur among the tiles crossed by the border. The tiles 39 and 101 are crossed by two borders and they illustrate both situations. At the same level, other F-sons of a G-centre are further and, indeed, they belong to different sectors. They belong either to a sector which is outside the sector defined by the root of the initially considered tree, or they belong to a sector which is inside the area of the tree. In the first case, as sectors define a partition starting from a given level, the property of the lemma follows. In the second case, it is not difficult to see that the border of a sector involves **8**-centres which occur periodically along the border as we go down along it. As **8**-centres have only F-sons, these F-centres do not generate trees. This is why, trees are rather 'far' from such a border. And so, using the levels we introduced in the mantilla, we can see that the trees which are generated at the same level always occur in sectors which have no border in common. Look at figures 13 and 14. Also, figure 19 contains two examples of the situation when borders of different trees are closest at possible. The tiles 39 and 101 are crossed by two borders. The tile 39 is crossed by the right-hand side border of the tree rooted at 2 and it is also crossed by the created left-hand side border of the tree rooted at the tile 104. For the tile 101, it is crossed by the right-hand side border of the tree rooted at 2 and also by the just now created right-hand side border of the tree rooted at the tile 264 as the latter tree is inside the former. Note that this is the single possibility for a tree to be so closed to another one. 'Old' trees are indeed very far from each other.

Now we get an important corollary of Lemma 8:

LEMMA **9** *In the mantilla, two trees of the mantilla have either disjoint areas or one area contains the other.*

Proof. Assume that we have two trees A_1 and A_2 such that their areas intersect and that none of them contains the other. Let τ_i be the root of A_i, $i \in \{1, 2\}$. Let τ be a tile of the intersection. In the tree A_1, there is a path from τ to τ_1 which consists of tiles of A_1. As $\tau_1 \notin A_2$, there is a last tile of A_1 on the path, say σ_1, which meets the border of A_2. As σ_1 is on the border of A_2, there is a last tile of A_2, among those which are on the border from σ_1 to τ_2, say σ_2 which meets the border of A_1. And so, σ_2 contains both the border of A_2 and the border of A_1. Considering the triangle defined by τ_1, τ_2 and σ_1, the border of A_2 must meet the border of A_1, a contradiction with Lemma 8. ■

Now, we define the following notion:

DEFINITION **3** *A* **thread** *is a set $\mathcal{F}$ of trees of the mantilla such that:*

(i) if $A_1, A_2 \in \mathcal{F}$, then either $A_1 \subset A_2$ or $A_2 \subset A_1$;
(ii) if $A \in \mathcal{F}$, then there is $B \in \mathcal{F}$ with $B \subset A$, the inclusion being proper;
(iii) if $A_1, A_2 \in \mathcal{F}$ with $A_1 \subset A_2$ and if A is a tree of the mantilla with $A_1 \subset A$ and $A \subset A_2$, then $A \in \mathcal{F}$.

DEFINITION **4** *A thread $\mathcal{F}$ of the mantilla is called an* **ultra-thread** *if it possesses the following additional property:*

(iv) there is no $A \in \mathcal{F}$ such that for all $B \in \mathcal{F}$, $B \subset A$.

LEMMA **10** *A set $\mathcal{F}$ of trees of the mantilla is an ultra-tread if and only if it possesses properties (i) and (ii) of definition 3 together with the following:*

(v) for all $A \in \mathcal{F}$ and for all tree B of the mantilla, if $A \subset B$, then $B \in \mathcal{F}$.

Proof. Indeed, an ultra-thread satisfies (v). Otherwise, let $A \in \mathcal{F}$ and B be a tree of the mantilla such that $A \subset B$ and $B \notin \mathcal{F}$. From (iii) we get that for any tree C of the mantilla such that $B \subset C$, then $C \notin \mathcal{F}$. From Lemma 9, if $A \subset B$, A is a sub-tree of B and so, considering the path leading from the root of A to the root of B, there are at most finitely many trees D of the mantilla such that $A \subset D \subset B$. Note that if two trees D_1 and D_2 of the mantilla contain A, we have $D_1 \subset D_2$ or $D_2 \subset D_1$ by Lemma 9. And so, considering the biggest tree D between A and B with $D \in \mathcal{F}$, we obtain an element D in $\mathcal{F}$ such that for all $A \in \mathcal{F}$, $A \subset D$. This contradicts (iv). And so, if B is a tree of the mantilla which contains A, it belongs to $\mathcal{F}$.

Conversely, if a set $\mathcal{F}$ of trees of the mantilla satisfy (i), (ii) and (v), it obviously satisfies (iii) and (iv). ■

Accordingly, an ultra-thread is a maximal thread with respect to the inclusion.

Note that the mantilla may possess ultra-threads and it may possess none of them. Indeed, consider the algorithm of sub-section 4 and apply the following strategy:

- at time t_{2n}, in step 3, for the choice of C_{n+1}, we take an F-centre;
- at time t_{2n+1}, in step 3, for the choice of C_{n+1}, we take a G-centre, choosing at random between a G_ℓ- and a G_r-centre.

Then it is clear that the sequence constructed by C_n defines an ultrathread.

Consider now another execution of the algorithm of sub-section 4, where the strategy is now:

- at time t_n, in step 3, take for C_{n+1} an **8**-centre.

Then as the sectors defined by C_n are increasing sectors, all the threads existing at time t_n have a maximal tree at some level with respect to C_n. As the sequence of flowers above C_n do not contain the root of a tree, we have that the maximal trees we define at time t_n are not included in a tree, by induction on the construction of sequence $\{C_n\}$. The tree which appears at higher levels generates trees which are all outside the sector defined at time t_n.

Here are additional properties of the ultra-threads.

LEMMA **11** *Let $\mathcal{U}$ be an ultra-thread. Then, $\mathcal{U} = \{A_n\}_{n\in\mathbb{Z}}$, where $A_n \in \mathcal{U}$ for all $n \in \mathbb{Z}$ and $A_n \subset A_{n+1}$, the inclusion being proper. We also have that $\bigcup_{n\in\mathbb{Z}} A_n = \mathbb{H}^2$.*

Proof. By properties (ii) and (v) of the ultra-threads, there is a sequence $\{C_n\}_{n\in\mathbb{Z}}$ such that $C_n \subset C_{n+1}$ for all n in $\mathbb{Z}$, the inclusion being proper. As C_n is a sub-tree of C_{n+1}, there is a path which goes from the root of C_n to that of C_{n+1}. Along these paths, there are finitely many trees of the mantilla. By (v), these trees also belong to $\mathcal{F}$. Accordingly, we obtain $\{A_n\}$ by appending these trees to $\{C_n\}$.

From our study of trees issued from a G-centre crossed by the border of a given tree of the mantilla, we know that we have the following property. If A and B are two trees of the mantilla with $A \subset B$, the inclusion being proper, consider the set of tiles A' which is obtained by appending a layer of one tile along the borders of A and outside A. Then, we have that $A' \subseteq B$.

Now, fix a tile τ_0 in A_0. From what we just noted, we obtain that $B_1 \subset A_1$ and, by induction, that $B_n \subset A_n$ where B_h is the ball of radius h around τ_0. Accordingly, $\bigcup_{n\in\mathbb{Z}} A_n = \mathbb{H}^2$. ■

LEMMA **12** *Let $\mathcal{U} = \{A_n\}_{n\in\mathbb{Z}}$ and $\mathcal{V} = \{C_m\}_{m\in\mathbb{Z}}$ be two ultra-threads. Then, there are two integers n_0 and m_0 such that $A_n = C_m$ for all n and m such that $n - n_0 = m - m_0$.*

Proof. Indeed, consider A_0. Then, as $\bigcup_{n\in\mathbb{Z}} C_n = \mathbb{H}^2$, there is m_0 such that C_{m_0} contains the root of A_0. Now, by Lemma 9, necessarily, $A_0 \subset C_{m_0}$ and so, $C_{m_0} \in \mathcal{U}$ by property (v) of the ultra-threads. This means that there is n_0 such that $A_{n_0} = C_{m_0}$. Now, by construction of $\{A_n\}$ and $\{C_m\}$, there is no tree of the mantilla between A_n and A_{n+1} and, similarly, between C_m and C_{m+1}. Accordingly, $A_{n_0+1} = C_{m_0+1}$. By induction, we get $A_{n_0+k} = C_{m_0+k}$ for all $k \in \mathbb{N}$. ■

2.5 Isoclines

In [18], we have a new ingredient. We define the status of a tile as **black** or **white**, defining them by the usual rules of such nodes in a Fibonacci tree.

Then, we have the following property.

LEMMA **13** *It is possible to require that* **8***-centres are always black tiles. When this is the case, a seed is always a black tile.*

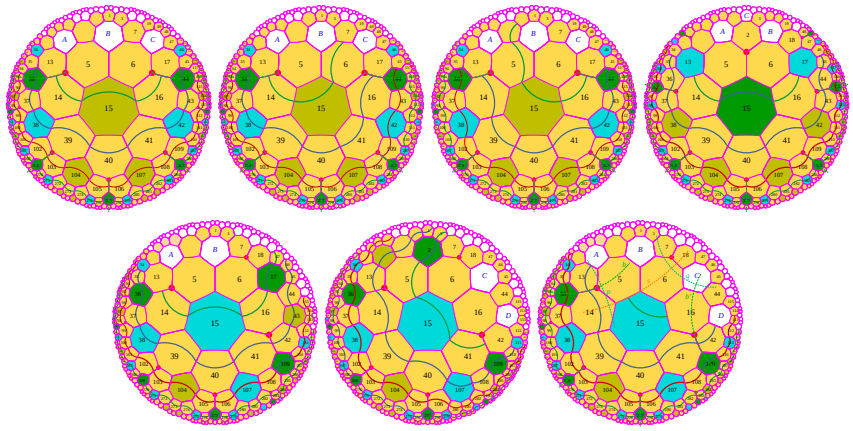

FIG. **20** The black tile property and the levels:
On the first row: the three cases for an F-secot and the single case of an **8**-one. On the second row, the three possible cases for a G-centres.

Proof. The argument is based on the pictures of figure 21. On these figures, we can see the differenciation between black and white nodes performed by arcs drawn on the tiles. One kind of arc joins the mid-points of two edges of the heptagon which are separated by one edge. The other joins the mid-points of two edges which are separated by two consecutive edges of the heptagon. The figure illustrates this definition on the tile of an F-centre. As we shall soon see, the same tile of the mantilla may occur as a black tile or as a white one.

Of course, once we define a tile as a black or a white tile, its sons are defined according to the usual rules of a standard Fibonacci tree, see [24]: a black node has two sons, a black and a white ones; a white node has three sons, a black and two white ones. In both cases, the black son is also the leftmost.

Starting from the pircture of an **8**-centre in figure 20, the last one in the first row, we can see that the sectors attached to the sons of the centre are, from the left to the right: $Fw61$, Fb, Fb, $Fw72$, were Fb is the node which is represented on the left-hand side of figure 21, $Fw61$ is the node which is represented on the right-hand side of the figure. The figure clearly indicates the reason of the name of the latter tile. For what is $Fw72$, it is symmetric to $Fw61$ with respect to the reflection axis of the latter tile exchanging the sides 1 and 7, for instance, but renumbering the tile in the same way as previously after the reflection, as the axis of the reflection is not changed. We can see the induced sons of the new defined centres. In fact, we obtain the sons of any centre, step by step, using table 8.

On the middle picture of figure 20, we can see that along a ray crossing **8**-centres along a reflection axis, if we define the **8**-centre as a black tile and its

petals $1\overline{4}7\circ$ and $157\circ$ as black and white tiles respectively, then this attributes are kept by indution along the position of the tiles on the ray. From this, defining the patterns in each sector, we find out that the configurations are reproduced by the recursive definition of the sectors: in fact, we have nine kinds of sectors: one kind for **8**-centres, three kinds for the F-centres, one black and two white ones, and four kinds for the G-centres: two kinds of G_ℓ-centres, a black and a white ones, and the same for G_r-centres. This defines eight different situation of sectors. Now, as in each sector the above properties are satisfied for the sons of the centre of the sector, they are also satisfied inside the sectors by the recursive structure of the sectors and by the property which we established on the borders of sectors.

TABLE **8** Table of the relations between the centre of a sector and its sons, taking into account the incidence of the isoclines.

centre	sons:			
Fb	G_rw	Fb	Fb	$G_\ell w$
$Fw61$	G_rw	Fb	Fb	$G_\ell b$
$Fw72$	G_rb	Fb	Fb	$G_\ell w$
$G_\ell w$	G_rb	Fb	$G_\ell b$	
$G_\ell b$	G_rb	Fb	$G_\ell w$	
G_rw	G_rb	Fb	$G_\ell b$	
G_rb	G_rw	Fb	$G_\ell b$	
8	$Fw61$	Fb	Fb	$Fw72$

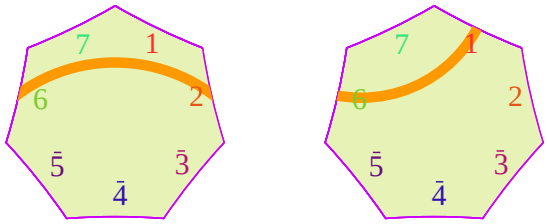

FIG. **21** The black tile property and the levels:
On the left-hand side, a black F-centre. On the right-hand side, a white F-centre, here, the case $Fw61$.

Note that figure 20 represents seven pictures only as, in fact, $G_\ell w$ and $G_r w$ are identical sectors: their difference lies in the father of the sector. It does

not stand in the same place with respect to the centre. Remember that, in a G-sector, the G-centre has two centres in contact with its parental tiles, see the places B and C for tiles to be fixed in figure 14. For a G_ℓ-centre the father is in B, while the father is in C for a G_r centre. ■

It is not difficult to note the following. Number the sides of a heptagon from 1 up to 7, starting from the side which is shared by the father and counter-clockwise turning around the tile. This defines the **local numbering**. In this numbering, the arc joins the mid-point of the sides 2 and 7 in a white node and the mid-points of the sides 3 and 7 in a black node.

TABLE **9** Table of the centres and petals equipped with the isoclines.

tile	*st*	edges	relative	tile	*st*	edges	relative
F	B	6-2	6-2	11∘2	B	((−•)-(2-1))	7-3
	W	6-1	6-1	11∘2	W	((−•)-2)	7-2
	W	7-2	7-2	37∘7	B	(7-(3-7))	2-5
8	B	$\overline{6}$-$\overline{2}$	$\overline{6}$-$\overline{2}$	37∘7	W	((7-3)-(3-7))	3-5
G_ℓ	B	2-$\overline{6}$	2-6	1∘14	W	((1-4)-(4-1))	3-5
G_ℓ	W	1-$\overline{6}$	1-$\overline{6}$	$\overline{5}$∘77	B	((7-$\overline{5}$)-(•−))	5-1
G_r	B	$\overline{2}$-6	$\overline{2}$-6	$\overline{66}$7∘	W	($\overline{6}$-$\overline{6}$)	2-4
G_r	W	$\overline{2}$-7	$\overline{2}$-7	1$\overline{22}$∘	W	($\overline{2}$-$\overline{2}$)	4-6
2∘77	B	((7-2)-(•−))	5-1	11∘$\overline{3}$	B	((−•)-($\overline{3}$-1))	7-3
2∘77	W	(2-(•−))	6-1	47∘7	W	((7-4)-(4-7))	3-5
1∘1$\overline{3}$	B	((1-$\overline{3}$)-1)	3-6	1∘15	B	((1-5)-1)	3-6
1∘1$\overline{3}$	W	((1-$\overline{3}$)-($\overline{3}$-1))	3-5	1∘15	W	((1-5)-(5-1)	3-5
1∘$\overline{4}$7	W	((1-$\overline{4}$)-($\overline{4}$-7))	3-5	6∘77	B	((7-6)-(•−))	5-1
$\overline{5}$7∘7	B	(7-($\overline{5}$-7)	2-5	6∘77	W	(6-(•−))	6-1
$\overline{5}$7∘7	W	(7-$\overline{5}$)-($\overline{5}$-7)	3-5	137∘	B	((1-3)-7)	3-6
11∘6	B	((−•)-(6-1))	7-3	157∘	B	(1-(5-7))	2-5
11∘6	W	((−•)-6)	7-2				

At the level of a centre, looking at the different pictures of figure 20, we can see that the sons of a centre, in the sense of the Fibonacci tree, share a common side with another son and that this side is the side 7 in the local numbering, in the white son(s). This also can be checked for the second level of the Fibonacci tree, starting from the centre. Then, the property can be

continued by induction, thanks to the recursive structure of the sectors. Now, we already noticed that the structure of the sectors is similar to the structure of Fibonacci carpets which are described in [24, 14]. And so, we can continue the argument upwards. Accordingly, the arcs which we have described can be joined by the common edge of tiles which are on the same level of a Fibonacci tree. Now, as can be seen from the picture, which is a result of our above analysis of the status of the tiles along the border of a sector, the arcs also cross the sectors. The isoclines from the different sectors match, even when they are disjoint. Accordingly, the arcs constitute infinite paths which split their complement in the hyperbolic plane into two connected infinite parts. We shall call these infinite paths **isoclines** and we shall say that the isoclines cross the hyperbolic plane from one end to another.

In the sequel, it will be important to mark the path of an isocline on each tile of the mantilla. As can be seen by a careful study of the sectors based on figure 20 and on the tables 1 and 2, the 21 tiles which define the mantilla become now 33 tiles. They are displayed in table 9. In the table, we have indicated the position of the arcs in terms of the marks of the tile and also in a **relative numbering**. This numbering is obtained by starting from the red vertex of the tile when it is a petal and then, number the sides from 1 to 7 by counter-clockwise turning around the tile. For the centres, we keep the numbering of the mantilla.

From now on, we fix a numbering of the isoclines themselves. We number them periodically, from 0 up to 19, the number of an isocline crossing a center C being smaller than the number of the next isocline which crosses the sons of C. This numbering allow to define the directions **up** and **down** in the hyperbolic plane. The isoclines allow to define the directions **to the left** and **to the right**.

From the pictures of figure 13 we easily derive the following important property:

LEMMA **14** *Let the root of a tree of the mantilla T be on the isocline* 0*. Then, there is a seed in the area of T on the isocline* 5*. If an* **8***-centre A is on the isocline* 0*, starting from the isocline* 4*, there are seeds on all the levels.*

We have a very important density property:

LEMMA **15** *For any tile τ in a realization of the mantilla, fitted with the isoclines, there is a seed on an isolcine* 0 *within a ball around τ of radius* 21*.*

Proof. From figures 13, 14 and 15, there is an **8**-centre H at a distance at most 3 from τ. Let i be the number of the isocline on which H stands. Consider the ray issued from H which goes down along the axis of reflection of H which crosses its red vertex. If $i \in \{3..16\}$, then, going down along this ray, we find another **8**-centre H_1 on the isoclines 14, 15 or 16, depending on the remainder of i modulo 3 at a distance at most 12 from H. The different situations are examined by table 10 which, for each case, indicates a path from H_1 to a seed σ on an isocline 0.

These indications immediately follow from figures 13, 14 and 15 which display the structure of the sectors and from lemma 14. Indeed, in an **8**-sector, there are two F-flowers at distance 2 from the **8**-centre and which are white tiles: we indicate this by denoting them by Fw. There are also black F-flowers, denoted by Fb, also at distance 2. Now, the Fw-tiles are on the isocline $+1$ and the Fb-tiles are on the isocline $+2$. In the tree cases, the F-centre which appears on an isocline 0 is a seed. It can be checked that the distance from H_1 to the seed is 9, 6 and 6 when H_1 is on the isocline 14, 15 or 16 respectively. Accordingly, the distance from H to σ is at most 18, so that the distance from τ to σ is at most 21.

TABLE **10** Checking the density of the seeds: on a ray of **8**-centres.

node	iso.	dist.	node	iso.	dist.	node	iso.	dist.
8	14	9	**8**	15	12	**8**	16	12
8	16	+3	Fw	16	+2	Fw	17	+2
Fw	17	+2	Gb	18	+2	Gw	18	+2
G_r	18	+2	Fb	0	+2	Fb	0	+2
Fb	0	+2						

NOTE: The indication of the distance, in tiles, is relative to the node of the previous row, in the table. Also note that the distance indicated on the first line corresponds to H on an isocline 5, 3 and 4 repsectively. For another position, we subtract a mulitple of 3, according to the remainder of i mod 3.

We remain with the case when $i \in \{0..2\} \cup \{17, 18, 19\}$.

First, consider the case when $i \in \{17, 18, 19\}$.

In this case, we look at the centre A which is at the distance 3 from H, above H, on the continuation of the ray of **8**-centres issued from H. We know that A is on the isocline $i-3$.

If A is an **8**-centre, we are done, as A lies on an isocline 14, 15 or 16. The distance of a seed σ on the isocline 0 from A is at most 9, from table 10. Hence, the distance of the seed from τ is at most 15. These cases are indicated in table 11.

If A is not an **8**-centre, then it is an F- or a G-centre. The possibilities are given by table 11. Now, depending on which isocline A is, we split the cases in to two ones.

If A is on an isocline 16, there is a G-son of A on an isocline 18 when A is a G-centre or when it is an Fw-centre, see figure 20. Indeed, when A is an Fb-centre, as its G-son will be on an isocline 17, we have to proceed in another way. This is indicated in the table by another row below the one corresponding to the case denoted by Fw/G. On the new row, we have Fb on the column 16, indicating the position of the centre. As there is nothing else on the row, this means that we go up to the father of A. Again we have two cases, depending on

which father, on the same criterion as before as we are simply by two isoclines higher. Of course, the situation with Fw/G receives a similar solution: there is simply one more G-son on the path. Now, we can solve the case Fb, as it is on an isocline 14: it has a Gw-son on an isocline 15 and the black G-sons of this Gw-centre are on an isocline 16. Hence, we know how to find σ on the isocline 0. It is easy to check that the distance are what the table indicates.

TABLE **11** Table of the paths to σ when H is on an isocline 19, 18 or 19. The first column indicates the distance from τ to σ. The second indicates the distance from H to σ and the third one indicates the distance between A and σ. The columns entitled 0, 19, 18, 17, 16, 15 and 14 indicate the element of the path on the isocline with the number of the column. When the path goes to the next row, there is no number on the first three columns.

			0	19	18	17	16	15	14
				8					
12	9	+6	σ				**8**		
10	7	+4	σ		G		Fw/G		
							Fb		
14	11	+8	σ		G		G		Fw/G
16	13	+10	σ		G		Gb	Gw	Fb
					8				
12	9	+6	σ					**8**	
14	11	+8	σ				**8**	F/Gb	
								Gw	
14	11	+8	σ					**8**	
						8			
14	11	+8	σ						**8**
12	9	+6	σ		G		G		Fw/G
14	11	+8	σ		G		Gb	Gw	Fb

NOTE: The difference between the numbers in the first three columns is 3, the distance from τ to H.

Next, we have the case when A is on an isocline 15. Now, as we assume that A is an F- or G-centre, we split the situation into two cases, depending on whether A is a Gw-centre or not. If it is not, we find an **8**-centre at a distance 2 from A on the isocline 16. This is easy to check on figure 20. And then, we use the path indicated in table 10. If A is a Gw-centre, then we can see from the same figure that its parental **8**-centre is on the same isocline as itself. And so, we get a **8**-centre on an isocline 15, at a distance 2 from A.

We arrive to the last case when A is on an isocline 14. Now, we split the cases as for the isocline 16, as long as we are now by two isoclines higher. We have just two introduce another G-son to the path: it is always possible to have a G-son of a G-centre by two isocline below, at a distance 2 of the father, as usual.

Second, consider the case when $i \in \{0..2\}$.

Whatether A, we are on an isocline $i-3$, *i.e.*, an isocline 19, 18 or 17. If A is an **8**-centre, then we can apply the results of the previous table: the maximal distances from A to the seed are now 13 for the isocline 19 and 11 for the isoclines 18 and 17. For the maximal distances from τ to σ, this gives us 19 and 17 respectively.

Now, we have to look at what happens when A is an F- or a G-centre.

First, we start when A is on the isocline 19. If A is not a Gw-centre, then at a distance 2 from A, we find an **8**-centre on an isocline 18 and so, from there, by table 11, we arrive to a seed σ on an isocline 0 by a path of length at most 11. Accordingly, this gives a distance from τ to σ which is at most 19.

TABLE **12** Table of the paths from H to σ when H is on an isocline 2, 1 or 0.

		2	1	0	19	18	17	16	15
		8							
19	13				**8**				
					F/Gb				
19	2+11					**8**			
					Gw				
							F/G		
14	2+2+4							Fw/G	
18	2+2+8							Fb	
18	2+2+8								F/Gb
18	2+2+8								Gw
			8						
17	11					**8**			
						F/G			
18	2+10							F/G	
18	2+10						F/G		
				8					
17	11						**8**		
16	10						F/G		

If A is a Gw-centre, we can go from there at a distance 2 to an **8**-centre on the same isocline 19. We would get a maximal distance of 21. But we can get a better result. Take the father B of this Gw-centre which is necessarily at a distance 2 and on the isocline 17, see figure 20. Then, we take again the father C of B. Now, C is at a distance 2 from B, either on the isocline 16 or on the isocline 15. If C is on an isocline 16, we split this case into two situations which we already analyzed in table 11: the case Fw/G and the case Fb. In the first case, C is at a distance 4 from σ and so A is at a distance $2+2+4=8$ from σ. In the second case, C is at a distance 8 from σ and so A is at a distance 12 from σ.

We remain with the case when C is on an isocline 15. This time, we split the situation into the case F/Gb and the case Gw. In both cases, table 11 shows us that C is at a distance at most 8 from a seed σ on the isocline 0. Accordingly, this tells us that σ is at a distance at most 18 from τ.

Now, we arrive to the case when A is on an isocline 18. Now, as A is assumed to be not an **8**-centre, its father B is an F- or a G-centre at a distance 2 from A and on the isocline 17 or on the isocline 16. Now, we have met the former situation in table 11 and the latter in the discussion when A is on an isocline 19. And so, we find the indications of the table: if B is on an isocline 17, its distance to a seed σ of the isocline 0 is at most 10. If B is on an isocline 16, its distance to a seed σ is also at most 10.

At last, we arrive to the case when A is on an isocline 17. We already computed the distance of an-F or a G-centre on an isocline 17 to a seed σ of the isocline 0, and we have found that it is at most 10. Accordingly, in this case, τ is at most at a distance 16 from σ.

Accordingly, the longest distance between τ and σ which we find in this discussion is 21. Which proves the lemma. ■

3 A parenthesis on brackets

Now, we turn to the basic process of the construction. This process is also used by Berger and by Robinson in their respective proofs. However, the process, alghough different, is more explicit in Berger's presentation where it is one dimensional, while Robinson directly deals with the two-dimensional extension of the same process. To better understand the process, we look at it from an abstract point of view. In a first sub-section, we shall consider the case when the process evolves on the whole line. In a second sub-section, we shall look at what happens if we restrict it to a ray.

3.1 The infinite models

Consider the following process:

We have a bi-infinite word of the form ${}^{\infty}(RMBM)^{\infty}$. We call this the **row** 0. We define the next **rows** k as follows. Assume that the row k is of the form ${}^{\infty}(R\_^{2^k-1}M\_^{2^k-1}B\_^{2^k-1})^{\infty}$. The word $R\_^{2^k-1}M\_^{2^k-1}B$ is called the **basic pattern** of generation k or the k**-basic pattern**. We superpose these rows one above the other in such a way that the letter R or B of the row k+1 is put over the M of a k-basic pattern. To better visualize the process, we consider the even rows as written in blue and the odd rows as written in red.

These rows can also be obtained from one another by a cancellation process: on the row k, we re-write with blanks the letters R and B and the M letters are re-written R or B according to the following rule. At random, we fix one M at the mid-point of a basic pattern and then, we replace this M by R. The next M to the right is left unchanged and the second one is replaced by B and the third one is again left unchanged. Starting from the following M we repeat

this process periodically. We also repeat the reverse sequence of actions to the left of the initially chosen M.

Now, the letters define positions in a natural way for any subword which we shall consider. We shall call **intervals** the set of positions delimited by the R and the B of a basic pattern. We shall specify blue or red interval according to the colour of the delimiting R and B. We shall also consider the set of positions defined by a B followed by the next R. We shall call this a **silent interval**, also specifying red or blue, depending on the colour of the delimiting B and R. When speaking of silent intervals, the ordinary one will be called **active**. At this point, we notice that active and silent intervals of the same generation have the same length and the same stucture of proper sub-intervals, whether active or silent.

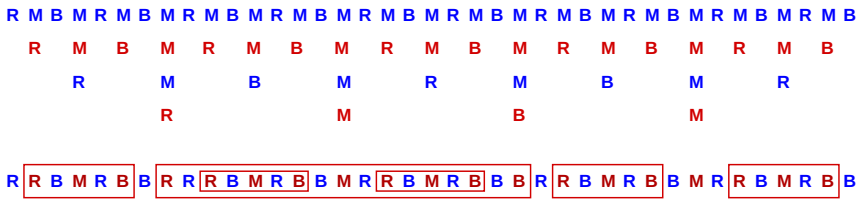

FIG. **22** The abstract rows and the transparent letters: inside the long red frame the transparent letters which are not in the smaller red frames.

Now, assume that we superpose the rows of the generations from 0 to $2n+1$. In this superposition, we assume that the blanks and the blue letters are transparent. We are interested in counting the number f_n of letters inside a red active interval of the generation $2n+1$ which are not contained in a red active interval of a previous generation. This is illustrated in figure 22. Such letters will be called **free**. Note that, from this definition, the letters which are the ends of a red interval cannot be free.

We have the following property which can easily be derived from figures 22 and 23 by induction.

LEMMA **16** *The number of free letters inside a red interval of generation* $2n-1$ *is* 2^n+1*, with* $n \geq 1$*.*

Proof. Denote by f_n the number of free letters in a red interval of the generation $2n+1$. By the definition of the constructio, we can see that active and silent intervals of the same generation can be transformed into each other by a simple shift of the length of these intervals. As the this length is a multiple of the lengths of the intervals of smaller generations, such a shift changes nothing for the sub-intervals. In particular, the structure of the sub-intervals of an acitve and a silent interval of generation n is the same, as already mentioned.

From figures 22 and 23, we can see that in a red active interval I of the generation $2n+1$, with $n \geq 1$, there are two red active intervals of the generation $2n-1$. The complement in I of these two red active intervals consists into

an open silent interval J of generation $2n-1$, and two intervals J_1 and J_2 of equal lengths which are a half of J. Clearly, what is free in J, J_1 and J_2 remains free in I. This counting gives us: $f_n = f_{n-1} + 2.\left(\frac{f_{n-1}-1}{2}\right) = 2.f_{n-1} - 1$, as f_n is odd, which is easy to see: the mid-point of a red active interval is free. As $f_1 = 3$, we get the expression of the lemma for f_n. ■

Now, we can also ask the same questions for the blue intervals, considering that now, blank and red letters are transparent. We easily get the following result, again by induction:

LEMMA **17** *The number of free letters inside a blue interval of the generation* $2n$ *is* 1 *for* $n > 0$.

Proof. The same argument leads us to the same induction relation with g_n the number of free letters in a blue interval and the induction starts from $n = 1$. Now, $g_1 = 1$ and so, we find $g_n = 1$ for all n. ■

The result of lemmas 16 and 17 explain why we shall consider the red intervals in our construction.

The free letters also have another interesting property in the red intervals.

LEMMA **18** *Let* $a_1, \ldots, a_{2^n+1}$ *be the positions of the free letters in a red interval of the generation* $2n+1$*, the first position in such an interval being* 1*, the ends being not taking into account. Then* $a_{i+1} - a_i \geq 2$ *except for* $i = 2^n$ *and* $i = 2^n+1$ *for which* $a_{i+1} - a_i = 1$.

The proof is done by induction on n, the property being already true for the generation 1. Note that in the proof of lemma 16, we had to look at halves of intervals of the form $]BMR[$. In such intervals, the central M is never counted as well as the ends. Accordingly, by induction, the contribution of a half consists of isolated free letters.

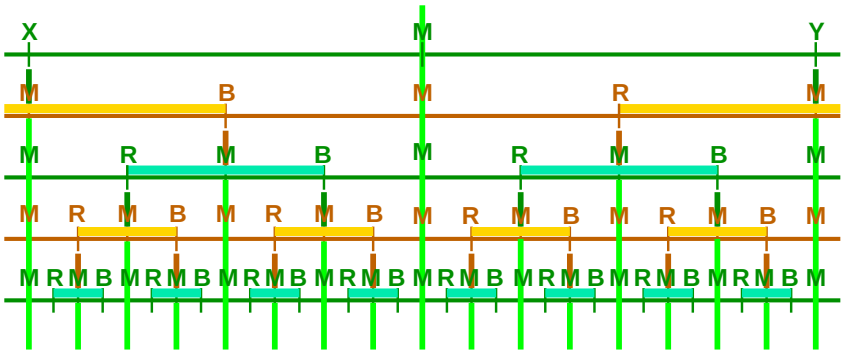

FIG. **23** The silent and active intervals with respect to mid-point lines. The light green vertical signals send the mid-point of the concerned interval to the next generation. The colours are chosen to be easily replaced by red or blue in an opposite way. The ends X and Y indicate that the figure can be used to study both active and silent intervals.

We can describe the structure of the red active intervals contained in a bigger red active interval and of the free letters with better precision. First, it is not difficult to see that the free letters come from letters which are already present in the generation 0:

LEMMA **19** *Let I be a red active interval of the generation $2n{+}1$, with $n > 0$. Let x be a letter R, M or B belonging to a blue active interval of the generation $2m$, with $0 < m \leq n$. Then x cannot be a free letter.*

The proof comes from the simple observation that, by construction, the R and the B of a blue interval of a positive generation $2n$, with $n > 0$, are generated by a red active interval of generation $2n{-}1$. And so, They cannot be seen in a red interval of a generation m, when $m > 2n$.

Now, we can describe the positions of the red active intervals and of the free letters contained in a given active interval. They are given by the following lemma, giving a much more precise information:

LEMMA **20** *Let I be a red active interval of the generation $2n{+}1$. Then, I can be split into its ends, its free letters and a finite set of interval which exactly contains 2^k intervals of the generation $2(n{-}k){+}1$. Similarly, if J is a blue active interval of the generation $2n$, then J can be split into its ends, its unique free letter and a finite set of intervals which exactly contains 2^k intervals of the generation $2(n{-}k)$.*

Proof. Consider H_n an interval of generation n. Using the argument which we used for the proof of lemmas 16 and 17, we obtain that

$$(*) \qquad |H_{n+2}| = 2.|H_n| + |H_n| - 2 + 2.\frac{|H_n| - 3}{2} + 2$$

,

where $|H_n|$ is the number of letters contained in H_n.

This gives us $|H_{n+2}| = 4|H_n| - 3$, leading to $|H_{n+2}| - 1 = 4(|H_n| - 1)$. As $|H_1| = 5$ and $|H_0| = 3$, we get $H_{2n+1} = 4^{n+1} + 1$ and $H_{2n} = 2.4^n + 1$.

Rewriting (*) as $|H_{n+2}| - 3 = 2|H_n| + 2(|H_n| - 3)$, and replacing H_n by the just computed value in the first term of the second member of the latter equation, we get, by elimination, for odd generations:

$$\boxed{|H_{2n+1}| - 3 = 2^{n+1} + \sum_{k=0}^{n-1} 2^{n-k}(4^{k+1} + 1)}$$

and, for the even ones:

$$\boxed{|H_{2n}| - 3 = \sum_{k=0}^{n-1} 2^{n-k}(4^k + 1)}$$

From this decomposition in numbers, we get the splitting indicated in the lemma: in the left-hand side part of the equality, the subtraction represents the ends of the interval together with its mid-point. ■

We conclude this sub-section with an additional important information on the silent interval, whose structure is very different from that of the active ones.

Say that a finite sequence $\{I_k\}_{k\in[0..n]}$ of silent intervals is a **tower** if and only if for each $k \in [0..n]$, I_k belongs to the generation n and if the mid-point of these intervals is the same position in I_n which thus, contains all of the members of the sequence. Note that if $\{I_k\}_{k\in[0..n]}$ is a tower, we have $I_k \subset I_{k+1}$ for all k with $0 \leq k < n$. The common mid-point of the silent intervals of a tower is called the **mid-point** of the tower. The last interval in the tower which contains all of them is called the **area** of the tower. We also say that this last interval **closes** the tower.

We have the following lemma:

LEMMA **21** *Let I be a silent interval of generation n. The silent intervals which it contains or intersect can be partitioned into finitely many towers. The set of the mid-points of these towers contains the mid-point of I. For generations $n \geq 2$, it also contains the both ends of I. At last, for the towers which are contained in I and whose mid-point is not that of I, their areas belong at most to the generation $n-2$ and their mid-points are ends of proper intervals of I.*

The proof of this lemma is simply by induction on the generation to which I belongs. It can be illustrated by figure 23.

This gives a simple algorithm to construct the active and silent intervals generation after generation, considering that each generation is put on another line which we call **layer**.

Initial step:

$n := 0$;

the current layer is the layer n; the active and silent intervals of this generation are determined.

Induction step:

i) The mid-point of the active intervals of the generation n which are determined on the layer n send a red signal to the layer $n+1$: it is the current **end signal** which consists of two kinds of signal. Each second signal is called R and the others are called B, the initial R being taken at random.

ii) The mid-point of the silent intervals of the generation n send a light green signal to the further layers: it is the current **mid-point signal**.

iii) The layer $n+1$ stops the end signals. The R-signals define the beginning of an active interval of the generation $n+1$ and the next B-signal received on the layer defines the terminal end of the considered active interval. The end signals are absorbed by the layer $n+1$. The complement intervals are the silent intervals of the generation $n+1$. The current mid-point signals which meet the mid-point of a silent interval go on to the next layer. The

current mid-point signals which reach the mid-point of an active interval will emit the end signal of the next generation.

iv) $n := n+1$;

ALGORITHM **1** *The algorithm to construct the active and silent intervals, generation after generation.*

We shall go back to this algorithm in the next sub-section.

We conclude this sub-section with a look at the possible realizations of the abstract brackets. From now on, such a realization will be called an **infinite model** of the abstract brackets, **infinite model** for short. At each generation, we have two choices for defining the position of the active intervals of the next generation. Accordingly, this yields continously many infinite models, even if we take into account that if we fix a position which we call 0, there are countably models which can be obtained from each other by a simple shift with respect to 0. However, the different models do not behave in the same way if, for instance, we look at the towers of silent intervals. In this regard, we have two extremal models. In one of them, 0 is the mid-point of an infinite tower of silent intervals. As this model is symmetric with respect to 0, we call it the **butterfly model**. In another model, 0 is always the mid-point of an active interval of each generation. This model is also symmetric with respect to 0. We call it the **sunset model**.

As we shall later have to deal with the butterfly model, let us briefly indicate the following. Let a_n, b_n and c_n denote the addresses of the R, the B and the M of an active interval I of the generation n. Denote by d_n the address of the M which follows the B defined by b_n. If I_{n_1} is the active interval of the generation n for which a_n is the smallest positive number, we have $a_{n_1} = 2^n$, $b_{n_1} = 3.2^n$, $c_{n_1} = 2^{n+1}$ and $d_{n_1} = 2^{n+2}$. Note that a_{n_1} also gives the address of the left-hand side end of the silent interval with the smallest positive address in the sunset model.

We have the following 0-1 property for the infinite models:

LEMMA **22** *Consider an infinite model of the abstract brackets. We have the following alternative: either for any position x, x belongs to finitely many active intervals or, for any x, x belongs to infinitely many active intervals.*

The proof relies on the fact that if x belongs to finitely many active intervals, there is a layer n such that if x belongs to an interval of the generation m with $m \geq n$, then the interval is silent. Let I be the silent interval of the generation n which contains x. Then, it is plain that the tower to which I belongs is infinite. Otherwise, there would be an active interval containing x and belonging to a generation k with $k > n$, a contradiction. Now, as an infinite tower is unique when it exists, the property holds for any position.

3.2 The semi-infinite models

Now, we consider what happens if we cut the result of the previous process, as illustrated by figure 23, at some position.

To simplify things, we take the M of a silent interval of the generation 0. We imagine a vertical line δ starting from M, the layers being horizontal, and we say that δ cuts all the layers. By definition, we forget what happens on the left-hand side of δ and we look only at what remains on the right-hand side. Moreover, all active intervals which are cut by δ are removed. What remains will be called a **semi-infinite model**

There are a lot of realizations of the semi-infinite model. Say that when a position is contained by an active interval, it is covered by this interval.

Consider an infinite model of the abstract brackets, fix a position x and focus on the semi-infinite model defined by the cut at x. Then we have:

LEMMA **23** *Consider an infinite model of the abstract brackets and the position x of a cut. In the semi-infinite model defined by the cut at x, for any position y after x, y is covered by finitely many active intervals.*

The proof is straightforward from the following property:

LEMMA **24** *Consider an infinite model of the abstract brackets and the position x of a cut. Let y a position with $x > y$ and assume that in the model, any position is covered infinitely many often. Then, there is an active interval I which contains both x and y.*

From lemma 24, the proof of lemma 23 is easy: as active intervals of the same colour are either disjoint or imbedded, if an active interval J contains both x and y, this is also the case for any active interval I which contains J. This rules out all the active intervals of the same colour and of bigger generations which contain y. For the other colour, either all active interval containing y do not contain x or at least one of them contains x and so, we have the same conclusion for intervals of the other colour. Note that it is not difficult to construct infinite models where 0 is covered by infinitely many blue active intervals and by no red active interval.

Now, the proof of lemma 24 is not difficult. From one generation to the next one, the length of an interval gets twice bigger. This means that if $y \in I_n$, where I_n is an active interval of generation n, then $]y-\frac{|I_n|}{2}, y+\frac{|I_n|}{2}[$ is contained in K_{n+1}, the interval of generation $n+1$ which contains y. As infinitely many active intervals contain y, we may assume that $|I_n| > 2|y-x|$. Accordingly, $x \in K_{n+}$. If K_{n+1} is active, we are done. If not, K_{n+1} is contained in a tower of silent intervals which cannot be infinite, by the assumption of the lemma. Now, by construction, of the model, the area of a tower is contained in an active interval of the next generation. And so, K_{n+1} is contained in an active interval which, thus, contains both x and y. And so, both lemmas are proved.

From lemma 23, from the uniqueness of the infinite tower in the butterfly model and from lemma 24, we can draw the following conclusion:

LEMMA **25** *Let x be the position of a cut in a semi-infinite model. Let y be another position with $x < y$. Then, except if y is the position 0 in the butterfly model, y is always covered by an active interval.*

Deep results on the space of all these realizations are given by an acurate analysis to be found in [10]. The interested reader should have a look at this paper.

In the next two sub-sections, we deal with the implementation of these models first, in the Euclidean plane, and then, in the hyperbolic plane. The study of the semi-infinite models is especially needed by the implementation in the hyperbolic plane.

4 The interwoven triangles

In this sub-section, we make the first step to lift up the infinite models of abstract brackets to the hyperbolic plane. This consists in a detour via the Eucidean plane.

We lift up the intervals as **triangles** in the Euclidean plane. The triangles are isoceles and their heights are supported by the same line, called the **axis**, see figure 24.

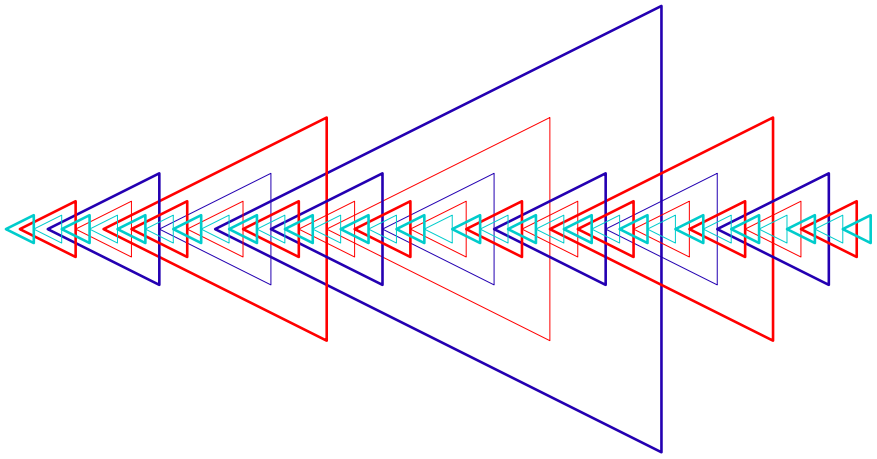

FIG. **24** *An illustration for the interwoven triangles.*

From now on, we restrict the word **triangle** to the objects which represent an active interval of the infinite model. For the silent intervals, also represented in our lifting, we use the word **phantom**. For properties shared by both triangles and phantoms, we shall speak of **trilaterals**. For the set of all trilaterals, we shall speak of the **interwoven triangles**.

The interwoven triangles have a lot of properties which they inherit from the infinite models. A first one corresponds to the non intersection property of the active intervals.

LEMMA **26** *The triangles of generation n+2 do not meet the triangles of generation n. Accordingly, the area of a triangle of generation n is contained in the area of some triangle of generation n+2.*

The proof comes from the same property for the active intervals. If the triangles would meet, their intersection would produce an intersection in the projections.

Note that the property does not hold for the phantoms. For the phantoms, we can collect them into towers, exactly as this was done for the silent intervals. We have:

LEMMA **27** *Phantoms can be split into* **towers** *of embedded phantoms. The phantoms of a tower have the same mid-point. This mid-point may be the vertex of a triangle or the mid-point of a basis of a triangle. In a tower, the colours of the phantoms it contains alternate and each phantom of a tower contains phantoms of all smaller generations.*

This is a direct consequence of lemma 21. As for towers of intervals, we shall say that the biggest phantom of a tower **closes** the tower.

The problem of intersections between trilaterals can be made a bit more exact. We have the following general properties.

LEMMA **28** *Between trilaterals, the crossings occur between legs of one figure and the basis for the other figure.*

LEMMA **29** *A leg of a trilateral is never cut inside the open interval delimited by the mid-distance line and the basis of the trilateral.*

The easy proof of lemmas 28 and 29 rely on the proof of lemma 20 and on the following property. To formulate it, consider two intervals $I = [x, u]$ and $J = [y, v]$ on the axis, x, y, u and v being positions of letters. Let T_I be the isoceles triangle, with its vertex at x, its legs parallel to the legs of the interwoven triangles, and its basis cutting the axis at u. Similarly, define T_J from J. Denote by $ar(T_I)$ and $ar(T_J)$ the areas of T_I, T_J respectively. Then, obviously, we have:

LEMMA **30** *Let $I = [x, u]$ and $J = [y, v]$ be two intervals on the axis. Assume that $x < y$. If $u < y$, then, $ar(T_I) \cap ar(T_J) = \emptyset$. If $y < u < v$, then the basis of T_I cuts the legs of T_J. If $v < u$, then $ar(T_J) \subset ar(T_I)$.*

Now, from the analysis of towers of phantoms and from the construction of the generation $n+1$ from the generation n, we have:

LEMMA **31** *A trilateral T of a generation $n+1$ exactly meets two triangles P_1 and P_2 of generation n: the legs of T meet the basis of P_1 while the legs of P_2 meet the basis of T. If T is a triangle, it also meets a trilateral F of generation $n+2$: the legs of F meet the basis of T.*

LEMMA **32** *A trilateral T of generation $n+1$ meets all the phantoms contained in the triangles P_1 and P_2 of genertaion n which generate T. The intersections occur by the bases of the phantoms inside P_1 meeting the legs of T and by the basis of T meeting the legs of the phantoms inside P_2, at their mid-point.*

From the construction of the abstract brackets, we get a simple algorithm to construct the interwoven triangles.

The generation 0 is fixed by alternating triangles and phantoms.

When the generation n is completed, a vertex of a triangle or a phantom is put on the intersection of the axis with the mid-distance line of a **triangle** of generatoin n. This vertex grows legs of a colour which is opposite to that of the generation n: here too, blue and red are opposite of each other. The legs grow until they meet a green signal, travelling on a horizontal line. If the trilateral is a triangle, the legs stop the green signal. If the trilateral is a phantom, the green signal crosses the legs. In both cases, the legs go on until they meet a basis of their colour. They stop it and constitute a trilateral of generation $n+1$. Now, the intersection of the basis of the trilateral with the axis requires a vertex: of a triangle if the basis belongs to a phantom, of a phantom if the basis belongs to a phantom. The process is repeated endlessly.

The detection of the green signal and of the correct basis are facilitated by the following mechanism: the legs of red triangles emit red horizontal signals which have a laterality. A right-hand side leg emits a right-hand side signal and a left-hand side leg emits a left-hand side signal. This allows to detect what corresponds to the free letters and which we call the **free rows** of a red triangle.

In [18], we proved:

LEMMA **33** *The interwoven triangles can be obtained by a tiling of the Euclidean plane which can be forced by a set of* 190 *tiles.*

In sub-sections 6.2 and 6.3, we describe the tiles, taking into account the properties of the above lemmas. In [18], the corresponding tiles are displayed in a square format, as required for *à la* Wang tiles. Note that the set of prototiles referred to by the lemma also provides the detection of the free rows of red triangles which are marked by an appropriate signal, called the **yellow** signal.

5 Implementing the interwoven triangles in the hyperbolic plane

The idea of the implementation in the hyperbolic plane is based on the fact that the isoclines which we introduced in sub-section 2.5 provide us with the horizontals which are needed to construct a space-time diagram.

From lemma 14, we define the isoclines 0, 5, 10 and 15 to play the rôle of the rows in the Euclidean implementation. The trilaterals will be constructed on trees of the mantilla. The vertex is realized by a seed, and the legs are supported by the borders of the tree rooted at the seed. The basis is defined by an isocline which cuts both borders of the tree.

As there are 6 seeds on the isocline 5 inside the tree defined by a seed on the isocline 0, there are 6 trilaterals of generation 1 raised by a triangle of generation 0. And so, contrarily to what happens in the Eucidean construction, we have several trilaterals of the same generation for the same set of isoclines crossed by the legs of these trilaterals.

Call **latitude** of a trilateral the set of isoclines which are crossed by its legs, vertex and basis being included.

We shall look at a thread as a frame for the implementation of a semi-infinite model of the abstract brackets. In case of ultra-threads, we can even implement an infinite model. But, even when there are ultra-threads, there are also threads, so that semi-infinite models cannot be avoided. Now, due to the working of the Euclidean implementation, the realizations associated to the threads cannot be independent: the same latitude cannot be used both for a triangle and for a phantom of the same generation. Consequently, the implementation of the semi-infinite models must be **synchronized**. The semi-infinite models must be considered as different cuts of the same infinite model, implemented in such a way, that the latitudes of the triangles match. Consequently, the possibility of the realization of the infinite model in the case of ultra-threads brings in no harm: it can be viewed as a cut at infinity.

As we have infinitely many threads, it is not difficult to see that there will be infinitely many trilaterals within a given latitude.

The goal of the synchronization is to guarantee that the algorithm describe in sub-section 4 will be in action here too, up to a few tunings needed by the synchronization. These changes will concern the definition of the axis of the implementation, and the synchronization of the horizontal signals: the vertices, the bases of trilaterals, the mid-points of their legs and the horizontal signals emitted by the legs of a triangle.

5.1 The scent

By definition, we decide that all seeds which are on an isocline 0 are **active**. This means that they actually grow legs of a triangle of generation 0. We can reformulate lemma 15 by saying that **the set of active seeds is dense in the hyperbolic plane**.

Next, an active seed diffuses a **scent** inside its trilateral until the fifth isocline, starting from this seed, is reached. Seeds which receive the scent, and only them on the isoclines 5, 10 and 15, become active. The other seeds of these isoclines become **silent**: they do not give rise to a trilateral.

An active seed also triggers the green signal when it reaches an isocline 15. By construction, the generation 0 is not determined by the meeting of a green signal: the change from the first half of the leg to its second half is performed when the isocline 5 is met. But, for the other generations, the construction is determined by the meeting of a green signal, always on an isocline 15.

We can see that the scent process construcs a tree. The branches of the tree materialize the thread which implements the considered semi-infinite model. Note that the above synchronization mechanism fixes things for spaces between

triangles but also inside them. Indeed, these spaces become larger and larger and so, starting from a certain latitude, the isoclines 0 produce active seeds which are inside these spaces, creating new implementations of semi-infinite models.

5.2 Synchronization: the mechanisms

Due to the occurrence of several trilaterals within a given latitude, we have now to require that all triangles, red, blue and blue-0, emit a signal along each isocline which meets their legs. The signal has the colour of the triangle and it has the laterality of the leg which emits it. The signal will be called **upper** as, in the tiles, it will be placed over the path of the isocline. The signal will be emitted by the legs of triangles, except the vertex which never emits this signal. This is a simplification with respect to the implementation described in [16, 18]: it also reduces the number of tiles. Now, as in [16, 18], we require that the corners of a phantom also emit an upper signal of its colour and of the laterality of the corner.

Various problems

Now, in between two contiguous triangles of the same latitude, horizontal signals of the same colour but with a different laterality will meet. We have to allow such a meeting. It will be performed by an appropriate tile which we call the **join-tile**. There is a join-tile for red signals and another for blue signals. The join-tile, see the pattern illustrated by figure 25, illustrates such a junction. Note that, on the left-hand side, we have the right-hand side signal and that, on the right-hand side, we have the left-hand side signal. Now, the opposite junction does not exist. This is conformal with the working of the algorithm of sub-section 4. Moreover, the opposite junction cannot be obtained from this one, as completely turning tiles is impossible in our setting. This is guaranteed by the existence of the isoclines and by their numbering.

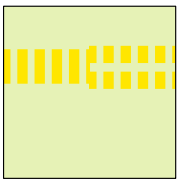

FIG. **25** *The pattern of a join-tile.*

We also require that an upper horizontal signal of a given laterality may cross a leg of a trilateral of the same colour only if it has the same laterality as the leg. When the colours are different, the crossing is always permitted, whatever the lateralities of the leg and of the signal.

From the impossibility to get the opposite junction to that which is realized by a join-tile, we obtain the following principle:

LEMMA **34** *An upper horizontal signal with a constent laterality cannot join two legs of the same trilateral.*

Proof. This is an easy corollary of the rule about the meeting of the legs with an upper horizontal signal. ■

The second mechanism which we introduce to force the synchronization of different constructions is that all bases on a given isocline merge. This changes the tiles for the corner, but this does not affect the algorithm of section 4. This also does not change the fact that corners emit an upper horizontal signal of their colour and of their laterality.

Now, the upper signals allow to differentiate the various parts of a basis. If a basis has an upper horizontal signal of its colour, we are outside a trilateral of the generation of the basis. If not, we are inside. We say that the basis is **covered** if it is accompanied by an upper horizontal signal of its colour. Otherwise, we say that the basis is **open**.

This distinction is important. When a leg meets a basis: if it is the first half of a leg, *i.e.* between the vertex and the mid-point of the leg, it meets the basis without changing it. When the second half of leg meets a basis, it crosses it if the colour is different. If the colour is the same, it crosses it only if the basis is covered. Indeed, from lemma 34, an upper horizontal signal cannot go from one leg of a trilateral to the other: there must be a triangle of the same colour in between. And so, an open basis does not cross the second half of a leg of a trilateral of the same colour. Accordingly, for the second half of the leg, when the leg meets such a signal, this means that the expected basis is found.

Now, there is a problem if we consider the situation of a missing trilateral. In the same latitude, other trilaterals are realized. This comes from the following result.

LEMMA **35** *Within a given latitude corresponding to an interval of the model realized by the tiling, there are infinitely many trilaterals.*

Proof. Consider the lowest row β of the latitude. As we know, the interval I corresponding to the considered latitude, we also know the highest row κ of the latitude. Now, fix a tile τ on β. There is at least one **8**-centre H over κ such that the ray ρ crossing the **8**-centres below H, look at figures 13, 14 and 15, meets the isocline of β on the left-hand side of τ. We may assume that there is an isocline 0 between H and κ. Considering a seed σ on this isocline which is on the left-hand side of H, it is now plain that the tree rooted at σ is on the left-hand side of ρ and that, as all the triangles of the generation 0 starting from σ are present, there is a trilateral associated to β and κ inside the tree rooted at σ. By taking the reflection in ρ of this construction, we can prove the same property for the right-hand side of the tile τ. Now, taking two tiles τ_1 and τ_2, with τ_1 on the left-hand side of τ_2, we have a trilateral on the left-hand side of τ_1 and another one on the right-hand side of τ_2. Repeating this argument, we get infinitely many trilaterals. ■

Now, consider two such trilaterals T_1 and T_2, with T_1 on the left-hand side of T_2 and such that there is no other trilateral of this latitude in between T_1

and T_2. Each T_i, $i \in \{1, 2\}$, contains a triangle P_i such that P_i contributes to the generation of the basis β of T_1 and T_2. We may assume that there is no triangle of the latitude of P_1 between P_1 and the right-hand side leg of T_1 and, we may assume the same for P_2 and the left-hand side leg of T_2. Consider the upper horizontal signal σ which accompanies β and which is produced by the right-hand side corner of T_1. It is of the colour of β which is opposite to the colour of P_1. The signal σ crosses the legs of the copies of P_1 which are in between T_1 and T_2. Consider such a copy P. Inside P, whose mid-distance line is on the isocline of β, σ meets towers of phantoms of the generations smaller than that of P. Now, if β crosses the phantoms of a tower and if there are at least two phantoms in the tower, as the colours of the phantoms alternate in a tower of them, we get a contradiction with lemma 34.

We postpone the solution to this problem after the presentation of a second problem of this kind.

Indeed, if we assume that the bases of triangles of the same generation and the same latitude match, the mid-distance lines of trilaterals of the same latitude also match. Let ι be the isocline 15 of the mid-distance lines. Now, we have towers of phantoms inside these trilaterals whose mid-distance line is also supported by ι. We already know that, within a given latitude, there are infinitely many trilaterals, see lemma 35. Consequently, all of them have the same colour and all of them are triangles or all them are phantoms. Now, in between two consecutive **triangles**, there are phantoms of smaller generation which have the same mid-distance line as these triangles. Such phantoms do occur inside a triangle, this is clear from the study of the abstract brackets and the tower structure of the phantoms. But this also occurs in between consecutive triangles. This comes from the fact that the seeds of the isoclines 0 are all active. Accordingly, they trigger the generation of new semi-infinite models of the same infinite model.

The conclusion is that, in between two triangles of a positive generation, of the same latitude and on the isocline of their mid-distance line, there is a green signal inside the triangles, and there are also others outside them. Now, for the correctness of the algorithm, it is important that triangles stop the green signal and that phantom do not stop it. Accordingly, these different green signals must not meet when they travel on the same isocline.

We have a common solution for these problems, but their exact implementations present a few differences. Also, it will be useful to have a closer look on what happens in between consecutive triangles. Lemma 35 only gives a qualitative information which is not enough to clearly understand the reason of the situation. Now, we turn to this point and later, we shall present the solutions to the problems which we raised in this sub-section.

A precision

In order to go further than lemma 35, we start from the following remark.

Consider a trilateral T_0 of generation $n+1$. If this trilateral is realized, by definition of the construction, there is a **triangle** T_1 of generation n such that the vertex of T_0 is on the mid-distance line of T_1. We shay that T_1 is the **father**

of T_0. Note that a trilateral has a single father, but several ones may have the same father. If $n > 0$, we can repeat this argument. In this way, we construct a sequence $\{T_k\}$, $k \in \{0..n\}$, such that T_{i+1} is the father of T_i, $i \in \{0..n-1\}$. It is plain that T_n belongs to the generation 0. We say that T_i, with $i \in \{1..n\}$ is an **ancestor** of T_0 and that T_n is its **remotest ancestor**. In many cases we shall also call **remotest ancestor** the vertex of T_0. The context will be clear whether we speak of the seed or of the tree.

We can formulate the following property which is proved in [21].

LEMMA **36** *For any trilateral T, its remotest ancestor belongs to the generation* 0. *If n is the generation of T, then the distance, in number of isoclines* 0, 5, 10 *or* 15 *from the vertex of T to the vertex of A is $2^{n+1}-1$. Now, let T_1 and T_2 be two trilaterals of the same generation within the same latitude. Then, there is no trilateral of the generation of T_1 in this latitude between T_1 and T_2, if and only if there is no seed between the remotest ancestor of T_1 and that of T_2.*

Proof. The existence of the ancestors follows from the algorithm of sub-section 4 and from the process of selection of the active seeds by the scent. Indeed, consider a trilateral T. If it belongs to the generation 0, we are done. If not, its father exists. Otherwise, the vertex of T would be the starting point of the scent. But, as the generation of T is positive, its vertex is on an isocline 5 or 15. But, an active seed on such an isocline comes from another active seed by the scent. This proves the existence of the father and, by induction, of the remotest ancestor. The computation of the distance comes from the fact that the amplitude of a latitude of generation n is $2^{n+1}+1$, taking inot account the isoclines 0, 5, 10 and 15 only. Now, the father of this trilateral T has 2^n+1 as its height. It is easy to see that the distance from the vertex of T to the vertex of its father is 2^n. And so, as the summation goes unitl the distance is 1, as the height of a trilateral of the generation 0 is 3, we have that the distance to the vertex of the remotest ancestor is $\sum_{k=0}^{n} 2^k = 2^{n+1}-1$. Now, the conclusion about T_1 and T_2 is easy. If there were a third trilateral T_3 in between T_1 and T_2, its remotest ancestor would be in between that of T_1 and that of T_2. Conversely, if there were a seed σ in between them, as σ is on an isocline 0, it is active and so, it would generate a succession of triangles of successive generations until the father of T_1, by synchronization with the descendents of the remotest ancestor of T_1. By synchronization, the descendent of σ would generate a trilateral P of the same generation as that of T_1 and P would stand between T_1 and T_2. ■

From the proof of the lemma, we can derive an important information on the trilaterals inside a given latitude.

LEMMA **37** *Let T_1 and T_2 be two trilaterals of the same positive generation $n+1$ and within the same latitude. Let ι be the isocline of their mid-distance lines. Assume that there is no trilateral of generation $n+1$ in between T_1 and T_2. Then, there is a phantom of generation n in between T_1 and T_2 whose mid-distance line is also on ι.*

Proof. From lemma 36, the problem boils down to see whether there are seeds on the closest isocline 0 which lies above the vertices of T_1 and T_2. The closest distance between two seeds σ_1 and σ_2 on the same isocline, measured in the number of tiles crossed by the isocline between σ_1 and σ_2 is 26. It is realized by the F-sons of the G_ℓ and the G_r-sons of a black F-flower. The biggest distance is 416, which is reached at the twelfth isocline from an **8**-flower. This is proved by the recursive structure of the tiling by its splitting into the sectors defined in sub-section 2.2 and by a checking of the first fourteen isoclines from the centre of a sector by a computer program. Now, two consecutive white nodes give rise to two non interescting Fibonacci trees which have both 144 tiles on their fifth level. Accordingly, as the distance in isoclines from the remotest ancestors of T_1 and T_2 to their vertices is at least 5 and as there are at least 10 white nodes between σ_1 and σ_2, the distance between the vertices of T_1 and T_2 is big enough to give room to a lot of active seeds. In each of them, by synchronization and by what happens inside T_1, there is a phantom of generation n: its latitude is placed between the latitude of the triangles of generation n which contains the basis of T_1 and the latitude of the triangle which contains the head of T_1. ■

Now, we are ready to turn to the solutions of the problems which were raised at the beginning of this sub-section. The idea is to create signals which will go from a triangle to the next one in such a way that the signal 'overpass' the biggest concerned phantom of a tower within the considered latitude. The signal will satisfy two constraints: it must not disturb the working of the algorithm of sub-section 4 inside each phantom of the tower; it will convey its characteristics unchanged, as if the tower of phantom were not present.

We shall see that both constraints, apparently a bit contradictory, can be satisfied within a satisfactory compromise.

We start with the green signal: its solution is simpler.

A solution for the green signal

To solve the problem, we introduce another upper horizontal signal, the **orange signal** which shares the isoclines 15 with the green signal. Now, contrarily to the green signal which has no laterality, the orange signal exists in to versions only: a left-hand side and a right-hand side ones. They both occupy the indicated isoclines with the green signal, but alternately, never on the same segment of the isocline, even inside a tile.

Clearly, when a leg of a triangle meets the green signal which is inside it, the leg turns to its second half, it stops the green signal and, at the same time, it emits an orange signal of the laterality of the leg, outside the triangle. We can see this signal as an **antenna** of the triangle which looks forward to handle the other antenna which is emitted, from the other side, by the closest triangle of the same latitude. Now, during this search, the signal meets phantoms on its way, as it can be seen from lemma 37.

When the orange signal meets the first phantom standing in front of it, it climbs up along the leg of the phantom until it reaches the vertex. There, it goes down along the other leg, until it meets the isocline which contains the green signal which is inside the phantom, on the other side of the leg, in the tile

which realizes the junction of the leg with the green signal and, also, the turn to the second half of the leg. This tile also sends an orange signal on the right isocline, to go on its travel to the orange signal of the opposite laterality which is running to it, at some point, in front of it.

Note two points: during this climbing up and down, the signal keeps its laterality. Inside the phantom which supports the orange signal on the upper parts of its legs, there may be other phantoms for which the same green line is used to make the separation between the first and second halves of their legs. Note that the just described climbing of the orange signal can be repeated for other phantoms of the same generation standing in between our triangles, within the same latitude. This is repeated until the signal, coming from the next triangle meets the one we consider. Both signals can be joined by a tile similar to that of figure 25.

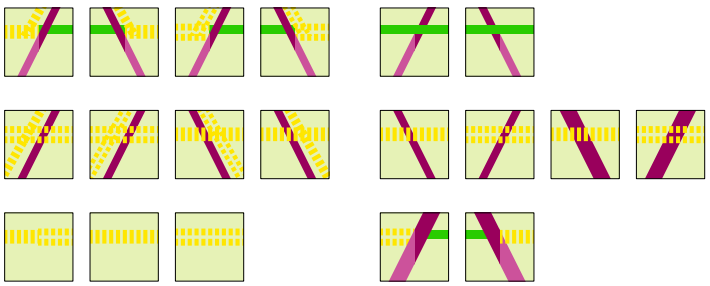

FIG. **26** The tiles for the antennas of triangles. A solution which also works for horizontal signals.

Now, legs of trilaterals can be crossed by an orange signal: this is possible if the signal travels on an isocline which is not the mid-distance line λ of the trilatral. Such a situation occurs: from the study of the abstract brackets, we know that a phantom contains inside itself the same trilaterals as a triangle of its generation. For these inner triangles, their mid-distance lines do not travel on the isocline of λ. Accordingly, the orange signals emitted by inner triangles cross the legs of the trilaterals whose mid-distance line is on λ, either in their first half or in their second one. We provide tiles for such a crossing, see figure 26, noticing that here too, we apply the rule that the orange signal of a given laterality must cross legs of the same laterality. As proved in [21], in between two consecutive triangles, there is a finite interval $[a, b]$ on the isocline of their mid-distance line such that, on the left-hand side of a, legs which cross the topmost isoclines of the latitude belong to a bigger generation and all of them are right-hand side legs. On the right-hand side of b, legs which cross the topmost isocline of the latitude belong to a bigger generation and all of them are left-hand side legs. Consequently, the join-tile can be placed at any tile of the interval $[a, b]$ which is not inside a phantom. In fact, as a corollary of lemmas 36 and 37, we can prove the following:

LEMMA **38** *Consider two consecutive triangles of the same generation and within the same latitude. Then, there is at most one leg of a trilateral of a bigger generation which crosses the topmost isocline of the latitude between the two triangles.*

Proof. Indeed, denote by T_1 and T_2 the two triangles and consider such a leg. Let T be the trilateral to which this leg belongs. Its remotest ancestor lies on a much higher isocline than that of the remotest ancestor of T_1. From the argument of lemma 37, we conclude that either the remotest ancestor of T_1 or that of T_2 falls within T. Now, if there where another leg, from the same argument, there would be room for an active seed on the isocline of the remotest ancestor of T_1 in between that of T_1 and that of T_2, which is a contradiction with lemma 36. ■

From this study, we also conclude that lemma 34 applies to the horizontal orange signals. In particular, if an orange signal crosses a leg of a trilateral, this means that there is a triangle of a smaller generation inside this trilateral. It is indeed the case, as a trilateral of a given generation n, with $n \geq 2$, always contains trilaterals of smaller genration than the generation $n-1$.

A solution for the horizontal signals

The solution for the horizontal signals is inspired from the previous one.

Let us go back to the situation of two triangles T_1 and T_2 of the same generation, within the same latitude, with no triangle of the same generation and the same latitude in between. Let P_1 and P_2 be the triangles which generate the basis of T_1 and T_2 and which are the closest to the appropriate leg of T_1 and T_2, as in the initial description of the problems. The right-hand side leg of T_1 emits right-hand side upper horizontal signals and the left-hand side leg of T_2 emits left-hand side upper horizontal signals, all of them of the colour of T_1. Let n be the generation of T_1 and assume that $n \geq 2$. If there were no triangle nor phantom between T_1 and T_2, this is the case for the generations 0 and 1, the join-tile of the appropriate colour would be the solution.

Now, inside the latitude of T_1, we find two triangles of generation $n-2$, S_1 and S_2 and three phantoms F_1, F_2 and F_3 with the following conditions: S_1 is above S_2, F_1 is above S_1, F_2 is between S_1 and S_2, and F_3 is below F_3. In fact, within the latitude of any of these five trilaterals, we may find several copies of the same trilateral. Now, if an upper horizontal signal comes from T_1 on an isocline which meets a leg of S_1 or S_2, as the left-hand side legs of S_1 and S_2 emit left-hand side upper signals, they meet the signals sent by T_1 with the join-tile. On the right-hand side of S_1 and S_2, the right-hand side legs emit a left-hand side signal and so, we have the same situation with the next copies of S_1 and S_2, until the last right-hand side signals again meet the left-hand side signals emitted on the same isoclines by the left-hand side leg of T_2. Again, the join-tile solves this situation.

Now, for the upper signals travelling on an isocline which meets F_i, the situation is different, as a phantom does not emit signals, except at its corners. However, there is also a simple solution. If the phantom contains a triangle of its colour, this triangle will emit the upper signals which are not stopped by the legs of the phantom as we may assume that their laterality is that of the legs of

the phantom. But the phantom has free rows, exactly as a triangle of the same generation. We already met this property: the structure of the inner trilaterals of a phantom is the same as that of a triangle of its generation. Now, for a free row, lemma 34 forbids the signal to cross the phantom. Now, we can do the same as what we did for the green signal. We simply allow the upper horizontal signals to climb up the leg of the phantom when they meet a free row of the phantom. In the case of a blue phantom, we have exactly the same situation as for the green signal as a blue trilateral exactly has one free row, namely on its mid-distance line.

In a red phantom, the situation is a bit more complex, as there are a lot of free rows. In fact, starting from the deepest upper signal within this latitude, the signal climbs up along the left-hand side leg and stops all the upper signals travelling on the isocline of a free row, inside F. When the climbing signal arrives at the vertex, it goes down, keeping its laterality. Now, going down along the righ-hand side leg of F, each time it meets the isocline of a free row of F, it emits an upper signal of the same laterality outside the phantom and it goes on going down. When the going down signal or the climbing up one meets the isocline of a non-free row inside F, the upper signal travelling on the isocline crosses the leg of F as it will meet a leg of a red triangle. To simplify the managing of this case, the climbing up signal starts from the basis of F and the going down one stops at the basis of F. Again, the laterality of the signal is unchanged while passing over the vertex, as this is the case for the orange signals. Now, the conclusion is clear: the climbing up and going down signals realise two combs on each side of the phantom and they gather up upper signals of the same laterality arriving on the free rows of the phantom. On one side of F, this laterality is different from that of the upper signals which cross the legs of F.

Now, we can see that the two above conditions are satisfied: inside the red phantom, nothing is disturbed and outsie the phantom, the signals behave as if the phantom and its inner phantoms were not present. Also, lemma 34 applies to the signals which travel on the isoclines of the free-rows.

It is easy to check that the join-tile must be used for the red signals which travel on the isoclines of the free-rows of trilaterals which they meet. Due to the conservation of the laterality during the passing of the phantoms, the join-tile must be used but it can be used only once. As lemma 34 is still in force, the signal cannot be used inside the phantom on the isocline of a free row: using the join-tile, we would get wrong lateralities on both sides.

For the upper horizontal signals, we remember the rule: when they meet the leg of the first phantom of their colour at a free row of the phantom, the signal goes up along the leg, possibly joining a similar signal of the same colour and the same laterality, already climbing up along the phantom. In this situation, a red signal also sends a similar red signal along the leg of the phantom, but downwards. When the upper horizontal signal meets the leg of the first phantom of its colour at a non-free row, possibly using the join-tile, it crosses the leg of the phantom and a possible climbing signal.

Note a difference with the orange signal which climbs up along the first

phantom which it meets on the mid-distance line.

Let us give a last precision which will be useful for the description of the tiles.

When we consider two consecutive triangles T_1 and T_2 of the same generation n and within the same latitude, the biggest phantom P which we find on the mid-distance line of T_1 between T_1 and T_2 is of generation $n-1$. And so, the colour of P is opposite to that of T_1. However, in between T_1 and T_2, there are other towers, of lower size, as it follows from another application of lemma 37. For some of these towers, it is possible that their biggest phantom has a generation number of the same parity as n. In this case, the orange signal and the horizontal one of the colour of T_1 will climb up along the leg of the same phantom. Now, we have to not forget that inside a phantom which deviates a horizontal signal, as the free rows remain free, the inner phantoms do not receive a horizontal signal and so, the tiles must also forsee this possibility.

At last, it is interesting to notice that, in the butterfly model, see subsection 3.1, the mechanism of the orange signal forces the green signal to run over the whole isocline which is the mid-point of the latitude which contains no triangle. Indeed, the laterality constraints of the tiles for the crossing of legs of trilaterals prevent an orange signal to run at infinity.

Now, we can conclude that the tiling forces the construction of trilaterals, generation after generation, as indicated by the algorithm of sub-section 4.

6 Completing the proof

6.1 The computing areas

The active seeds were defined in sub-section 5. They allow to define the trilaterals in the hyperbolic plane. Now, to define the **computing areas**, we ignore the blue triangles and their associated blue signals, the phantoms of any colour with the corresponding signals, green and orange signals, as well as the covered parts of the bases of red triangles. Accordingly, we focus our attention on the red triangles only with what occurs inside them: red and yellow signals.

We have already mentioned that lemma 34 applied to horizontal red signals, allow to detect the free rows inside the red triangles. We have also mentioned that the yellow signal, without laterality, marks the free rows of the red triangles.

The free rows of the red triangles constitute the horizontals of the grid which we construct in order to simulate the space-time diagram of a Turing machine.

Now, we have to define the verticals to complete the implementation of the grid in which we perform the simulation.

The vertical consist of rays which cross **8**-centres. We have already met such rays when we defined the border of a sector in sub-section 2.2. Now, such rays have to be connected with a tile of the border of a tree of the manitlla, attached to a red triangle. Figure 27 illustrates how this connection is realized in the different cases of the tile of the border of a red triangle which receives a yellow signal. As indicated in [15, 18], the border of a tree is periodic after the tile

which follows the root of the tree. The periodic pattern consists of the three tiles: $11 \circ 2$, G_r and $1 \circ 15$ for the right-hand side border and $6 \circ 77$, G_ℓ and $37 \circ 7$ for the left-hand side one. In each case, the vertical goes to the closest **8**-centre which is in the area of the tree.

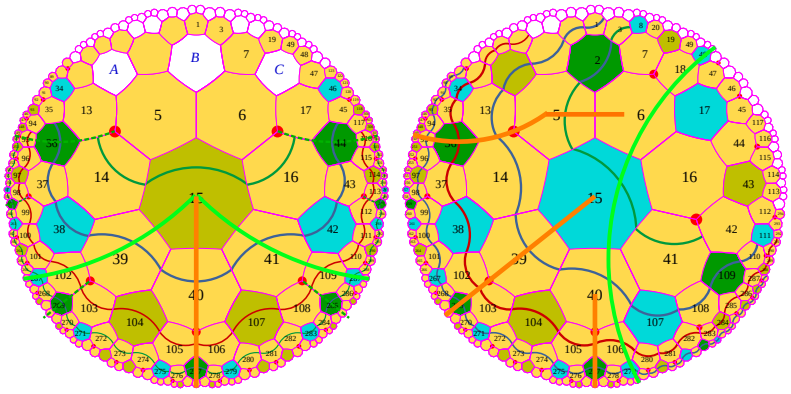

FIG. **27** The vertical starting from a point of the border of a triangle which represents a square of the Turing tape.
On the left-hand side: the case of the vertex. On the right-hand side, the three other cases for the right-hand side border are displayed on the same figure.

Note that, in figure 27, the vertical signal is represented by a ray. This is not exactly the case. Looking at the left-hand side picture of the figure, the signal goes from the tile 15 to the tile 40, then from the tile 40 to the tile 105 and from there to the **8**-centre, the tile 277. In terms of petals and of the denotations of tables 2, 1 and 8, the route is as follows:

$$Fb,\ 1\overline{4}7 \circ w,\ 2 \circ 77w,\ \mathbf{8},$$

and then, periodically: $1\overline{4}7 \circ w,\ 2 \circ 77w,\ \mathbf{8}$.

In the right-hand side picture of figure 27, the three cases of signals starting from a tile of the right-hand side border are represented. In terms of petals and centres, the aperiodic part of the routes, up to the first **8**-centre, is given as follows:

- from a tile $11 \circ 2$: $11 \circ 2b,\ 137 \circ b,\ 2 \circ 77w,\ \mathbf{8}$;
- from a tile G_r: $G_r b,\ 47 \circ 7w,\ 6 \circ 77w,\ \mathbf{8}$;
- from a tile $1 \circ 15b$: $1 \circ 15b,\ 2 \circ 77w,\ \mathbf{8}$.

Similar initial parts of verticals can be defined for the left-hand side border of a tree. This is left as an exercise to the reader.

The verticals represent the history of a square of the Turing tape. Accordingly, each tile of the vertical which is on the border represents an empty square, *i.e.* a square containing the blank. The computing signal starts from the seed. It travels on the free rows. Each time it meets a vertical, this means that the head of the Turing machine scans a square of the tape: the square whose content is conveyed by this vertical. As the current state of the machine is conveyed

by the computing signal, the corresponding instruction can be performed. If the direction of the motion of the head is not changed and if the corresponding border is not reached, the computing signal goes on on the same row, and now, the vertical conveys the new content of the same square of the tape. Otherwise, the computing signal goes down along the vertical signal with the new state of the Turing machine, the new content of the tape and the direction of the move of the head. When the next free row is met, the new content goes on on the vertical and the computing signal goes on its travel on the new row, in the direction indicated for the move and with the new current state.

Concrete details for the implementation are dealt with in the next sub-section, devoted to the precise description of the tiles. They are rather close to the classical proofs.

6.2 Description of the tiles: the proto-tiles

In this sub-section, we shall describe as precisely as possible the tiles needed for the constructions defined in the previous sub-sections, the tiles associated with the computing areas being described in the next sub-section 6.3. As we introduced several changes with respect to [18, 15], the present description introduces a few changes and append a few types of new tiles. Also, we proceed to the counting of the tiles in a different way.

The set of tiles to which we turn now is called the set of **prototiles**. A prototile is not a true tile. Indeed, a tile is a copy of a prototile. Better, a tile is the indication of two data: the location of a tile in the heptagrid and the indication of a copy of the prototile which is placed at this location.

The set of prototiles forces the construction of the mantilla with the isoclines. It also forces the activation of the seeds and the consecutive construction of the interwoven triangles, including the detection of the free rows in the red triangles.

In the definition of the tiles, lemma 25 plays an important rôle. As the tiles have a very **local** character, it is important to look at all possibilities. In many regards, lemma 25 tells us that, putting aside the exceptional case of the position 0 in a realization of the butterfly model, any tile is always eventually in some triangle T. The fact that T itself is or not inside a bigger triangle depends on the cut of the model which is implemented by the thread to which T belongs. On another hand, the accompanying signal of the same colour of a basis allows us to know by its presence or absence whether the considered tile of the basis is inside or outside a trilateral of the generation of the basis.

All the prototiles are constituted by tiles of the format given by figure 8 on which we append several signals.

All signal which appear on a prototile may be described as a **superposition** of **elementary** signals. In their turn, elementary signals are defined in terms of a few **basic** signals combined by the applications of **masks**.

We have four kinds of basic signals: vertical, horizontal, uniform and lateral signals. There are also colours associated to the signal as well as a thickness.

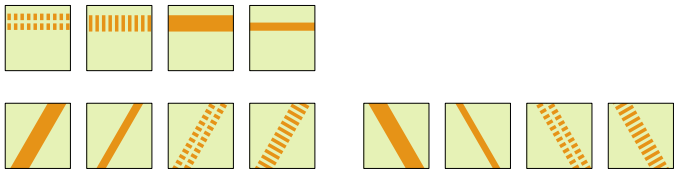

FIG. **28** The basic signals for the prototiles.
First row: horizontal signals. Second row: vertical signals. On the left-hand side: the left-hand side verticals; on the right-hand side: the right-hand side ones.

Figure 28 illustrates these signals, but without colours. It is not difficult to imagine them in the appropriate colours defined in sub-section 5.

Note that the tiles of figure 28 are squares. This is suited for the Euclidean implementation. Now, it is not difficult to see that it is also convenient for the hyperbolic plane. The correspondence between the sides of a square and those of a regular heptagon is easy. Denote the sides of the square by the self-evident notations n, w, s and e, and denote the sides of a heptagon by its local numbering. The correspondance is given by table 13. It is also illustrated by figure 29.

TABLE **13** Correspondence between the square and heptagonal tiles. For the latter ones, the correspondence also depends on the status of the tile: black or white.

square	heptagon	
	black	white
n	1,2	1
w	3	2
s	4, 5, 6	3, 4, 5, 6
e	7	7

Note that from the study of sub-sections 5 we know that the vertical signals connected with a trilateral go along black tiles only. A left-hand side signal goes from the side 1 to the side 4, and a right-hand side signal goes from the side 2 to the side 6. As the local numbering is known by the tile by the position of the isocline signal, the tile also knows the laterality of a vertical signal.

For the colours, we distinguish between the **skeleton** signals and the **control** ones. The skeleton signals materialize the trilaterals. The control signals implement the horizontal signals emitted by the trilaterals, the scent and the signals which they emit as well as the auxiliary synchronization signals which we introduced in sub-section 5.2.

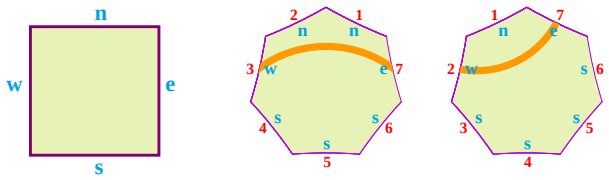

FIG. **29** The translation from a square tile onto heptagonal ones.
From the left to the right: the square, a black heptagon and then, a white one.

For the skeleton, we have three colours: **blue-0**, **blue** and **red**. The blue-0 colour is given to the generation 0 and only to it. The blue colour is given to the generation with a positive even number, and the red colour is given to those with an odd number. This is dictated by the construction of sub-section 4. The distinction between triangles and phantoms is implemented by the thickness of the signal. Triangles are represented by thick signals. Phantoms are represented by thin ones. We distinguish between the first and the second halves of legs by **hues** in the colours. In red trilaterals, the first half is dark while the second half is light. In blue-0 and blue trilaterals, the first half is light and the second half is dark. The basis always has the same hue as the second half of the legs: this is conformal to the matching at corners. Note that the blue-0 colour is needed to force the generation 0. Blue-0 and blue triangles determine the red trilaterals. By the distinction between blue-0 and blue, the red triangles determine blue trilaterals only.

Now, the elementary signal involve **masks** which allow to cut out a part of the basic signal. There are four kinds of masks: the left-hand side mask, which hides the right-hand side half of the tile; the right-hand side mask, which hides the left-hand side half; the upper mask, which hides the lower half of the tile and the lower mask, which hides its upper half. Also, elementary signals have a colour and, for horizontal signals, they have a **position**.

To define this latter notion, we define five **channels**, from top to bottom, numbered from 1 up to 5:

- **channel 1**, the signals emitted by the legs: blue or red, left-hand side or right-hand side; note that the dotted structure representing the lateralitites allow us to have both red and blue horizontal signals on the same channel;
- **channel 2**, the special signal traveling on the mid-distance lines of a trilateral: green or orange; remember that the green signal is uniform while the orange one has a laterality;
- **channel 3**, the signal of the isocline crossing the tile; it joins the mid-point of the side 2 or 3 to the mid-point of the side 7;
- **channel 4**, the signal of a free row, if any;
- **channel 5**, the skeleton signal of a basis.

For vertical signals, we have two channels: one for the skeleton signal, necessarily that of a leg, possibly with a mask, and one more for a possible orange signal or a coloured one or even both, always with a laterality which is independent of the laterality of the leg.

We can notice that the possible values for the channels are not completely independent. As an example, if the tile is on an isocline 0, the skeleton is necessarily that of a phantom of generation 0. We know that there is a possible yellow signal on the channel 4. On another hand, if the tile is on an isocline 5, there is no yellow signal and the skeleton is necessarily that of a red phantom or of a red triangle, in fact of generation 1.

We may define the tiles as follows. First, we define the general compatibility conditions. For this purpose, we define three parts of a leg, excluding vertices and corners which we consider as characteristics of the bases. The three parts are: the first half of the leg, the mid-point tile and the second half of the leg. Similarly, we can define three attributes for the bases: vertex, plain and corner. By definition, a plain basis is a part of the basis where there is no vertex and no corner. Now, we can define a table, see table 14 below, which indicates the possible meetings of legs with bases. We append a fourth row for an empty leg: this means that we have a basis which meets no leg for the considered tile. Note that, on another hand, a leg always meets a basis. Indeed, in the case of a butterfly model, we shall consider that the green signal which crosses the hyperbolic plane from the left to the right is accompanied by the basis of an infinite trilateral. But, as bases travel on isoclines 0, 5, 10 and 15 only, we have a fourth column for no basis, which corresponds to the meeting of the legs with the other isoclines.

And so, we have nine basic cases, denote them by $C_{1,1}$, $C_{1,2}$, $C_{1,4}$, $C_{2,2}$, $C_{3,2}$, $C_{3,3}$, $C_{3,4}$, $C_{4,2}$ and $C_{4,4}$, in obvious notations. Now, in each case, there are conditions which restrict the choice of the parameters which enter the definition of the leg and/or the basis.

From the lemmas of sub-section 4 and 5, we have the following constraints. Note that in theses conditions, when not specified, the word 'leg' alone means 'leg of a trilateral'.

- c_1: the leg of a triangle may meet an open basis of a triangle, only if the colours are different;
- c_2: a horizontal lateral signal crosses a leg of its colour only if its laterality is that of the leg;
- c_3: the first half of a leg meets covered or uncovered bases, leaving them unchanged in this regard;
- c_4: the second half of a leg meets covered bases only;
- c_5: when there is a yellow signal, always inside a red triangle, there is no horiontal red signal inside the triangle, on this row;
- c_6: the yellow signal never travels on the isoclines 5; it may travel on the others;
- c_7: the green an orange signals occur on isoclines 15 only;
- c_8: an orange signal cannot cross the mid-point tile of a trilateral;

- c_9: an orange signal crosses first and second halves of legs, only of its laterality.

Certain constraints concern all the situations, namely c_5, c_6 and c_7. Others concern several cases or sometimes a single one.

TABLE **14** *Compatibility conditions of a leg with a basis. The last row indicate the case when the basis is present but not the leg. The last column indicates the case when the leg is present but not the basis.*

	vertex	plain	corner	empty
first half	YES	YES	NO	YES
mid-point	NO	YES	NO	NO
second half	NO	YES	YES	YES
none	NO	YES	NO	YES

If there were no constraints, it would be enough to multiply the number of possible signals for each channel, horizontal and vertical, and to multiply all of them in order to count the tiles. As this is not the case, we have to exactly number the cases which satisfy the required constraints: they will be taken into the counting, and only them.

First, we look at the case $C_{4,2}$, for which the number of constraints is the smallest. Then, we shall look at the situation of legs which do not meet a basis, the cases $C_{1,4}$ and $C_{3,4}$, first and second halves respectively.

Case $C_{4,2}$

The possible values for the different horizontal channels are given by table 15, below. The table indicates 3600 possible patterns. However, as we shall soon see, this is a very high estimate. As an example, we can see that the choice of certain values is more restricted on certain isoclines than on the others. And so, the actual number is much lower.

Let us briefly explain the indicated values of the horizontal channels which we denote by hc_i, with $i \in \{1..5\}$, in the table.

For hc_3 and hc_4, the values immediately follow from the definition of the channel. For hc_1, we have two possible colours, blue and red, two possible lateralities, L and R and for each one, but not together, there is the possibility of a join pattern. Also, there are cases when the basis is accompanied by a single signal. This is the case, for a blue one, inside the triangles of generation 1. This may be the case, for a red signal, on an isocline 15. There may be both signals on most isoclines 15 and there may be no horizontal signal at all in the channel 1 on an isocline 15, for instance inside a phantom of generation 0.

For hc_2, the five values which are indicated correspond to the possibilities dictated by the definition. Note that a signal is present on this channel only

on an isocline 15. For hc_5, as there is a basis on each isocline 0, 5, 10 or 15, we have three possible colours and the choice of a triangle or a phantom. The value of this latter parameter is called the **status** of the basis.

TABLE **15** Denotation of the possible values on the horizontal channels of a tile.

hc_1	hc_2	hc_3	hc_4	hc_5
ϵ, $b\xi$, $r\xi$, bj, rj, $b\xi_1 r\xi_2$, $bjr\xi$, $b\xi rj$	ϵ, g, $o\xi$, oj	0, 5, 10, 15	ϵ, y	$\gamma\xi$, $\gamma \in \{b_0, b, r\}$, $\sigma \in \{\tau, \varphi\}$
15	5	4	2	6

NOTE: In hc_1, $\xi, \xi_1, \xi_2 \in \{L, R\}$.

In the counting of the prototiles corresponding to the case $C_{4,2}$, we separate the cases according to the number of the isoclines, so that hc_3 has a single value in each case. These values are indicated in table 16. The encercled number which is in the first column of the table indicates the case which is analyzed by the corresponding the row. Just below, a row with small numbers indicates the number of possible values for each channel. The product is indicated, for this case, in the last column. The row with the small numbers is called the counting row.

Let us first consider the case of an isocline 0. We know that, in this case, the basis is that of a phantom of generation 0: we have a thin blue-0 basis. If we are on an isocline 10, the basis is that of a triangle of generation 0 and so, we have a thick blue-0 basis. This fixes the value of hc_5 when that of hc_3 is fixed.

Assume that there is a yellow signal in the channel 4: this is the case under the row (1) in table 16. Accordingly, we are inside a red triangle of generation 1. And so, there is no red signal on the channel 1. There may be a blue signal if we are in between the triangles of generation 0 which generate the basis of this red triangle. And so, we exactly have the indicated numbers of the counting row.

Next, assume that there is no yellow signal in the channel 4: this is the case under (2) in table 16. Then, the tile may be almost anywhere. It is not difficult to see that the occurrence of both red and blue horizontal signals can easily be realized on an isocline 0 or 10. Let us see that the case when there is no signal on the channel 1 and the case when there is only one coloured signal in this channel are also possible. The case when there is no signal occurs inside a red phantom P of generation 1: the rows inside P are free but they are not marked as yellow, as we are inside a phantom. Now, inside P there are triangles of the generation 0. There is a basis of such a triangle T inside P. Inside T, the basis is open, and so it has no blue signal. This is for the isocline 0. Now, P also contains a phantom P_0 of generation 0. The same argument as for T, applied to the basis of P_0 gives us a situation where there is no signal in the channel 1

on an isocline 0. Now, outside P_0 or T, we have parts of the considered bases which are covered. Accordingly, we have the occurrence of a blue signal without red signal. It remains to see that the situation with a red signal without a blue one is also possible. This is the case, for instance, in between two triangles of generation 1, inside a trilateral of generation 0. From lemma 34 and from the configuration of the join-tiles, there cannot be a horizontal blue signal inside a blue 0 trilateral.

TABLE **16** Table of the values for the horizontal channels of a tile in the case $C_{4,2}$.

	hc_1	hc_2	hc_3	hc_4	hc_5	#
(1)	ϵ, $b\xi$, bj	ϵ	0 | 10	y	$b_0\varphi$ | $b_0\tau$	
	4	1	2	1	1	8
(2)	*all*	ϵ	0 | 10	ϵ	$b_0\varphi$ | $b_0\tau$	
	15	1	2	1	1	30
(3)	*all*	ϵ	5	ϵ	$r\sigma$	
	15	1	1	1	2	30
(4)	ϵ, $b\xi$, bj	g	15	y	$b\sigma$	
	4	1	1	1	2	8
(5)	ϵ, $r\xi$, rj	g	15	ϵ	$r\sigma$	
	4	1	1	1	2	8
(6)	ϵ	g	15	ϵ	$b\sigma$	
	1	1	1	1	2	2
(7)	$\gamma\xi$, γj, $\gamma j\overline{\gamma}\xi$, $\gamma\xi_1\overline{\gamma}\xi_2$, $\gamma\xi\overline{\gamma}j$	$o\xi$, oj	15	ϵ	$\overline{\gamma}\sigma$	
	11	3	1	1	4	132
total:						218

NOTE: *all* indicates all the 15 values of table 15 for the channel 1.

Now, let us consider the case of an isocline 5: it is under (3) in table 16. We always have a red basis, either of a triangle or of a phantom. Of course, there is no yellow signal and we have again ϵ on the channel 2. We have just to check that all cases are possible for the channel 1. Again, the occurrence of both blue and red signals is not difficult to realize. Let us see that the case with no signal is possible: from the discussion of the previous case, this is the case inside a blue-0 triangle T_0 which generates the basis of a triangle T of the generation 1. The basis of T is open inside T, hence it has no red signal and it has no blue signal inside T_0. This same situation, on the basis of T and outside

the triangles of generation 0 gives us a situation where we have a blue signal only. The situation of a red signal only occurs around the vertex of T which is also on an isocline 5, but inside another triangle T_1 of generation 0. Accordingly, there is no red signal. But the vertex of T may be in a part of an isocline 5 which is not covered by a red phantom. And so, in this case, the red signal is alone present.

Now, we arrive to the situations of an isocline 15. First, we consider the case when we have both a yellow and a green signal, then the situation when we have the green signal only and, at last, the situation when we have the orange signals, which, clearly, rule out a yellow signal.

So, if the green and the yellow signal are both present, which is the case under (4) in table 16, the tile is on the mid-distance line of a red triangle. By the algorithm of sub-section 4 and by the synchronization principles, see sub-section 5.2, the basis occuring in the channel 5 is blue. It cannot be a blue-0 basis, as red triangles do not generate the generation 0. Of course, the status of the basis is not fixed. We know that there is no red signal on the channel 1. There may be no blue one: this is the case if the trilateral corresponding to this basis exists at this point of the considered latitude. If it does not exist, the basis is covered and so, we then have a blue signal on the channel 1. This situation may happen. Consider to contiguous active seeds σ_1 and σ_2 on an isocline 0 with, for instance, σ_1 on the left-hand side of σ_2, on the isocline of the remotest ancestor of T. Consider the rightmost branch β_1 defined by the scent starting from σ_1 and the leftmost branch β_2 defined by the scent starting from σ_2. Then, within the same latitudes of trilaterals along β_1 the trilaterals which are realized between β_1 and β_2 belong to smaller generations than that of T within its latitude.

Assume that we have no yellow signal, but that the green signal is still present. As the green signal is present, we are inside a trilateral, on its mid-distance line.

If we are inside a triangle, it must be blue, as a red one would require the occurrence of a yellow signal. And so, the basis on the channel 5 is red. The red basis may be open or covered, depending on the realization or not of the red trilateral possibly generated by the blue triangle.

If we are inside a phantom P, we have the green signal and no yellow one. If we are on the mid-distance line of the infinite tower of a realization of the butterfly model, there is no blue nor red signal on the channel 1. This case is (6) in table 16 when the basis is blue and it is with (5) when the basis is red. And so, assume that the tower to which P belongs is finite. Let T be the triangle which closes the tower. As we have no yellow signal, T is necessarily a blue triangle and we have the already discussed situation and so, the possible accompanying signal is red only.

The situations are grouped under (5) and (6). Under (5), we only have the case when the basis is red. Under (6), we have the case when the basis is blue. Note that, in this case, it cannot be accompanied by a blue signal in the channel 1, which corresponds to the butterfly model.

At last, we have the situation when we have an orange signal in the channel 2, which is under (7) in table 16.

In this case, we are necessarily on a covered basis, on the common mid-distance line λ of two triangles T_1 and T_2 of colour γ, between T_1 and T_2. Note that, as we are on an isocline 15, the colour cannot be blue-0 as the mid-distance line of a blue-0 triangle is an isocline 5. Note that the seeds on λ generate a basis of colour $\overline{\gamma}$ which we find on the channel 5. Depending on whether the trilateral associated to this basis is realized or not on the considered part of λ where our tile is, the basis is opened or not and so, me may have a signal $\overline{\gamma}$ on the channel 5. Accordingly, we have all the situations indicated by the table.

Now, table 16 only looks at the horizontal channels of the tile. Now, the tile must be superposed to a tile of the mantilla. We have 33 patterns for these tiles and so, this gives us 7194 prototiles. However, we have to take into account that the tiles may receive or not the scent. Below, table 17 indicates the structure of the tiles with respect to the scent depending on the pattern of the mantilla and of the number of the isocline.

TABLE **17** Table of the effect of the scent on a basis. For each entry, the left-hand side indicates what happens if the tile does not receive the scent and the right-hand side indicates what happens when the scent is received.

	0	5	10	15
seed	**e/t**	**i/t**	**i/t**	**i/t**
others	**i/h**	**i/h**	**i/h**	**i/h**

NOTE: **e**, **i**, **t**, and **h** mean **emit**, **idle**, **transmit** and **halt** respectively.

Indeed, from the table we check that when the tile receives the scent, it stops it if it is not a seed. If it is a seed, it transmits it. If the tile does not receive the scent, it does nothing, except a seed on an isocline 0 which then, emits the scent.

Accordingly, for each tile, we have exactly two different possibilities with respect to the scent. And so, this defines 14,388 prototiles. In fact, we can significantly reduce this number by introducing the following constraints:

- c_{10}: a tile can receive at most one join-pattern for horizontal signals of the same colour with lateralities;
- c_{11}: a join-tile for horizontal signal with lateralities of the same colour must be placed on the border of a sector.

Note that, in table 16, we already implemented the constraint c_{10}. The constraint c_{11} does not appear in the table, but it appears in the counting. From c_{11} we conclude that the patterns of the table must be multiplied by 33 when no j occurs in the pattern and, when this is the case, the corresponding tile must be multiplied by 3. Indeed, we consider that, in terms of tiles, the border of a sector is defined by the tiles described in sub-section 6.1. Taking into account these constrain together with the effect of the scent, we obtain that

table 16 defines 8,988 prototiles.

Case $C_{1,4}$

Now, we turn to the situation when the tile is on the first half of a leg and when it does not meet a basis.

As a general remark, note that for a triangle, we have two lateralities and three possible colours, which makes 6 cases. For a phantom, we have still two lateralities and three possible colours. But a phantom may receive an orange signal or a coloured lateral signal or both. For each colour and for each laterality of the leg, these possibilities, for a phantom, represent 9 cases. We discuss them according to the isoclines and the possible patterns of the mantilla.

TABLE **18** Counting the first half of the legs.

	triangle	phantom	isocline	mantilla	partial
blue-0	2	18	4	1	80
blue	2	18	1	1	20
blue	2	18	16	3	960+80
red	2	18	2	1	40
red	2	18	16	3	960+80
total					2220

NOTE: On each row, we sum up the first two columns and then, we multiply the result by the product of the two next column. This new result is put on the last column. The added numbers in the last column indicate the contribution of additional tiles for the scent which is counted in the other rows.

For the blue-0 trilaterals, the first half concerns the isoclines 1..4 for a triangle and the isoclines 11..14 for a phantom. It is not difficult to see that the tiles of the mantilla which are on these places are fixed by their position on the border and by their distance from the root. Which justifies the corresponding row of the table.

Now, the situation is different for the blue and red trilaterals. What remains is that the first tile following the root is always the same. It occurs on the isoclines 16 for the blue trilaterals and on the isoclines 6 or 16 for the red triangles. For the other isoclines, any tile belonging to a period of a border is possible. There is three possibilities for each laterality. Also note that the isoclines which are concerned by the case $C_{1,4}$ are the isoclines 1..4, 6..9, 11..14 and 16..19 which means 16 isoclines.

Now, we have to consider the possible contribution of the scent. The first half of a blue-0 trilateral always contains the scent, by definition of the scent. The scent is also present on the legs for the first five isoclines following the root. But these isoclines may also not bear the scent when the length of the

leg becomes important. And so, we have to append the tiles for the scent: they concern the four isoclines which follow the root and so on each isocline, the tile of the mantilla is fixed by its position on the border. Accordingly, this makes $20\times4 = 80$ new prototiles for each colour. They appear on the appropriate row of the table. Accordingly, we obtain 2,220 prototiles for the case $C_{1,4}$.

Case $C_{3,4}$

This time, we consider the case of a second half. We have the same analysis as previously with several simplifications. For the phantoms, there is no orange signal, nor blue climbing signal. However, there may be a red climbing signal for a red phantom. Moreover, on the second half, we are always on the periodic part of the border, the tiles being still fixed by the position in the case of the blue-0 trilaterals. At last, there is no scent to be taken into account.

The information is gathered in table 19.

TABLE **19** Counting the second half of the legs.

	triangle	phantom	isocline	mantilla	partial
blue-0	2	2	4	1	16
blue	2	2	16	3	192
red	2	6	16	3	384
total					592

NOTE: On each row, we sum up the first two columns and then, we multiply the result by the product of the two next column. This new result is put on the last column.

Case $C_{1,1}$

Now, we deal with the vertices of the trilaterals. First, we notice that their pattern can be described in terms of basic signals, combining them with appropriate masks. Denote by $L_\pi\gamma\sigma\xi$ the basic signal of a leg, where the status σ is in $\{\tau,\varphi\}$, where the colour γ is in $\{b_0,b,r\}$, where the laterality ξ is in $\{L,R\}$ and where π indicates which half of the leg we consider, with π in $\{1,2\}$. Denote by μ_α the operator consisting in applying a mask, with α in $\{u,d,\ell,r\}$. Then, the vertex of a phantom has the general form $\mu_d(L_1\gamma\varphi L)+\mu_d(L_1\gamma\varphi R)$, and that of a triangle has the general form $\mu_d(L_1\gamma\tau L)+\mu_d(L_1\gamma\tau R)$, see figure 31. Fitted with appropriate colours, we call these signals **elementary**. It is not difficult to see that, for triangles, we have just defined 3 patterns. For phantoms, we have this number of patterns multiplied by the number of cases connected with the possible presence of climbing signals. As there are two lateralities for each signal and as two of them at most can be present, the orange one included, when there are two signals, we get 27 patterns. And so, there are 30 elementary signals representing a vertex.

However, a vertex stands on an isocline 0, 5, 10 or 15 and so, it is accompanied

by a basis. We take benefit of table 16 in order to extract the bases and their accompanying signal which can be met by a vertex. From the constrain c_{11}, we know that we can rule out any basis which has the join-pattern of a horizontal signal. We discuss the different cases according to the isoclines. For each one, table 20 indicates the vertices and the bases which meet.

On an isocline 0, we can only have the vertex of a blue-0 triangle: a single pattern. Now, on an isocline 10, we only have the vertex of a blue-0 phantom, and we know that there are 9 patterns. On an isocline 5, we have a red trilateral: either a red triangle, 1 pattern, or a red phantom, again 9 possible patterns. On an isocline 15, we have the vertices of blue or red trilaterals. For each colour, the counting of the isocline 5 shows that we have 10 patterns, and so we get 20 patterns, as indicated in the table.

Let us look at the possible meetings with a basis.

On an isocline 0, we may meet only a basis of a blue-0 phantom. All cases of table 16 are possible.

TABLE **20** The counting of the prototiles for the vertices.

isocline	0	5	10	15	total
vertex	$b\tau$	$r\sigma + K$	$b\varphi + K$	$\gamma\sigma + K$	
	1	10	9	10+10	
basis	y, $b\xi y$, ϵ, $b\xi$, $r\xi$, $b\xi_1 r\xi_2$	ϵ, $b\xi$	ϵ, y	$\gamma\sigma + K$	
	12	3	2	3+4	
scent	2	1	1	1	
#tiles	24	30	18	70	142

NOTE: K represents the repetition of the same pattern entailed by the different possible lateral signals accompanying the leg of a phantom, also at the vertex.

Now, consider the case of an isocline 5. The vertex is raised inside a blue-0 triangle. Accordingly, there is no horizontal blue signal. There may be a red signal on the channel 1. And so, only three cases are possible, those which are indicated by the table.

In the case of an isocline 10, by construction of the scent, we are inside a red trilateral of generation 1 whose vertex is on an isocline 5: there cannot be a red signal. And so, the father of this red trilateral exists, which is a blue-0 triangle. This means that the basis where occurs the vertex on the isocline 10 is open: there cannot be a blue signal. Now, there can be a yellow signal, hence the two signals indicated by the table.

At last, we arrive to the situation of an isocline 15. By definition of the construction of the trilaterals, there is a green signal as the vertex is on an

isocline 15: it is generated on the mid-distance line of a triangle. By the scent constraint, the vertex is inside a blue-0 phantom. And so, there cannot be a blue signal. There can be a red signal, in this case the trilateral is red, as the basis can be covered as already noticed. If there is no red signal, there can also be a yellow signal: the basis is blue, and so is the vertex. At last, there can be no signal at all, for instance on the mid-distance line of a tower of phantoms. And so, independently of the colour of the vertex, there may be no signal or a red one on the channel 1. There can also be a yellow signal, only if the vertex is blue. And so, we have the cases indicated in the table. As we separately multiply the indications of the basis and the vertices for the isocline 15, depending on the colour of the vertex, we obtain the 70 patterns indicated in the last row of the table.

Accordingly, we find 142 prototiles.

Case $C_{1,2}$

This time, we arrive to an important sub-case, also from the point of view of the number of prototiles: this case corresponds to the crossing of the first half of a leg with a basis.

We present the counting of the tiles in table 21 and we describe the tiles in the justification of the counting. Note that the table contains four column which correspond to four items among the seven rows of table 16. For a convenient correspondence between the tables, the columns of table 21 have the same number as the corresponding row of table 16. The first column of table 21 indicates the case of the leg, together with a multiplicative coefficient used in the counting: 2 for a triangle, as the leg has two possible lateralities, 18 for a phantom as, besides the laterality of the leg, the phantom may be accompanied by an orange signal, a coloured one or both signals. In the second row of the table, we remind to which isocline the different cases refer. Then, each row indicates the case of the leg. The last column indicates the number of the patterns.

Now, in the table, we assume that the laterality of the leg is fixed. It is called ξ. Also note that the legs are either blue or red. The colour blue-0 is ruled out: the leg of a trilateral of generation 0 meet either an isocline 5 or an isocline 15, but it is always at the mid-point tile of the leg. And so, we have four cases for the leg which we denote by $b\tau$, $b\varphi$, $r\tau$ and $r\varphi$. Also note that from lemma 8, the condition c_{11} rules out the presence of a join tile on the leg of a trilateral. This significantly reduces the number of tiles.

The first remark deals with the selection of the columns. Indeed, the cases (4), (5), and (6) of table 16 concern the case when a basis is acompanied by a green signal. By the principles of the algorithm of sub-section 4, the meeting of a leg with a green signal triggers the change from the first half to the second one which is materialized by the mid-point tile of the leg. By definition, the first and second halves of a leg do not contain this tile. Accordingly, these rows are ruled out.

Consider the first half of a leg of a blue trilateral T. We shall discuss the case of a triangle and of a phantom at the same time.

TABLE **21** The counting of the prototiles for the crossing of bases with the first half of a leg of a trilateral.

cases	①	②	③	⑦	total
isocline	0,10	0,10	5	15	total
$b\tau$, 2	y, $yb\xi$ + $yb\xi$	ϵ, $b\xi$, $b\xi r\xi_2$ + $b\xi$, $b\xi r\xi_2$	$b\xi$, $b\xi r\xi_2$	$b\xi$, $b\xi r\xi_2$ | $b\xi r\xi_2$ + $r\xi_2$, $b\xi r\xi_2$	
	2+1	4+3	6	3×2+(2+2×2)	56
$b\varphi$, 18	y, $yb\xi$ + $yb\xi$	ϵ, $b\xi$, $b\xi r\xi_2$ + $b\xi$, $b\xi r\xi_2$	$b\xi$, $b\xi r\xi_2$	$b\xi$, $b\xi r\xi_2$ | $r\xi_2$, $b\xi r\xi_2$	
	2+1	4+3	6	(3+4)×2	540
$r\tau$, 2	$yb\xi$ + $yb\xi$	$r\xi$, $b\xi r\xi$ + $r\xi$, $b\xi r\xi$	$b\xi r\xi$ + $b\xi$, $b\xi r\xi$	$b\xi_2 r\xi$ + $b\xi_2$, $b\xi_2 r\xi$ | $r\xi$, $b\xi_2 r\xi$	
	1+1	2+2	3	6+2×3	56
$r\varphi$, 18		ϵ, $b\xi_2$, $b\xi_2 r\xi$ + $b\xi_2$, $b\xi_2 r\xi$	$b\xi r\xi_2$ + $b\xi_2$, $b\xi_2 r\xi$	$b\xi_2$, $b\xi_2 r\xi$ | $r\xi$, $b\xi_2 r\xi$	
	0	5+4	6	(4+3)×2	522
total:					1174

NOTE: In the columns ① and ②, the sign + separates the case of an isocline 0, on the lef-hand side, from that of an isocline 10, on the right-hand side. Similarly, in the column ⑤, when needed, the sign + distinguishes between the case of the basis of a triangle and that of a phantom respectively. In the column ⑦, the symbol | distinguishes between the case when γ is blue, and the case when it is red. Inside a fixed colour of γ, if present, the sign + distinguishes between triangles and phantoms as for the column ⑤.

If we meet the isocline 0, we have the basis of a blue-0 phantom. As we have the case ①, the yellow signal is present. The basis may be covered or not: this defines 2 cases, and it is easy to see that both cases occur. An open basis of a blue-0 phantom is crossed by any leg which is triggered on the isocline 15 which crosses this phantom. Such a situation occurs with any blue trilateral of generation at least 2. The situation with a covered basis is obtained when a trilateral of generation $n+2k$, with $k > 0$ cuts the basis of

a triangle of generation n which it contains. On the isocline 10, the basis is that of a triangle. It is necessarily a triangle of generation 0. Now, a triangle of generation 0 contains no trilateral and it triggers trilaterals of generation 1 only. Accordingly, a leg of a blue trilateral cannot occur inside a **triangle** of generation 0. And so, the only possible meeting with a basis on an isocline 10 is with a blue signal.

Now, consider the case (2). We still meet an isocline 0 or 10 but, this time, the basis is not accompanied by a yellow signal.

If we meet the isocline 0, we again have the basis of a blue-0 phantom. Note that T belongs to a positive even generation. And so, this isocline 0 is crossed by red trilaterals of the generation 1. If such a red trilateral is a triangle, we necessarily have a red signal together with the blue signal. If it is a phantom, we may have a blue signal only. This is the case if the leg comes from a vertex which is inside a tower of phantoms with at least one alternation. Now, notice that we cannot have the red signal alone, as inside a triangle R of the generation 1, there is at least an isocline 0 with a blue signal on it which is generated by a phantom of generation 0 which must exist, as R exists. Now, as another possibility, it is easy to see that the leg may be crossed by both a red and a blue signal. In all cases the blue signal has a single laterality: that of the leg. And so, we have the signals listed in the table.

If we meet the isocline 10, we have the basis of a blue-0 triangle T_0. The basis must be covered, by the same argument as we have seen in the case (1). But it is also accompanied by a red signal as T contains at least legs of red triangles of generation 1. And so, the isocline 5 which crosses T_0 must be covered when it crosses T as T belongs to a bigger generation. And so, we necessarily have the signals $b\xi$ or $b\xi r\xi_2$, giving rise to 3 cases. Note that $b\xi$ occurs when a triangle of generation 2 cuts the basis of a triangle T_0 of generation 0, of course outside T_0.

Now, consider the case (3). This time, the leg meets an isocline 5. Hence, we have a red basis. It cannot be generated by T, as T belongs to a bigger generation. The basis may be covered or not: if T is generated by a triangle T_1 of generation 1, then the basis is open and it has a blue signal, emitted by the father of T_1. Now, the red basis may be that of a phantom of generation 1. Again, we have the same situation as T may be raised in a tower of phantoms with at least one alternation. In the other situations, blue and red signals are both present.

At last, we arrive to the case (7). In fact, we can have here a discussion in general terms. From the analysis performed to establish table 16, we know that the signal $\gamma\xi$ is present, ξ being fixed and γ being possibly either blue or red. We also know that there is a basis of the colour $\overline{\gamma}$. Consider two consecutive triangles T_1 and T_2 of the colour γ within the same latitude. On the isocline λ of their mid-distance line, which is an isocline 15, they generate a basis of the colour $\overline{\gamma}$. In between T_1 and T_2, the basis is covered by a signal oR and oL. From lemma 38, see sub-section 5.2, we know that there is at most one leg of a generation higher than that of T_1. Accordingly, the situation which we

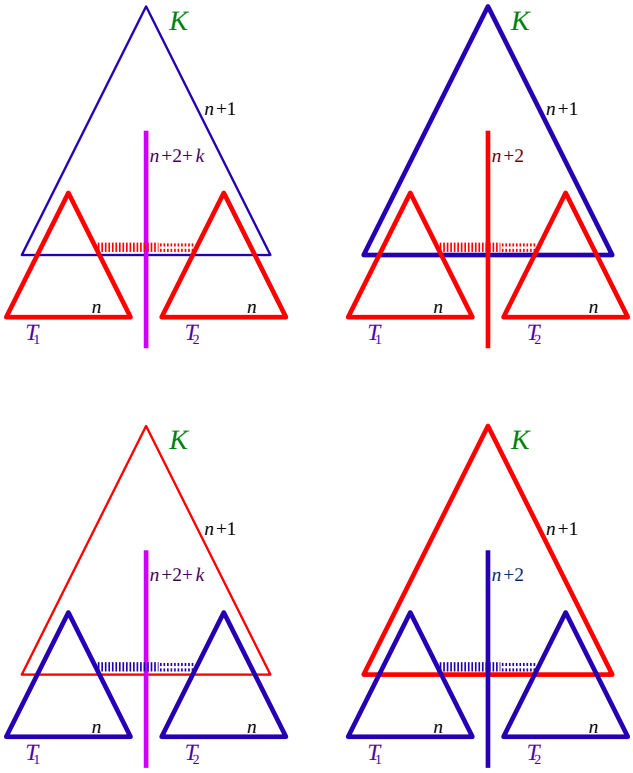

FIG. **30** The situation in between consecutive triangles of the same generation and latitude. The triangles, the small ones in the figure belong to the generation n. Note the signals of their colour, $\gamma\xi$, in between them. When it exists, K is represented by the big triangle. On the left hand-side, the case when K is phantom, the leg may be red or blue, purple on the picture. On the right-hand case, the case when K is a triangle: the leg is of the colour γ, necessarily.

considered is just the one we have just described. If the trilateral corresponding to the basis $\overline{\gamma}$ does not exist on this part of λ, then there is a signal $\overline{\gamma}\xi$ or $\overline{\gamma}\xi_2$, depending on the colour of the leg and on the colour $\overline{\gamma}$. If the trilateral exists, denote it by K, then the basis $\overline{\gamma}$ is open and so the signal $\gamma\xi$ or $\gamma\xi_2$ is alone. We know that if n is the generation of T_1, that of K is $n+1$. If K is a triangle, the mid-distance line of K generates a trilateral M of generation $n+2$ of the colour γ which may freely cut the basis $\overline{\gamma}$: it is the leg which we consider. If K is a phantom, its mid-distance line generates a trilateral M of generation $n+2+k$ which may have a colour independent of γ. Now, as K is a phantom, the leg

of M may freely cut the basis of K, whatever its colour. Moreover, whether K is a triangle or a phantom, from lemma 29, the meeting between the leg and the basis $\overline{\gamma}$ occurs within the first half of the leg. The situation is illustrated by figure 30.

Applying this argument to our situation, we can see that all the combinations permitted by table 16 are possible, provided that the compatibility conditions on the colours of legs and basis are observed. Later on, we shall refer to this by saying that the case (7) is only limited by combinatoric constraints.

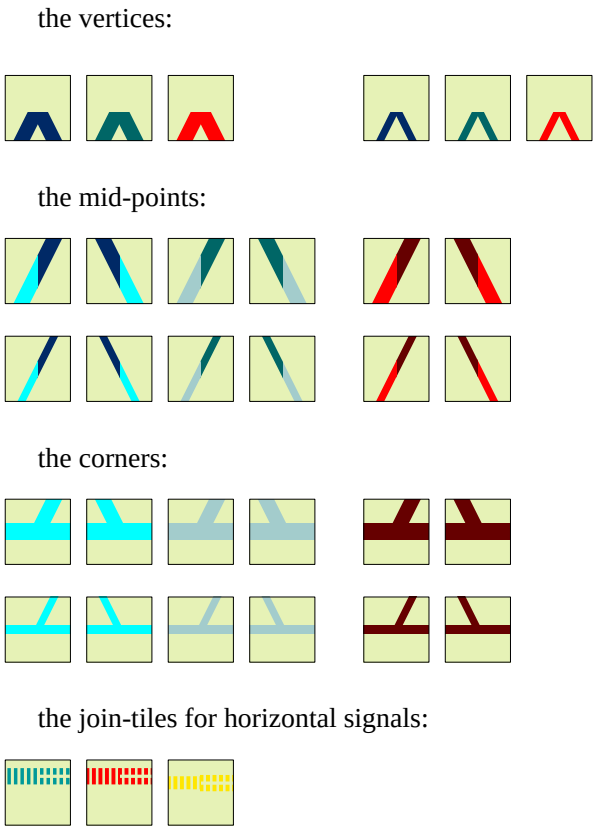

FIG. **31** The elementary patterns for the skeleton of the construction.

For the present situation of a first half of a leg, we have the following possibilities.

In any case, we have the signal of the colour γ. We have this signal alone if K exists. If K does not exist, we also have to append the signal of the colour $\overline{\gamma}$.

If γ is the colour of the leg, we have the following possibilities: $\gamma\xi$ and $\gamma\xi\overline{\gamma}\xi_2$, which means 3 cases. Moreover, in each case, the status of the basis β of the colour $\overline{\gamma}$ is free. And so, we have 6 patterns.

If the colour of the leg is $\overline{\gamma}$, the signals are $\gamma\xi_2$ and $\gamma\xi_2\overline{\gamma}\xi$. Now, in the case when the signal $\overline{\gamma}\xi$ is present, the status of β is free. However, when the signal $\gamma\xi$ is alone, β must be a basis of a phantom if the leg belongs to a triangle and β can also be a basis of a triangle otherwise. This means that if the leg belongs to a phantom we have 8 possible patterns, but if the leg belongs to a triangle, we have only 6 possible patterns.

Accordingly, we have 12 possible patterns when the leg belongs to a triangle and 14 of them when it belongs to a triangle. Consider now the case of the first half of a leg of a red trilateral T. Again, we shall discuss the case of a triangle and of a phantom at the same time.

With the case (1), the situation is a bit different with respect to the case with a blue leg.

The presence of a yellow signal is possible with a red leg of a triangle only. As we have a free row, we are either on an isocline 0, an isocline 10 or an isocline 15, but this latter case is ruled out. On the isocline, we have a blue-0 basis of a trilateral. Note that, inside the red triangle, the corresponding trilateral exists thanks to the scent mechanism. This means that the basis is always accompanied by a blue signal. This gives us 4 cases for the case (1). Note that the leg of the triangle emits a horizontal red signal outside the triangle and of the laterality of the leg.

Now, consider the case (2). This time, the basis is not accompanied with a yellow signal. In the case of a triangle, either we have a free row or a row with a horizontal red signal. In this case, we have a red signal $r\xi$. As it travels on an isocline 0, the red signal is accompanied by a blue signal. Indeed, the red signal comes from inner red triangles which contain inner blue or blue-0 triangles or at least part of them, those triangles existing from the scent principle.

In the case of a red phantom, we know that the free rows exist, exactly as for a red triangle, but they are not marked by a yellow signal. So, in this case, the blue-0 basis is accompanied by a blue signal. There is one case when the blue-0 basis is not covered: this the case when a red phantom of generation $2n+1$, with $n > 0$, is generated. This occurs inside, on the mid-distance line of a blue-0 phantom, hence for an isocline 15. In the other cases, the blue-0 basis is always accompanied. If the isocline does not correspond to a free row, we have the red signal $r\xi$. For the same reasons as with a leg of a red triangle, the red signal is accompanied by a blue signal. Note that the laterality of the blue signal is free.

Now, we arrive to the case (3). This is the case when the red leg meets an isocline 5. If we have the leg of a red triangle T and a red basis of a triangle R, R must be inside T, as we are within the first half of a leg of T and so, the basis is covered as required. This red basis is generated by a blue or blue-0 triangle of a generation smaller than that of R and which exists by the scent principle. Accordingly, we have a signal $b\xi_2 r\xi$. If the leg of T meets a red phantom, we have the same conclusion when the basis comes from an inner phantom P: the corner of P emits the required signal $r\xi$. And the same argument as for R shows that we have also a blue signal. Now, the leg of T may cross the open basis of a red phantom P which is not inside T. This happens when the vertex

of T is on an isocline 15. The legs of T first cross the bases of phantoms which belong to a tower, crossing the bases inside their phantom. As the colours of the phantoms alternate in a tower, we have also the crossing of an open basis of a red phantom. However, this basis of the phantom is generated by a blue or blue-0 triangle of a smaller generation and so, the red leg crosses a blue signal alone.

Consider the case when we have a leg of a red phantom P crossing a red basis. As the structure inside P is the same as the structure inside a red triangle of the same generation, we have at least the same signals. However, we cannot find the situation where the leg would cross an open basis of a red triangle: this is possible inside the triangle which generates the basis, but then, the basis is covered by a green signal, which is impossible, by construction, on an isocline 5. And so, we have the same conclusion as for the leg of a red triangle.

At last, we arrive to the case (7). This the case when the leg of our red trilateral T meets an isocline 15. The discussion which we had in the case of a blue leg also applies here in the same way exactly, also see figure 30. And so, we have 6+6 patterns when T is a triangle and 8+6 of them when T is a phantom, as indicated by the representation of the possible cases in the table.

For the counting of the prototiles, as the legs meet three possible tiles of the mantilla only, these tiles being fixed by the laterality of the leg, we obtain $1174 \times 3 = 3522$ prototiles.

Case $C_{2,2}$

This case concerns the meeting of a leg of a trilateral with a basis at its mid-point. As for the vertices, we can define an elementary signal to represent this part of the leg when the first half changes to the second one. We take the same representation of the legs as for the vertices. But now, we use a left- and a right-hand side masks. The signal is $\mu_\ell(L_2\gamma\sigma\xi) + \mu_r(L_1\gamma\sigma\xi)$. Figure 31 illustrates the application of these operators.

According to the algorithm of sub-section 4, the basis must have the green signal, excepted for triangles of generation 0 which have their mid-distance line on an isocline 5.

We display the description and the counting in table 22 which is organized as table 21.

We start our study with a blue-0 triangle. In this case, the mid-point occurs on the first isocline 5 which is met by the leg from its root. This corresponds to the situation of a basis described in the case (3). The basis is red and it may be open or covered. Indeed, the basis is open if the corresponding trilateral of generation 1 exists. If it does not exists at this place, it exists somewhere else in the same latitude from lemma 35. And so, the basis is covered. Note that both lateralities of the red signal may occur, of course not on the same tile. This gives the number of tiles indicated by the table.

Next, we look at the case of a blue-0 phantom. This case is different from the previous one as now, the mid-point of the leg occur on an isocline 15 by the meeting with a green signal. The difference of behaviour of the green signal

which may or may not cross the leg is taken into account by the multiplicative coefficient which represents the different situations of the phantom: alone, with an orange signal, or a lateral blue signal or both signals.

TABLE **22** The counting of the prototiles for the crossing of bases at the mid-point of a leg.

cases	③	④	⑤	⑥	total
isocline	5	15	15	15	total
$b_0\tau$, 2	ϵ, $r\xi_2$ $+\epsilon$, $r\xi_2$				
	3+3	0	0	0	12
$b_0\varphi$, 18		$\epsilon + \epsilon$	ϵ, $r\xi_2$ $+\epsilon$, $r\xi_2$	$\epsilon + \epsilon$	
	0	1+1	3+3	1+1	180
$b\tau$, 2			ϵ, $r\xi_2$ $+\epsilon$, $r\xi_2$		
	0	0	3+3	0	12
$b\varphi$, 18		$\epsilon + \epsilon$	ϵ, $r\xi_2$ $+\epsilon$, $r\xi_2$	$\epsilon + \epsilon$	
	0	1+1	3+3	1+1	180
$r\tau$, 2		ϵ, $b\xi_2$ $+ \epsilon$, $b\xi_2$			
	0	3+3	0	0	12
$r\varphi$, 18		ϵ, $b\xi_2$ $+ \epsilon$, $b\xi_2$	ϵ, $r\xi$ $+\epsilon$, $r\xi$	$\epsilon + \epsilon$	
	0	4+4	2+2	1+1	252
total:					648

Consider that the leg is in the case ④, which corresponds to the meeting of a blue basis accompanied by a green signal and a yellow one. This means that the phantom is contained in a red triangle. In this case, the basis is open as the triangle exists, due to the yellow signal. And so, we have a single case for each kind of basis.

Now, consider that the leg is in the case ⑤, which corresponds to the meeting of a red basis accompanied by a green signal. If the trilateral exists, the basis is open, otherwise, it is covered. And so, we have three cases for each kind of basis.

At last, we notice that the case of a blue basis with a green signal and no

other signal corresponds to the case of the mid-distance line of the infinite tower of the butterfly model. Two possibilities exist for the blue basis: thin or thick.

This time, we turn to the case of a blue trilateral T.

In this case, the meeting happens on an isocline 15.

If T is a triangle, we necessarily have a red signal along the mid-distance line, together with a green signal and so, we are in the case (5) or in the case (6).

In the case (5), the basis is open if the corresponding trilateral exists, otherwise it is covered. In the case (6), we are in the case of no accompanying signal. This is the case of the mid-distance line of the infinite tower of the butterfly model. By definition, this line is never crossed by a triangle. And so, this situation is ruled out.

If T is a phantom, the cases (4), (5) and (6) are all possible. In the first two cases, the discussion is similar to that of the case of a blue-0 phantom. However, in the case (4), the basis may be accompanied by a blue signal and the condition c_{12} applies. Also, in the case (6), the phantom may cross the mid-distance line of the infinite tower of the butterfly model. It crosses it at its mid-point, as required. Hence the counting indicated in the table.

Now, we discuss the situation for the leg of a red trilateral T.

This time, the case (5) is ruled out for a red triangle. In the case (4), we are, typically, in a red triangle which exists, thanks to the yellow signal. Moreover, the blue basis may be open or covered, depending on the existence or not of the corresponding trilateral. And so, we have 6 cases. The case (6) is also ruled out for a triangle which may not cross the mid-distance line of the butterfly model.

Consider the case of a red phantom. This time, all cases are possible with an isocline 15. We have a similar discussion as for a blue-0 phantom: the arguments are the same, and in the case (4), we also have the possibility of a blue signal.

The computations performed by the table give us 648 patterns. Again, as we are on a leg of a trilateral, three tiles of the mantilla are used for each laterality. As the laterality is already counted, we have $648 \times 3 = 1944$ prototiles.

Case $C_{3,2}$

This case concerns the crossing of the second half of a leg with bases.

We have a discussion which is very similar to the case $C_{1,2}$. However, the case is simpler as we have an important new constraint, namely the constraint c_4: the second half of a leg meets covered bases only.

Here also, we organize the discussion according to the cases of table 16. Now, as in the case of table 21, the cases (4), (5) and (6) are ruled out as they all contain a green signal: the meeting with this signal is impossible in the second half of a leg as well as it was impossible in the first half. Also, as in the case of the first half, blue-0 trilaterals are ruled out from this discussion, for the same reason.

With respect to the case $C_{1,2}$ we have another simplification: the orange signal does not occur on the second half of a phantom. For the same reason, there cannot be a lateral blue signal climbing along the second half of a leg: this may happen with the first half only. We remain with the possibility of

a lateral red signal climbing along the second half of a leg of a red phantom. This situation is taken into account by the multiplicative coefficient in the first column of table 23, as we did for table 21, with the same conventions on the representation of the content of the channel 1.

Below, table 23 displays the different cases and their counting.

First, we look at the case of a leg of a blue trilateral T meeting a basis on an isocline 0 or 10 with a yellow signal. This means that the trilateral is inside a red triangle. Its generation is bigger than the generation 0 and so, as the free row exists, the blue-0 basis cuts the leg of the blue trilateral outside the blue-0 trilateral. Hence, two cases.

Next, consider that we have still an isocline 0 or 10, but that there is no yellow signal. The corresponding blue signal comes from a blue-0 basis, and the corresponding trilateral exists inside T as T belongs to a bigger generation and from the scent principle. Accordingly, a blue signal is always present. There are cases when there is no other signal. Consider a big enough blue trilateral B. All isoclines which cross a first or a second half of a leg is crossed by a blue signal as a blue trilateral contains a single free row, its mid-distance line. Now, inside B, there are red trilaterals which also have free rows. This means that the free rows of these trilaterals do not contain a red signal inside the trilateral. As there is at least one phantom P, we know that outside P there is also no red signal: it is enough to consider that B is inside a bigger red phantom inside a tower which is in between two consecutive red triangles. In this case, the lines of the free rows of P cut the second half of the legs of P, accompanied by a blue signal only.

Now, a red signal may also be present in many other cases where a red triangle contains the blue-0 trilateral attached to the considered isocline 0 or 10.

Now, we arrive to the case of the meeting of an isocline 5, the case (3). There is a red basis which is always covered when it meets the leg of T from the condition c_4. Now, this red signal is also accompanied by a blue one. If there were no blue signal, this would mean that we are inside a trilateral of generation 1. This is possible for the first half of T, not for the second half.

At last, we arrive to the case (7), on an isocline 15.

Remember the discussion which we had in the same case with the first half of a leg. We have then noticed that the case of a horizontal signal of the colour γ alone was possible with the first half of a leg only. Accordingly, which is conformal to the condition c_4, we only have the signals $\gamma\xi\overline{\gamma}\xi_2$ when γ is the colour of the leg and $\gamma\xi_2\overline{\gamma}\xi$ when the colour of the leg is $\overline{\gamma}$. In both cases, the status of the basis of the colour $\overline{\gamma}$ is free. Accordingly, we get 8 possible cases in any case of the leg.

Now, consider the case of a leg of a red trilateral T.

In the case (1), we are in the case when the leg meets a free row of a red triangle. We have the signal $yb\xi_2$, as in the case of the first half of a leg. This crossing is impossible with the leg of a phantom, as in the case of the first half of a leg.

In the case (2), first consider the case when T is a triangle. As the basis is covered, we have the signal $b\xi_2$. Now, as we are not on a free row, otherwise, the yellow signal would be there, we also have a red signal. And so, the signal is $b\xi_2 r\xi$, whatever the status of the basis. This gives us 4 patterns only.

TABLE **23** The counting of the prototiles for the crossing of bases with the second half of a leg of a trilateral.

cases	(1)	(2)	(3)	(7)	total
isocline	0,10	0,10	5	15	total
$b\tau$, 2	$yb\xi$ + $yb\xi$	$b\xi$, $b\xi r\xi_2$ + $b\xi$, $b\xi r\xi_2$	$b\xi r\xi_2$	$b\xi r\xi_2$ | $b\xi r\xi_2$	
	1+1	3+3	2	(2+2)×2	36
$b\varphi$, 18	$yb\xi$ + $yb\xi$	$b\xi$, $b\xi r\xi_2$ + $b\xi$, $b\xi r\xi_2$	$b\xi r\xi_2$	$b\xi r\xi_2$ | $b\xi r\xi_2$	
	1+1	3+3	2	(2+2)×2	36
$r\tau$, 2	$yb\xi_2$ + $yb\xi_2$	$b\xi_2 r\xi$ + $b\xi_2 r\xi$	$b\xi_2 r\xi$ + $b\xi_2 r\xi$	$b\xi_2 r\xi$ | $b\xi_2 r\xi$	
	2+2	2+2	4	(2+2)×2	40
$r\varphi$, 18		$b\xi_2$, $b\xi_2 r\xi$ + $b\xi_2$, $b\xi_2 r\xi$	$b\xi_2 r\xi$ + $b\xi_2 r\xi$	$b\xi_2 r\xi$ | $b\xi_2 r\xi$	
	0	4+4	4	(2+2)×2	120
total:					232

NOTE: The factor 2 in the counting of the case (7) refers to the two possible statuses of the basis of the colour $\overline{\gamma}$.

When T is a phantom, the basis is also covered and so we have the signal $b\xi_2$. Now, we may be on a free row of the phantom, in which case, $b\xi 2$ is alone, or not, in which case, we also have $r\xi$. This gives us 8 patterns.

In the case (3), the leg meets an isocline 5 on which there is a red signal as the basis is covered. Now, this basis is generated by a triangle of generation 0 which always exists. As we are not inside a trilateral of generation 1 which does not contain any red trilateral, there is also a blue signal. Hence the signal $b\xi 2 r\xi$ whatever the status of T. This gives us 2 patterns in each case.

At last, we arrive to the case (7) for which we have the same situation as for a blue trilateral and, consequently, the same number of patterns.

From the table, we can see that this gives us 232 patterns. As the three tiles

of the period on the border of a tree are involved, and only them, as we are in the second half of a leg, we get 696 prototiles.

Case $C_{3,3}$

Now, we arrive to the case of the corners. This is the point where the second half of the legs meet the basis of their trilateral.

As for the tile for the mid-point of a leg, we can describe the skeleton structure of a corner by an appropriate assembling of basic signals. The elementary pattern is represented in figure 31 and it consists in the skeleton signal of the basis, on the channel 5 of the tiles, with a colour γ and a status σ. Then, we superpose the skeleton signal of the second half of a leg $L_2\gamma\sigma\xi$, for a corner of the side ξ. However, the superposition is not complete: it goes from the top of the tile until the channel 5. The part of the leg going from the channel 5 to the bottom of the tile is erased. This can be obtained by an appropriate new mask. There is also a lateral signal $\gamma\xi$ on the channel 1, but the signal does not cross the leg: it goes from the side 3 of the leg when $\xi = L$, along the channel 1, until it meets the leg. When $\xi = R$, it goes from the side 7, along the channel 1, until it meets the leg.

In the case of a red phantom, then we have $\sigma = \varphi$, the corner, associated to a red phantom which also bears a lateral red signal, bears the signal on a second vertical channel going through the same sides as the signal of the leg. This red lateral signal goes from the top of the tile until the channel 4. Its laterality is independent from that of the corner.

Now, this elementary pattern can be combined with the signals which travel on the other channels. As known from sub-section 4, the basis must be open inside the trilateral. This explains why the signal on the channel 1 coming from outside the trilateral is stopped by the leg.

When the basis travels on an isocline 15, which is the general case, it cannot contain a green signal. Accordingly, it meets an orange signal. It is crossed by the signal which also has the laterality of the corner.

The discussion is organized in table 24. It has the same cases as the crossing of a second half of a leg with a basis. However, here we have one more colour, as there are also blue-0 corners, for blue-0 triangles and for blue-0 phantoms.

Consider the case of a blue-0 trilateral.

As the corner of such a trilateral necessarily occurs on an isocline 0 or on an isocline 10, the cases (3) and (7) are ruled out.

In the case (1), we have a yellow signal and so, a single posibility for each laterality and for each kind of trilateral: remember that the basis is open inside the trilateral.

In the case (2), we have no yellow signal. We may have no signal at all, this happens inside a tower of phantoms, and we may also have a red signal: indeed, blue-0 triangles give rise to the trilaterals of generation 1 and on the mid-distance line of blue-0 phantoms which is an isocline 15, we may have the vertex of any trilateral, in particular, of red ones.

TABLE **24** The counting of the prototiles for the corners.

cases	①	②	③	⑦	total
isocline	0,10	0,10	5	15	total
$b_0\tau$, 2	y	ϵ, $r\xi_2$			
	1	3	0	0	8
$b_0\varphi$, 2	y	ϵ, $r\xi_2$			
	1	2	0	0	8
$b\tau$, 2				$r\xi_2$	
	0	0	0	2	4
$b\varphi$, 2				$r\xi_2$	
	0	0	0	2	4
$r\tau$, 2			$b\xi_2$	$b\xi_2$	
	0	0	2	2	8
$r\varphi$, 6			$b\xi_2$	$b\xi_2$	
	0	0	2	2	24
total:					56

NOTE: The factor 2 in the counting of the case ⑦ refers to the two possible statuses of the basis of the colour $\overline{\gamma}$.

Now, consider the case of a blue trilateral. Its basis is necessarily on an isocline 15, and so, we have to consider the case ⑦ only. Now, in this case, as the basis must be open, we have the single case $\gamma\sigma$, where γ is the colour which is opposite to the colour of the basis which is $\overline{\gamma}$, here blue.

Accordingly, this represents two patterns per laterality and per kind of trilateral.

Now, we consider the case of a red trilateral. We have exactly the same discussion as previously when the basis is on an iscoline 15, hence one pattern, basically. Now, there is another possibility with the trilaterals of generation 1 for which the basis is on an isocline 5. The basis is open, as required, but it has a blue signal as the basis is generated by a triangle of the previous generation which necessarily exists. And so, we have two cases both in the case of a triangle

and that of a pahntom.

This gives us 56 patterns. Now, the corner is on the border of a tree, after the second half of a leg. When the isocline of the basis is an isocline 15, we may have the three possible cases for a tile of a border of a tree, in the period of the border. But for the isoclines 0, 5 and 10, we always have the same tile. And so, we have to multiply the number of patterns on an isocline 15 by 3. Accordingly, we find 80 prototiles.

Case $C_{4,4}$

At last, we have the case when there is no basis and no leg. Of course, this situation exists. It is the case of the isoclines 1..4, 6..9, 11..14 and 16..19. All possible tiles of the mantilla can be met in this case, except the tile of an active seed. Accordingly, the number of prototiles would be $33 \times 16 = 528$.

However, we also have to take into account that the scent may also be dispatched to tiles within these latitudes. And so, the tiles may be crossed by the scent. The needed patterns are illustrated by figure 32. However, the number of tiles is not 528×2. Indeed, as already noticed in [18] and checked with the help of a computer program, not all tiles of the mantilla are involved by the diffusion of the scent. The reason is that within the frist four isoclines which are below the root of a tree of the mantilla, not all the tiles of the mantilla occur.

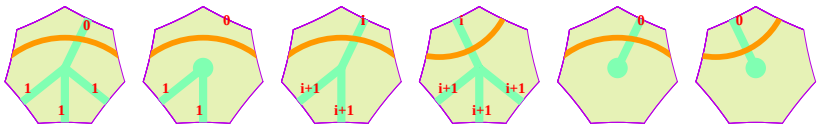

FIG. **32** The elementary patterns for the scent in the passive rows.

Their occurrence is indicated by table 25, also see [18].

TABLE **25** The counting of the tiles of the mantilla which are inside a tree of the mantilla in the first five isoclines, starting from a seed.

isocline	1	2	3	4		5
mantilla patterns	3	5	10	18	36	22

From table 25, we can see that 36 tiles of the mantilla are used for the isoclines 1..4. Note that this number takes into account the patterns, the number of the isoclines and the status of the tile. Now, the scent may also be activated on the isoclines 5, 10 and 15, so that the same tiles occur on the isoclines 6..9, 11..14 and 16..19 when the scent occurs. Accordingly, the number of these prototiles is $36 \times 4 = 144$. Appended to the 528 protiles which are used when there is no scent, we get 672 prototiles.

Now, we are in the position to count the total number of prototiles which are needed for the construction. To this purpose, we again use table 14, in which we

replace the YES/NO indications by numbers. Of course, NO is replaced by 0. For YES, we replace it by the number of prototiles which we have found for the corresponding case.

Accordingly, looking at table 26, we find that we need 18,856 prototiles for the construction.

TABLE **26** Counting of the prototiles by summing the partial totals of the previous tables.

	vertex	plain	corner	empty
first half	142	3522	0	2220
mid-point	0	1944	0	0
second half	0	696	80	592
none	0	8988	0	672
final account:				18,856

6.3 Description of the tiles: the meta-tiles

Now, we turn to the description of the meta-tiles which are the tiles needed for the simulation of the computation of a Turing machine. This part of the description corresponds to the sub-section devoted to the computing areas.

Figure 33 illustrates these tiles which we call meta-tiles as they are **variables** for prototiles. Indeed, the actual prototiles depend on the particular Turing machine whose execution is simulated by the tiling. For conveniency, in the following explanations, we denote the tiles by two numbers as follows: *a*-*b*, where *a* and *b* are the numbers of the row and the column respectively, where the tile stands in the figure.

The set of meta-tiles can be split into four groups of tiles, corresponding to the rows of figure 33. On the first row, we have the tiles used for conveying the information. On the second row, we can see the tiles used for performing an instruction. On the third row, we have the tiles which transmit the new information after performing an instruction. On the fourth row, we have the tiles for the halting of the machine.

We remind the reader that the tape of the simulated Turing machine is placed on the border of the tree, on the tiles where the border meets a free row of the concerned red triangle. The history of each square of the tape is represented by the verticals which run along a ray of **8**-centres which is the closest to the inital tile representing this square. The execution itself is materialized by what we call the **computing signal**. It is a signal which first conveys the current state of the Turing machine. The signal travels on the horizontals of the grid, materialized by the yellow rows of the red triangle where the simulation occurs. It also travels on the verticals which we have just mentioned. An instruction

is performed when the computing signal, travelling on a horizontal meets a vertical. The tile which is placed at this intersection, one of the tiles 2-1..2-8, represents all the data of the instruction: the current content of the tape, which arrives from the top of the tile; the current state of the Turing machine which is conveyed by the computing signal and which arrives on a side of the tile which is crossed by the isocline on which the tile stands. The exact side is determined by the motion of the head which is represented on the horizontal by a lateral yellow signal replacing the standard unilateral yellow signal for this part of the row. A right-hand side yellow signal indicates a motion to the right and a left-hand side yellow signal indicates a motion to the left. A lateral yellow signal enters the tile from the side of the opposite laterality.

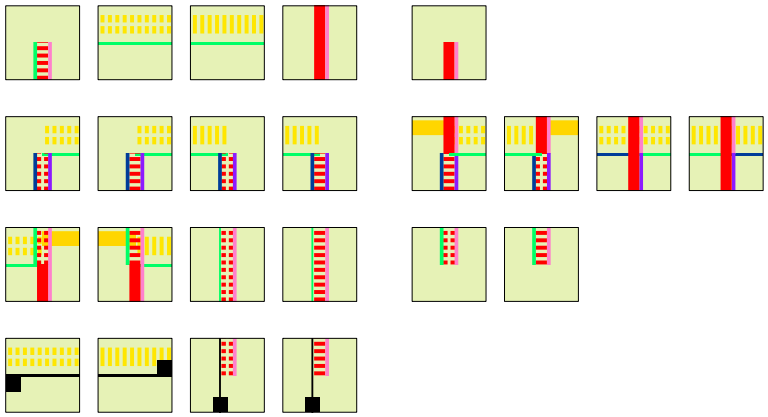

FIG. **33** The computing tiles.

The other part of a tile representing the execution of an instruction contains all the information of the output of the instruction: the new state of the machine which is now conveyed by the computing signal, the new content of the square which is transmitted by the same vertical and the new move of the head.

If the move is the same as the previous one and if the computing signal did not yet reached the border of the tree, the computing signal goes on on the same isocline. This situation is represented by the tiles 2-7 and 2-8. If the move is the same, but the instruction tile is on the border of the tree, we use the tiles 2-1 and 2-4.

If the move is the opposite, and we may assume, without loss of generatlity that we only have a move to the left or a move to the right, then the computing signal goes down along the vertical, using the tile 2-5 and 2-6 or the tiles 2-2 and 2-3 if the execution of the instruction happens on the border of the tree. Note that when the move is the same but the instruction is executed on the border, the computing signal also goes down along the vertical, which is clear from the tiles 2-1 and 2-4 used in this case.

When the computing signal goes down, during its travel along the vertical, until the next free row is met, it conveys three pieces of information. The new content of the square, specifically conveyed by the vertical, the new state of the Turing machine, temporarily conveyed in this way and the move of the next instruction, also temporarily conveyed in this way. The next move is represented by a lateral vertical signal whose laterality is that of the move.

When the next free row is met, the new content goes on along the vertical which again becomes unilateral, see the tiles 3-1 and 3-2. The vertical signal goes on conveying the new content of the square, using the tile 1-4. But the new state now travels on the new free row. On the new row, a lateral yellow signal replaces the unilateral yellow signal. The laterality of the new yellow signal is that of the move, which is indicated by the laterality of the upper part of the vertical signal of the tile 3-1 or 3-2. The side through which the computing signal exits has the laterality of the yellow signal, again see the tiles 3-1 and 3-2. On the new free row, the computing signal goes on its way, using the tile 1-2 or 1-3, depending on the direction of its move.

There is two ways to stop this simulation. In the first way, the machine calls its final state, which triggers the abutting of one of the tiles 4-1..4-4 to the instruction tile. As the tiles cannot be completely rotated, any tile from the tiles 4-1..4-4 blocks the construction of the tiling. In the second way, the halting state is not reached by the execution of the Turing machine program, but the basis of the triangle is met by the computing signal, travelling on a vertical. This situation is represented by the tiles 3-5 and 3-6.

Before turning to the precise description of the tiles and their counting, let us formulate two remarks. First, the tiles which we consider now are superposed with tiles of the mantilla, exactly as we have seen with the prototiles. Second, they are also superposed with the prototiles which we have seen but, in certain cases, they replace the prototiles. There is a simple rule to define this situation: the vertical signals are superposed to the signals of the prototiles. For the horizontal signals, the signal of the current state is superposed, but the motion signal, a lateral yellow signal, replaces the yellow signal of the concerned prototiles.

Note that not all prototiles are concerned with the computing signal. Basically, the basis signals containing the yellow signal are concerned together with the three tiles used for the border of a sector, following a ray of **8**-centres. Of course, the beginning part of a vertical belongs to an aperiodic part of the vertical. But a very few tiles are involved with this process and they mainly concern the tiles 1-5 and 2-1..2-4.

The counting of the tiles is displayed by table 27. We consider the main groups which are attached to the rows of figure 33.

Let us start with the first row of figure 33.

The firt tile is 1-1, which deals with the vertex of a red triangle. Looking at table 20, there are 3 cases of red vertices on an isocline 5 and also 3 of them on an isocline 15. Which makes 6 meta-tiles. Note that this tile can be

considered as a prototile: we may assume that the Turing machine always starts its computation in state 1 with a move to the right and, by assumption, it is on an empty square of the tape. We also may assume that the Turing machine always puts the symbol 1 in this square, but this is already not relevent to our purpose. Later, the tiles for the halting can also be considered as prototiles but all the other tiles are true meta-tiles.

Next, we have the meta-tiles 1-2 and 1-3 which convey the current state on a horizontal. This time, we have to know how many patterns are concerned by a yellow signal. For the plain bases, which is our case, table 16 indicates that there are 16 possible patterns. Now, any tile of the mantilla can be concerned. Moreover, any may or may not receive the scent. This gives us 2112 meta-tiles. Note that we find the same counting for the tiles 4-1 and 4-2 for the same reason: they stand on a yellow row.

At this point, we can divide the number of these meta-tiles by 2 by noticing that for a half of the 16 patterns accompanying the yellow signal, these patterns involve an isocline 15. Now, from lemma 19, in a red triangle, there is a single yellow row on an isocline 15, which is negligeable in comparison with the 2^n others in a red triangle of generation $2n+1$. And so, we decide that the computing signal will not travel on a yellow row when this row is accompanied by the green signal. Accordingly, this gives us 1056 meta-tiles of the type 1-2 and 1-3.

Then we have the tile 1-4.

These tiles travel on a vertical. And so, basically, they use 3 tiles of the mantilla, but they can meet any isocline, which we count in the patterns. This makes 60 meta-tiles. Note that this tile is not affected by the scent. This could happen from the vertex of a red triangle. However, the vertex makes use of the tile 1-1 which calls the tile 3-4 until the next yellow row is found. This exceeds the number of isoclines crossed by the scent along a vertical, as a vertical does not meet the border of an inner tree. However, the tile may be affected by the irregular part of a vertical. This happens with the tile 1-5 but, depending on the isocline which crosses the tile 1-5, the following tile 1-4 may fall again in the aperiodic part. In fact, 4 tiles are concerned by this aperiodic part: the tile $137 \circ b$ when the vertical starts from a tile $11 \circ 2b$, the tiles $47 \circ 7w$ and $6 \circ 77w$ when it starts from a tile G_r. The period is immediately reached after the first tile when the vertical starts from a tile $1 \circ 15b$. This comes from the study of sub-section 6.1 and it concerns the right-hand side border of a tree. Note that we have a symmetric situation on the left-hand side border. Accordingly, we have 6 patterns, but the concerned isoclines may be any one among the usual isoclines 0, 10 and 15 as there is no yellow row on an isocline 5. And so, we have 18 more meta-tiles which makes 78 meta-tiles.

Now, when the tile 1-4 crosses an isocline 0,5, 10 or 15, it crosses a plain basis and, inside a big enough red triangle, it may be any basis among the patterns which are defined by table 16. And so, taking into account that these different patterns contain the different cases of isoclines met by the tile, we get 654 new meta-tiles. Note that this counting again contains 12 tiles from the 60 ones

which we have already counted with all the isoclines: those which are on an isocline 0, 5, 10 or 15.

Next, we arrive to the tile 1-5.

This tile occurs on the border of the tree, at an instersection with a yellow row. This tile is the starting point of a vertical which does not receive the visit of the computing signal. Accordingly, we have the 8 patterns associated with a yellow row but, at the same time, as we are on the border of a tree of the mantilla, only 3 tiles are concerned for each border. Moreover, the scent does not reach such a tile. Accordingly, this gives us $8 \times 6 = 48$ tiles.

TABLE **27** Organization of the counting of the meta-tiles.

tiles	coef	patterns	mantilla	scent	total
1-1	1	V, 6	1	1	6
1-2, 1-3	2	Y, 8	33	2	1056
1-4	1	p, 16	3	1	48+18
1-4	1	B, 218	3	1	654
1-5	1	Y, 8	6	1	48
2-1..2-4	4	Y, 8	3	1	96
2-5..2-8	4	Y, 8	3	1	96
3-1, 3-2	2	Y, 8	3	1	48
3-3, 3-4	2	p, 16	3	1	96+52
3-3, 3-4	2	B, 218	3	1	654
3-5, 3-6	2	B, 11	3	1	66
4-1, 4-2	2	Y, 8	33	2	1056
4-3, 4-4	2	iso, 2	3	1	12
total:					4,006

This time, we deal with the second row of figure 33.

First, we have the tiles 2-1..2-4 which describe the execution of an instruction when the head of the Turing machine arrives at a square for the first time. This is why the execution happens on the border of the tree. Accordingly, the counting of the tiles 2-1..2-4 is the same as that of the tile 1-5, as they happen at the same place. Now, as the tiles take into account of which border of the tree is concerned, we have only 3 tiles of the mantilla to take into account. This defines 96 meta-tiles.

The tiles 2-5..2-8 deal with the standard execution of an instruction. This happens on a free row, and again 3 tiles of the mantilla are concerned. But they are not the same 3 tiles as in the previous case. Here, the three tiles are those which define a ray of **8**-centres. Accordingly, this again gives us 96 meta-tiles.

Now, we consider the tiles of the third row of figure 33.

The first two tiles of the row, the tiles 3-1 and 3-2 are also connected with the execution of an instruction: they concern the moment when the computing signal reaches a new free row on which it will look after the expected vertical of the next square of the tape to be visited. The counting is exactly the same as previously. As two tiles only are concerned, this gives 48 meta-tiles.

We now have to deal with the tiles 3-3 and 3-4. Here, the discussion is close to that of the tile 1-4. We have the same counting for the crossing with the basis and for the 16 passive rows of the mantilla, which gives us 750 meta-tiles. The aperiodic part of the verticals initiated by the tiles 2-1..2-4 or by the vertex 1-1, which gives us 18 new meta-tiles. But here, we have to take into account that the tiles coming from the vertex receive the scent. This gives exactly 4 new tiles, and as the vertex itself may be on any isocline 5 or 15, this gives 8 meta-tiles to append to the counting. And so, for these tiles, we get 802 meta-tiles.

At last, we arrive to the tiles 3-5 and 3-6. These tiles correspond to the interruption of the computation by the meeting of the basis of the red triangle. As we are inside the triangle, the basis is necessarily open. Now, on the isocline 15, it may be accompanied by a green signal or by an orange one and, this time, the meeting with a join tile is possible. We have also the possibility of an open red basis on the isocline 5 where there is neither green nor orange signal. Looking at table 16, we find 1 case with a green signal, 6 cases with an orange one and 4 cases for a red basis on an isocline 5, as a blue join-pattern is possible. Again, three tiles of the mantilla are possible, as we are on a vertical. This gives us 66 new meta-tiles.

At last, we consider the tiles of the fourth row of figure 33. These tiles deal with the halting of the Turing machine.

First, we have the case of a halting within a free row by the tiles 4-1 and 4-2. The counting is exactly the same as for the tiles 1-2 and 1-3 and so, we get 1056 meta-tiles.

Then, we have the case of a halting on a vertical: this is the case when the halting occurs on a change of direction of the head of the Turing machine. This situation is implemented by the tiles 4-3 and 4-4. Now, by their constitution, as the concerned execution of the halting instruction occurs on an isocline 0 or 10, the tiles 4-3 and 4-4 occur on an isocline 1 or 11. There is no basis on these isoclines and we have only to take into account the number of the isocline and the pattern of the tile of the mantilla. As we are on a vertical, there are three of them only. And so, we find 12 meta-tiles.

And so, we find exactly, 4,006 meta-tiles.

However, this number does not give us the exact number of prototiles which

we need if we know the program of the Turing machine. The actual number depends on the number s of symbols on the tape of the Turing machine and on the number q of states of the Turing machine. Here, we assume that the number of symbols contains the blank but, as usual, that the halting state is not taken into account in the number of states.

From this point of view, the tiles of figure 33 contain tiles with only a signal for the symbol on the tape, for example, the tile 1-4 and tiles with only a signal for the state of the head, for instance, the tile 1-2. Now, many tiles contain both symbols. If we consider the tiles of the second row of the figure, these tiles correspond exactly to the instructions of the Turing machine. But the number I of these instructions is not necessarily $q \times s$. In fact, we have $I \leq q \times s$. Now, a few tiles also depend on another parameter: the tiles of the third row only contain an entry of the table of the Turing machine: they contain the new symbol, the new state and the move to be performed by the head of the Turing machine. Now, the number X of different entries of the table is not necessarily the same as the number of instructions of the Turing machine. We simply have that $X \leq I$.

Let us count the number of tiles of each category:

- tiles depending on q only: 1-2 and 1-3 and so, 1056 tiles;
- tiles depending on s only: 1-4, 1-5 and 4-3, 4-4 and so, 780 tiles;
- tiles depending on I only: 2-1..2-8 and so, 192 tiles;
- tiles depending on X only: 3-1..3-6 and so, 916 tiles;
- prototiles: 1-1, 4-1, 4-2 and so, 1062 tiles.

This allows us to state the following result, taking into account the prototiles which we have counted is sub-section 6.2:

PROPOSITION **1** *Let M be a Turing machine which starts its computation from an empty tape, in state* 1*, goes to to the right and writes* 1 *on its first scanned cell. Denote by q the number of states of M, by s the number of its tape symbols, by I the number of its instructions and by X the number of different outputs produced by its instructions. Then, the set of tiles described in sub-sections* 6.2 *and* 6.3 *defines* $780 \times s + 1056 \times q + 192 \times I + 916 \times X + 19918$ *prototiles.*

7 A few corollaries

The construction leading to the proof of theorem 1 allows to get a few results in the same line of problems.

As indicated in [3, 4], there is a connection between the general tiling problem and the **Heesch number** of a tiling. This number is defined as the maximum number of **coronas** of a disc which can be formed with the tiles of a given set of tiles, see [11] for more information. As indicated in [4], and as our construction fits in the case of domino tilings, we have the following corollary of theorem 1.

THEOREM **2** *There is no computable function which bounds the Heesch number for the tilings of the hyperbolic plane.*

The construction of [15, 17] gives the following result, see [19, 23].

THEOREM **3** *The finite tiling problem is undecidable for the hyperbolic plane.*

Combined with the construction proving theorem 3 and a result of [24], the construction of the present paper allows us to establish the following result, see [20].

THEOREM **4** *The periodic tiling problem is undecidable for the hyperbolic plane, also in its domino version.*

In this statement, **periodic** means that there is a shift which leaves the tiling globally invariant.

Note that the analog of theorem 4 for the Euclidean plane was proved by Gurevich and Koriakov, see [5].

At last, in another direction, we may apply the argments of Hanf and Myers, see [6, 26], and prove the following result, see [18].

THEOREM **5** *There is a finite set of tiles such that it generates only non-recursive tilings of the hyperbolic plane.*

8 Conclusion

The first consequence is that, according to the countings of our sub-sections 6.2 and 6.3, we need a huge number of tiles.

Of course, we may wonder whether the number of tiles can be reduced. In the discussion about the tiles, we have seen that the constraints c_{10} and c_{11} about the join tile significantly reduced the number of prototiles. Also, the elimination of yellow rows accompanied by a green signal reduced the number of meta-tiles by a bit more than 2000 of them. Further reductions might be possible by a small tuning of the present signals. As an example, we could forbid yellow rows on the mid-distance line of a red triangle. This would reduce the present number of prototiles by a bit more than 400 tiles. Another smaller reduction could be obtained by requiring that horizontal blue signals crossing the leg of a red triangle along an isocline 0 or 10 should have the same laterality as the leg. This would spare a bit more than 150 prototiles. Now, all together, this represents a reduction of around 3.18 percents. On another hand, the latter suggestions of reduction increase the number of constraints and conditions, which makes the presentation less clear. This is why, they were not kept for the final counting.

Now, an attentive look at the tables of sub-sections 6.2 and 6.3 indicates that the reason of the big number of tiles lies in lemma 14 and in the number of tiles of the mantilla. A consequence of the lemma is the important number of passive tiles connected with the isoclines which do not bear the construction signals. And so, to get a significant reduction of the number of tiles means to find a new, simpler setting. Professor Goodman-Strauss advised me to do so. In fact, recently, I realized that this is possible. I have not the room, here,

to explain the idea. It is interesting to notice that this simplification allows to implement a similar implementation of the interwoven triangles in both the ternary heptagrid and in the pentagrid.

However, the number of prototiles induced by the signals for the crossing of the legs with the bases would almost be unchanged in the new setting, and this number represents a bit more than the third of the total number of prototiles. Accordingly, the reduction of the number of tiles might turn out to be not as drastic as desired. From what has just been said, we could expect to divide the number of tiles in a simpler environment, possibly by 2, but not much more.

The second consequence which could be derived from the construcion lies on a more abstract level. Let us look at the lifting of the abstract brackets to the interwoven triangles. At first glace, this seems to be a Euclidean construction. In the very paper, a whole section is devoted to the Euclidean implementation of the interwoven triangles. And in the next section, we still transfer this construction to the hyperbolic plane. It seems to me that the fact that this transfer is possible has an important meaning. From my humble point of view, it means that a construction which looks like purely Euclidean has indeed a purely combinatoric character. It belongs to absolute geometry and it mainly requires Archimedes' axiom. Note that absolute geometry itself has no pure model. A realization is necessarily either Euclidean or hyperbolic. We suggest to conclude that, probably, the extent of aboslute geometry is somehow under-estimated.

Acknowledgement

I am very pleased to acknowledge the interest of several colleagues and friends to the main result of this paper. Let me especially thank André Barbé, Jean-Paul Delahaye, Chaim Goodman-Strauss, Serge Grigorieff, Yuri Gurevich, Tero Harju, Oscar Ibarra, Hermann Maurer, Gheorghe Păun, Grzegorz Rozenberg and Klaus Sutner.

References

[1] Berger R., The undecidability of the domino problem, *Memoirs of the American Mathematical Society*, **66**, (1966), 1-72.

[2] Chelghoum K., Margenstern M., Martin B., Pecci I., Cellular automata in the hyperbolic plane: proposal for a new environment, *Lecture Notes in Computer Sciences*, **3305**, (2004), 678-687, proceedings of ACRI'2004, Amsterdam, October, 25-27, 2004.

[3] Goodman-Strauss, Ch., A strongly aperiodic set of tiles in the hyperbolic plane, *Inventiones Mathematicae*, **159**(1), (2005), 119-132.

[4] Goodman-Strauss, Ch., Growth, aperiodicity and undecidability, *invited address at the AMS meeting at Davidson, NC*, March, 3-4, (2007).

[5] Gurevich Yu., Koriakov I., A remark on Berger's paper on the domino problem, *Siberian Mathematical Journal*, **13**, (1972), 459–463.

[6] Hanf W., Nonrecursive tilings of the plane. I. *Journal of Symbolic Logic*, **39**, (1974), 283-285.

[7] Hopcroft, J.E., Motwani, R., and Ullman, J.D., *Introduction to Automata Theory, Languages, and Computation*, Addison Wesley, Boston/San Francisco/New York, (2001).

[8] Kari J., A new undecidability proof of the tiling problem: The tiling problem is undecidable both in the Euclidean and in the hyperbolic plane, *AMS meeting at Davidson, NC, Special Session on Computational and Combinatorial Aspects of Tilings and Substitutions*, March, 3-4, (2007).

[9] Kari J., The Tiling Problem Revisited, *Lecture Notes in Computer Science*, to appear in the volume **4664**, (2007).

[10] Levin L.A., Aperiodic Tilings: Breaking Translational Symmetry, *The Computer Journal*, **48**(6), (2005), 642-645.

[11] Mann C., Heesch's tiling problem, *American Mathematical Monthly*, **111**(6), (2004), 509-517.

[12] Margenstern M., New Tools for Cellular Automata of the Hyperbolic Plane, *Journal of Universal Computer Science* **6**N°12, 1226–1252, (2000)

[13] Margenstern M., Cellular Automata and Combinatoric Tilings in Hyperbolic Spaces, a survey, *Lecture Notes in Computer Sciences*, **2731**, (2003), 48-72.

[14] Margenstern M., A new way to implement cellular automata on the penta- and heptagrids, *Journal of Cellular Automata* **1**, N°1, (2006), 1-24.

[15] Margenstern M., About the domino problem in the hyperbolic plane from an algorithmic point of view, *iarXiv:cs.CG/*0603093 *v*1, (2006), 11p.

[16] Margenstern M., About the domino problem in the hyperbolic plane, a new solution, *arXiv:cs.CG/*0701096, (2007), January, 60p.

[17] Margenstern M., About the domino problem in the hyperbolic plane from an algorithmic point of view, *Technical report,* 2006-101*, LITA, Université Paul Verlaine − Metz*, (2006), 100p., available at:

http://www.lita.sciences.univ-metz.fr/˜margens/hyp_dominoes.ps.gzip

[18] Margenstern M., About the domino problem in the hyperbolic plane, a new solution, *Technical report,* 2007-102*, LITA, Université Paul Verlaine − Metz*, (2007), 106p., available at:

http://www.lita.sciences.univ-metz.fr/˜margens/new_hyp_dominoes.ps.gzip

[19] Margenstern M., The finite tiling problem is undecidable in the hyperbolic plane, *arxiv:cs.CG/*0703147*v*1, (2007), March, 8p.

[20] Margenstern M., The periodic domino problem is undecidable in the hyperbolic plane, *arxiv:cs.CG/*0703153*v*1, (2007), March, 12p.

[21] Margenstern M., About the domino problem in the hyperbolic plane, a new solution: complement, *arxiv*:0705.0086*v*4, (2007), May, 20p.

[22] Margenstern M., The Domino Problem of the Hyperbolic Plane Is Undecidable, *arxiv*:0706.4161, (2007), June, 18p.

[23] Margenstern M., The Fininte Tiling Problem Is Undecidable in the Hyperbolic Plane, *Workshop on Reachability Problems*, **RP07**, July 2007, Turku, Finland, accepted.

[24] Margenstern M., Cellular Automata in Hyperbolic Spaces, Volume 1, Theory, *OCP*, Philadelphia, to appear (2007).

[25] Margenstern M., About the domino problem in the hyperbolic plane from an algorithmic point of view, *Theoretical Informatics and Applications*, to appear (2008).

[26] Myers D., Nonrecursive tilings of the plane. II. *Journal of Symbolic Logic*, **39**, (1974), 286-294.

[27] Robinson R.M. Undecidability and nonperiodicity for tilings of the plane, *Inventiones Mathematicae*, **12**, (1971), 177-209.

[28] Robinson R.M. Undecidable tiling problems in the hyperbolic plane. *Inventiones Mathematicae*, **44**, (1978), 259-264.

[29] Turing A.M., On computable real numbers, with an application to the Entscheidungsproblem, *Proceedings of the London Mathematical Society*, ser. 2, **42**, 230-265, (1936).

[30] Wang H. Proving theorems by pattern recognition, Bell System Tech. J. vol. **40** (1961), 1–41.